# DYNAMICS OF THE CIRCADIAN RHYTHM IN DROSOPHILA MELANOGASTER

A Dissertation

Presented to the Faculty of the Graduate School

of Cornell University

in Partial Fulfillment of the Requirements for the Degree of

Doctor of Philosophy

by

Philip Brandon Kidd

January 2015

DYNAMICS OF THE CIRCADIAN RHYTHM IN DROSOPHILA MELANOGASTER

Philip Brandon Kidd, Ph.D.

Cornell University 2015

The circadian clock drives daily rhythms in many organisms and is a key regulator of diverse physiological functions, including metabolism, the immune system, and sleep. Circadian oscillators also have a variety of interesting dynamical properties, including spontaneous synchronization, entrainment by external stimuli, and temperature compensation of period. In this thesis, we first develop a variety of simple mathematical models, and then use those models to guide experimental work on two different aspects of circadian dynamics in the fruit fly *Drosophila melanogaster*. In the first set of experiments, we show that a carefully tuned light stimulus can disrupt the coherence of molecular circadian oscillations for several days, and use behavioral data to argue that this could be due to weak coupling between circadian neurons. In the second set of experiments, we use quantitative biochemical measurements to examine the mechanism of temperature compensation of the circadian period. We show that changes in temperature affect molecular oscillations by a simple rescaling of amplitude, and argue that this indicates that separate sub-processes of the circadian clock must be independently temperature compensated. We also investigate the mechanism of circadian temperature entrainment, and present evidence that the heat shock pathway is involved in communicating temperature to the circadian clock.

## BIOGRAPHICAL SKETCH

Philip Brandon Kidd was born September 13, 1984 in Miami, Florida. He soon moved to Hanover County, Virginia, and attended high school at the Governor's School for Government and International Studies in Richmond, where he learned French and Russian, languages that he has since mostly forgotten. In September 2002, Philip matriculated at Princeton University, where he majored in Physics and distinguished himself as a slightly better-than-average parliamentary debater. He graduated *magna cum laude* in 2006 with a thesis on metabolic regulation in *E. coli*, completed under the tutelage of Ned Wingreen. In the fall of that year he began his studies in Physics at Cornell University. In winter of 2010, he moved to New York City to work with Eric Siggia and Michael Young at The Rockefeller University.

To Lino

## ACKNOWLEDGEMENTS

My long and twisted path through graduate school could not have happened without the help and support of many different people. My long exploration of different areas of physics at Cornell was made possible by the help and understanding of many professors with whom I was associated: Chris Henley, Jim Sethna, John Guckenheimer, Eun-Ah Kim, and Chris Myers. I learned things from all of them that have been invaluable in my subsequent research career. I also have to thank my house- and classmates from those years, Srivatsan Chakram, Vikram Gadagkar, Ben Machta, and Justin Vines, with whom I had many hours of inspiring conversation about physics, science, and life.

My work at Rockefeller was supported by many other scientists. Alison North of the Bio-Imaging facility, Svetlana Mazel in the Cell Sorting facility , and Jeanne Chiavarelli-Giganti in the High Throughput Center provided experimental support. John Lis and Ralf Stanewsky generously provided fly strains. I must also thank members of the Siggia laboratory for their help. Aryeh Warmflash and Benoit Sorre gave invaluable advice about culturing and imaging mammalian cells. Paul François performed the research that inspired my work on temperature compensation, and we had numerous enjoyable talks about circadian rhythms over the years. My experience at Rockefeller would have been greatly impoverished without the wit and wisdom of Patrick Griffin, formerly of the Rockefeller Faculty Club. His gruff stoicism was the perfect foil when I needed to complain about something on a random Tuesday night.

All of my research at Rockefeller was performed in the laboratory of Michael Young, to whom I owe many thanks for his hospitality and scientific advice. The unenviable task of teaching me, a theoretical physicist ,to become a functioning molecular biologist was accomplished only by the heroic efforts of many

members of the Young lab. Nick Stavropoulos's deep knowledge of circadian rhythms and every other area of biology was incredibly important in answering the often bizarre questions of a newcomer to the field. Sheyum Syed taught me the art of molecular cloning, and as a fellow physicist, listened sympathetically to my occasional frustrations with doing biology. Alina Patke taught me to do mammalian tissue culture work and tolerated my intrusions into her fume hood with aplomb. Deniz Top instructed me in biochemical techniques, in particular the delicate ways of Western blotting, and in his capacity as my baymate, stopped me from concentrating too hard with his near-infinite supply of Archer and Family Guy clips. Lastly I have to thank Lino Saez. Lino was involved in my education in every experimental technique mentioned in this thesis and many more. He came up with wild ideas, pointed me towards interesting papers, and asked incisive questions whenever I gave group meeting. When I printed the form to schedule my B exam, Lino was the first person I wanted to show it to. He will be sorely missed by everyone who knew him.

I have to thank my committee members, Jim Sethna and Rob Thorne, for many useful discussions, and Rob for the use of his lab space during the construction of my custom incubator. Many thanks are due to my advisor, Eric Siggia, without whom none of this would have happened. His patience in the face of many setbacks, his rigorous and serious approach to doing biology, and his intolerance for any form of fuzzy thinking were critical to the completion of this thesis. I have grown immeasurably as a scientist under his tutelage.

Finally I have to thank my parents. They did everything to make sure I received the best education possible, gave me the freedom to follow my own path, and supported my many years as an impoverished graduate student with grace. I would be nowhere without them.

## TABLE OF CONTENTS


Biographical Sketch . . . iii
Dedication . . . iv
Acknowledgements . . . v
Table of Contents . . . vii

**1 Introduction** **1**
1.1 Function, ecology, and evolution of the circadian clock . . . 2
1.2 Genetics of the circadian clock . . . 6
1.3 Biochemistry of the circadian clock . . . 12
1.4 Anatomy of the circadian clock . . . 19

**2 Theoretical Considerations** **23**
2.1 Coupled oscillator models . . . 23
2.2 Period and phase of circadian rhythms . . . 29
2.3 Modeling temperature compensation . . . 36
2.4 Noise and bifurcations . . . 42

**3 Experimental Considerations** **47**
3.1 *Drosophila* behavior experiments . . . 47
3.2 Fluorescent imaging and tissue culture . . . 51
3.3 Western blots . . . 58

**4 Interneuronal Coupling and the Phase Singularity** **63**
4.1 Phase-resetting and the phase singularity . . . 64
4.2 Phase singularity in individual *Drosophila* . . . 69
4.3 Inferring coupling from average rhythm data . . . 75

**5 Temperature Sensation and Temperature Compensation** **82**
5.1 Temperature-insensitive clocks? . . . 84
5.2 Circadian temperature sensation . . . 94

**6 Conclusion** **101**
6.1 Future directions . . . 102
6.2 Evolution of circadian clocks . . . 106

**Bibliography** **110**

CHAPTER 1

# INTRODUCTION

Daily biological rhythms are ubiquitous in nature. Sleep and activity in animals, flowering and leaf movement in plants, and even metabolic activity in microorganisms are timed according to the passage of the twenty-four hour day. These rhythms are controlled not only by external cues of light and temperature, but by independent biological oscillations know as *circadian clocks*. The first scientifically documented observation of an endogenous circadian rhythm was made by Jean Jacques d'Ortous de Mairan in 1729, who showed that the daily leaf opening rhythm of the *Mimosa* plant persisted even when the plant was isolated from the sun in a dark room [33]. Even after de Mairan's experiment, it was widely believed that biological rhythms were controlled by environmental cues (such as temperature), until the 1823 discovery of Augustus Pyramus de Candolle that, in conditions of constant light, the period of the leaf opening rhythm of *Mimosa* was only twenty-two hours [32].

This observation that the natural period of endogenous biological rhythms is generally close to, but not exactly, twenty-four hours, led to the 1950's coinage by Franz Halberg of the term *circadian*, from the Latin *circa diem*, meaning about a day [69]. It was also in the 1950's that the field of insect circadian rhythm research was founded by Colin Pittendrigh at Princeton. Pittendrigh's interest in biological rhythms stemmed from his wartime work on malaria control in Trinidad, where he observed the precise daily timing of mating behavior in mosquitos [152]. This led to his pioneering of *Drosophila* as a model system for circadian research, based upon the marked daily rhythm in eclosion of adult flies from pupae (see, for example, [150]). Pittendrigh's research laid the

groundwork for the 1972 discovery by Konopka and Benzer of the first gene in *Drosophila* to influence circadian behavior, and indeed the first gene shown to influence any form of animal behavior at all (see [197] for a fascinating account of the life and work of Seymour Benzer). Using a chemical mutagenesis screen, Konopka and Benzer discovered three mutations in the *Drosophila period* locus, $per^0$, which led to a total loss of the endogenous exclusion rhythm, and $per^S$ and $per^L$, which led to a shift in the normally 23.5 hour period to 19 and 29 hours, respectively [101]. It was this discovery that marked the beginning of the modern era of circadian rhythm research.

## 1.1 Function, ecology, and evolution of the circadian clock

Circadian rhythms are known to be present in all animals (with a few notable exceptions), plants, many fungi, and photosynthetic microorganisms. Recent research suggests that the circadian clock may also be present in many other single-celled organisms, including *Archaea* [46]. In all cases, circadian clocks are known to satisfy three defining properties (the textbook of Dunlap [44] provides a good overview). First, the circadian oscillation is self-sustaining in the absence of external stimuli, and has a period of about twenty-four hours. Second, the circadian clock can be entrained by external rhythms of light or temperature. Third, the period of the circadian oscillation is temperature-compensated, that is, it does not vary with temperature in constant conditions. As we will see in the coming sections, the basic structure that generates spontaneous circadian oscillations, as well as the mechanism of light sensation, is well understood. However, the biochemical properties that determine the twenty-four hour period and the mechanisms of temperature compensation and temperature sensa-

tion remain unknown (see [161] for a review).

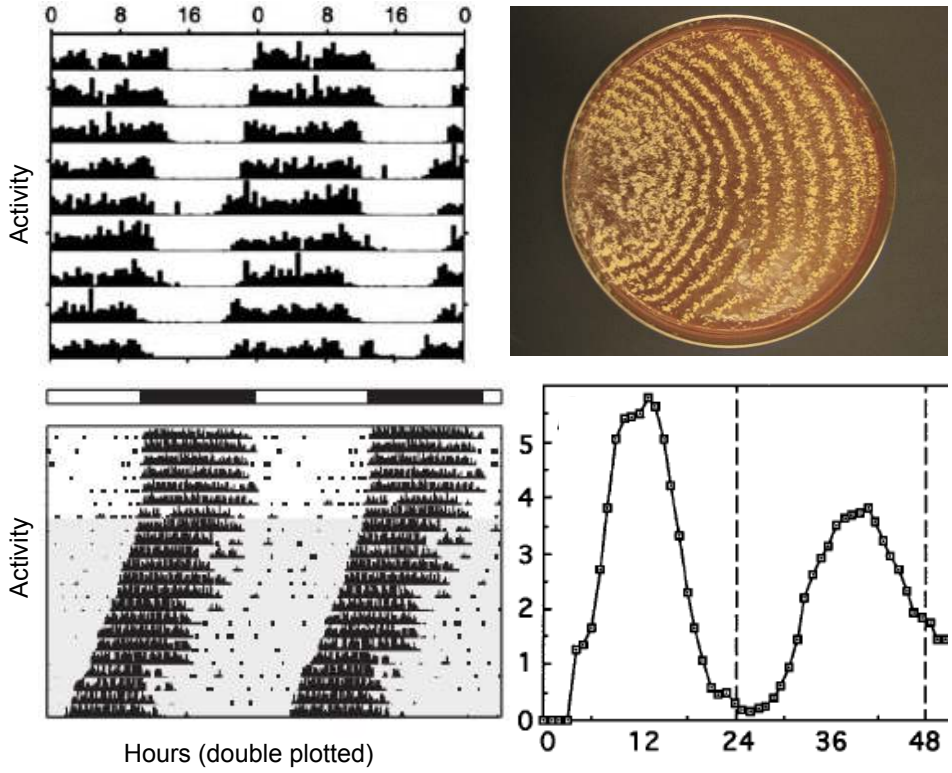


Figure 1.1: Measurable circadian outputs in various organisms. (Top left) *Drosophila* daily activity rhythms, as measured by crossing of a light beam in a linear tube. Crossings are counted in 30 minute bins and double-plotted, with the time axis marked in hours wrapped on in 24-hour intervals. From [38] (Top right) Rhythmic conidiation patterns in *Neurospora*. The white lines are conidium cells, which will release spores. From [170]. (Bottom right) Wheel running rhythms in mouse, showing the transition from a 24 hour rhythm under light entrainment, to the free-running period of about 23.5 hours. Plotted as in the top left. From [133]. (Bottom left) Relative luminescence over 48 hours from a cyanobacterial population transformed with firefly luciferase transcribed from the promoter for a rhythmically-expressed photosynthesis gene. From [119].

Though circadian biological rhythms have been observed in diverse organisms including sharks [204], nematodes [194], and the extremophile archaeon

*Halobacterium salinarum* [46], circadian rhythm research is primarily conducted in five model organisms: the fruit fly *Drosophila melanogaster*, the mouse *Mus musculus*, the bread mold *Neurospora crassa*, the cyanobacterium *Synechococcus elongatus*, and the model plant *Arabidopsis thaliana*. In *Drosophila* and mouse, circadian output is measured by observing activity rhythms, of wheel-running in the mouse [176], and of crossings of a light beam in the fly [158] (see Section 3.1 for more on fly circadian activity measurements). In *Neurospora*, circadian rhythms are marked by rhythmic conidiation (spore formation), producing regular patterns of white stripes on the growing fungus [13]. *Synechococcus* and *Arabidopsis* lack obvious external circadian markers, and their rhythms are generally observed using engineered luciferase reporters [100]. Figure 1.1 shows examples of some of these data.

The circadian clock has a diverse set of physiological functions. The phase of the clock regulates both the onset and duration of sleep in animals [210]. Mammals show circadian oscillations in body temperature [16] and in the levels of the hormones melatonin and cortisol [18]. Mice and *Drosophila* have been shown to have circadian rhythms of electrical activity in the brain, as well as regular circadian remodeling of synapses [87, 159]. In mice and humans, the circadian clock is expressed in the skin, where it has been shown to affect the differentiation of stem cells [20], and in the liver, where metabolic activity is regulated [11]. In fibroblasts, the timing of the cell cycle is strongly coupled to the circadian clock [136]. Circadian metabolic regulation leads to daily rhythms in the redox state of the key metabolites $NAD^+$/NADH [147]. The circadian clock is also expressed in the digestive tract [212] and ovaries [173] of *Drosophila*. In mice the circadian clock has been shown to regulate the differentiation of immune cells [42], and *Drosophila* with circadian disfunction are more susceptible

to infection [181].

Due to the critical regulatory functions of the clock, circadian disruption is associated with a wide array of medical problems. Familial advanced sleep phase syndrome (FASPS) [213] and delayed sleep phase disorder (DSPD) [5] have been shown to be associated with mutations in circadian genes. A variety of circadian-related medical problems are prevalent in shift workers (reviewed in [96]), in particular diabetes, obesity, and other metabolic syndromes [169]. Depression and bipolar disorder have been found in some cases to be related to circadian disfunction [126]. In mice, circadian defects have been shown to cause irritable bowel syndrome [4], and there is mounting evidence for a circadian component in other autoimmune diseases [103]. There is also a strong circadian bias in the occurrence of heart attacks [134].

The evolutionary importance of the circadian clock is clear from its varied medical and functional roles. Circadian defects have been shown directly to have strong fitness effects in *Drosophila* [104], as well as in cyanobacteria [211] and *Arabidopsis* [65]. However, firm explanations of the evolutionary origin of circadian rhythmicity remain elusive. As we will see in the next section, the significant differences in structure between eukaryotic and cyanobacterial clocks make it very likely that the circadian rhythm evolved independently at least twice. Additionally, though all eukaryotic clocks possess a common feedback loop structure (cf. [218] and the next section), and insect and mammalian clocks share a number of common components, there is very little sequence homology between the core proteins of the animal, fungal, and plant circadian oscillators. It is therefore unclear whether or not even eukaryotic clocks have a common evolutionary origin.

A number of theories have been proposed to explain the evolution of circadian oscillations. In cyanobacteria, light harvesting and nitrogen fixation reactions require different biochemical environments, and are heavily regulated by the circadian clock, leading to the proposal that a need for temporal regulation of metabolism drove the origin of the clock [190]. Another possibility is that the circadian clock originated as a means to prevent light-associated DNA damage [58]. The circadian clock is known to regulate the activity of DNA repair pathways [21], and some circadian genes bear sequence homology to genes involved in the DNA damage response [144]. The number of independent origins of the clock is also controversial. As we will see in the next section, prokaryotic and eukaryotic clocks are very different. Within the eukaryotes however, the presence of significant structural similarities combined with the lack of sequence homologies between kingdoms makes the question of evolutionary origins difficult to answer. In any case, as Theodosius Dobzhansky has famously observed, it is hopeless to understand the construction of biological mechanisms without reference to evolutionary processes [37]. As such, we will be returning to the question of evolutionary origins at opportune times throughout this thesis.

## 1.2 Genetics of the circadian clock

In the 40 years since the discovery of *period* by Konopka and Benzer, the genetic approach has led to the elucidation of the core structure of the *Drosophila* circadian oscillator in considerable detail. Figure 1.2 shows a diagram of the key components and their interactions. Similar work has also determined the structure of the clock in the mouse, *Neurospora*, *Synechococcus*, and to a somewhat lesser extent in *Arabidopsis* (see [219] for a comparative review). Figure

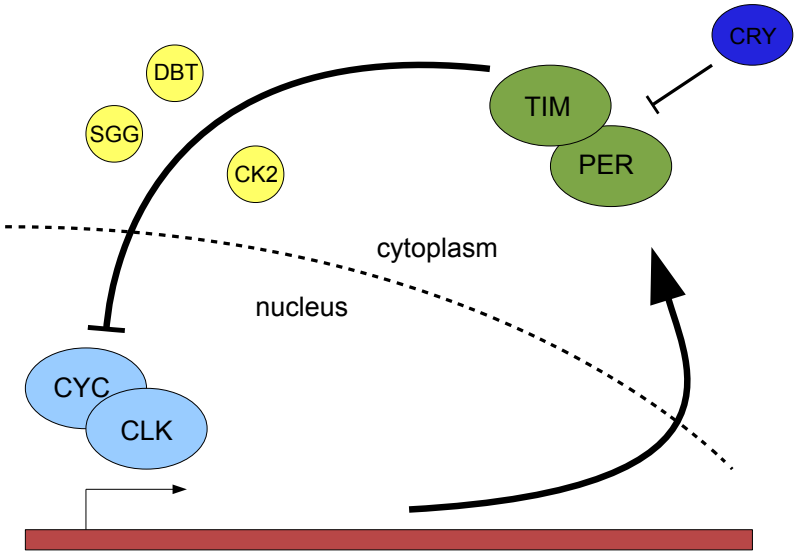


Figure 1.2: Diagram of the core components of the *Drosophila* circadian clock. The CLK:CYC transcription factor dimer activates production of the PER and TIM proteins, which dimerize and undergo a lengthy series of modifications in the cytoplasm, mediated by the kinases DBT, SGG, and CK2. These modifications lead to nuclear translocation of PER and TIM, where they repress the activity of the CLK:CYC dimer. Light resets the phase of the oscillation by activating the protein CRY, which leads to degradation of TIM.

1.3 shows the basic structures of the clock in *Drosophila*, mouse, *Neurospora*, and *Arabidopsis* side-by-side.

In Drosophila, the core of the circadian clock consists of four genes, whose corresponding proteins act as a pair of dimers. The CLOCK (CLK) and CYCLE (CYC) proteins dimerize to form a transcription factor which, in its active form, promotes the production of the PERIOD (PER) and TIMELESS (TIM) proteins [167]. PER and TIM form a dimer in the cytoplasm and, after undergoing a complicated series of biochemical modifications, translocate into the nucleus

and represses the activity of the CLK-CYC transcription factor ([31], and see [218] for an overview). It is this mechanism of delayed negative feedback that generates a self-sustained oscillation with a twenty-four hour period. The delay in nuclear translocation is generated by a series of interdependent chemical modifications of PER and TIM, affecting both stability of the proteins and their transport across the nuclear membrane (see [127] for a review). These modifications consist primarily of phosphorylation of serine and threonine residues by three key kinases: SHAGGY (SGG), a homolog of glycogen synthase kinase 3 [124], DOUBLETIME (DBT), a homolog of casein kinase 1 [157], and CASEIN KINASE 2 (CK2) [1]. The role of post-translational modifications in the clock will be discussed in more detail in the next section.

In *Drosophila*, CLK and CYC also promote production of two other transcription factors, VRILLE (VRI), and PAR DOMAIN PROTEIN 1 (PDP1) [28]. VRI acts to repress transcription of the *clk* gene, while PDP1 promotes *clk* transcription. The *vri*, *pdp1*, and *clk* transcription factors are all rhythmically transcribed with varying phases, and play a role in affecting downstream targets of the circadian clock. In particular, PDP1 is known to be required for normal activity rhythms [28]. Current research in circadian genetics is increasingly focused on downstream targets of the core clock, especially activity and sleep. A number of genes have been found that affect the quantity and quality of *Drosophila* sleep, including ion channels [19], regulators of protein degradation [180], and neurotransmitters [105]. Notably, none of these genes are involved in the function of the core circadian oscillation, and accumulating evidence suggests that the total quantity of activity and sleep (rather than the timing) is primarily regulated by homeostatic mechanisms, not by the core clock (see [154] for a recent review).

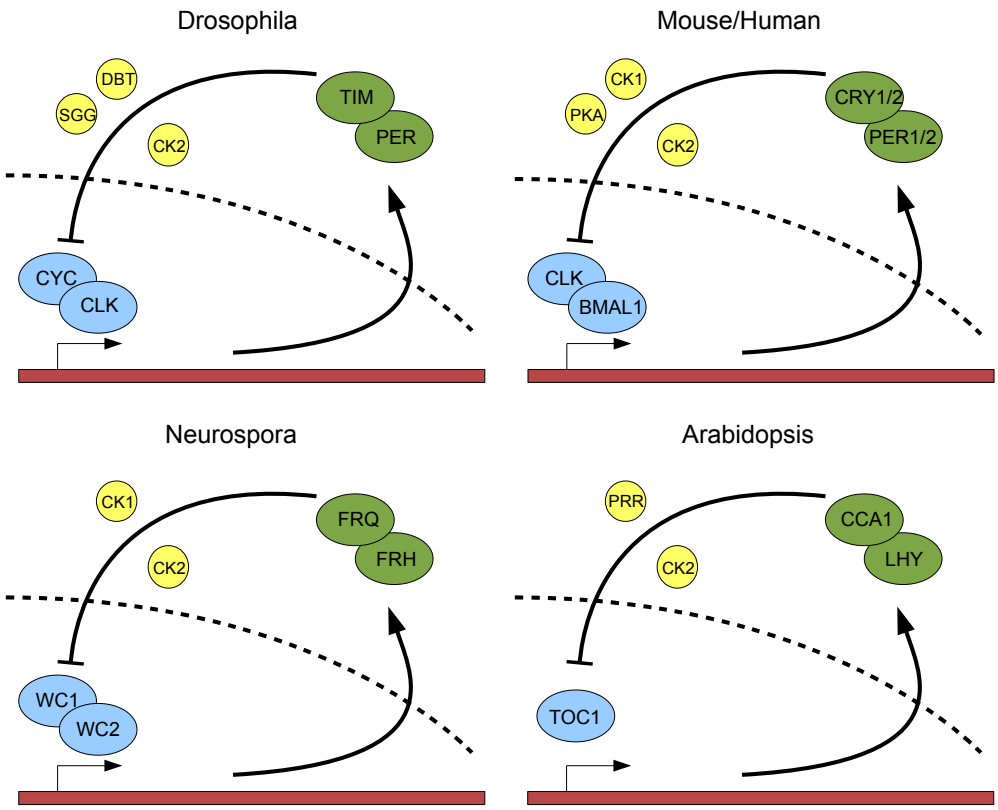


Figure 1.3: Remarkable conservation of the core structure of the circadian clock in *Drosophila*, *Neurspora*, mouse, and *Arabidopsis*. Transcription factors are shown in blue, negative regulators in green, and kinases in yellow. Homologous proteins across kingdoms have the same names, while differently named proteins serving similar roles generally lack any sequence homology.

As mentioned in the previous section, the double-dimer negative feedback loop structure of the *Drosophila* circadian clock is conserved in other eukaryotes. The basic structures of the circadian clocks in *Drosophila*, mouse, *Neurospora*, and *Arabidopsis* are shown together in Figure 1.3. Mammals possess three copies of the *period* gene, the first two of which are known to produce proteins which form a circadian complex that represses a transcription factor dimer made up of homologs of *clock* and *cycle*, known in mammals as *clock* and *bmal1* [97].

Though mammals posses a homolog of *Drosophila timeless*, its role in the circadian rhythm, if any, is unknown [63]. Instead, the mammalian PER proteins bind a pair of *cryptochrome* homologs, CRY1 and CRY2 [142]. This complex undergoes phosphorylation by mammalian CK1 and CK2, as well another kinase, PROTEIN KINASE A (PKA), followed by nuclear translocation and repression, in a process very similar to that of *Drosophila* [110]. The significant degree of sequence homology between animal circadian clocks makes it clear that they have a common evolutionary origin. *Neurospora*, however, is not known to have homologs of any of the core mammal or insect circadian genes. Nonetheless, the fungal circadian clock functions in a very similar manner. The master regulator FREQUENCY (FRQ) binds to the FRQ-interacting RNA helicase FRH, is modified by casein kinases 1 and 2, and translocates into the nucleus [55]. There, it represses the activity of a transcription factor dimer formed by WHITE COLLAR 1 and 2 (WC-1 and WC-2), which itself promotes transcription of FRQ [43]. Less is known about the makeup of the *Arabidopsis* circadian clock due to the difficulties of genetic screening in plants. However, it is known that *Arabidopsis* possesses a rhythmically expressed transcription factor *timing of cab expression 1* (TOC1), which produces and is repressed by a pair of proteins CIRCADIAN AND CLOCK ASSOCIATED1 (CCA1) and LATE ELONGATED HYPOCOTYL (LHY) [100]. CCA1 and LHY are also known to be modified by CK2, as well as a family of kinases known as pseudo-response regulators (PRRs) [70]. It is interesting that many of the same kinases participate in the circadian clocks of different eukaryotic kingdoms, particularly the casein kinases. However, these kinases are master regulators of numerous pathways, so their involvement in the circadian clock does not constitute strong evidence for a common evolutionary origin.

The circadian clock in cyanobacteria is quite different. In *Synechococcus*, the circadian rhythm involves only three proteins, KaiA, KaiB, and KaiC, and does not involve transcriptional feedback, in fact, it can proceed even when transcription and translation have been temporarily inhibited [186]. The cyanobacterial circadian oscillation can be reconstituted in vitro using only the purified Kai proteins and ATP [137]. This has allowed the biochemical functioning of cyanobacterial clock to be worked out in considerably more detail than that of eukaryotic clocks (see [123] for a review). The KaiC protein forms a hexameric enzyme, which is able to phosphorylate and dephosphorylate itself on two different sites on each of its six subunits [138]. In isolation, only the dephorylation (phosphatase) activity of KaiC occurs at an appreciable rate, but binding by KaiA promotes phosphorylation (kinase) activity [166]. Phosphorylation events lead to conformational changes in the KaiA/C complex that allow binding of KaiB, which inhibits the effects of the KaiA protein, leading to dephosphorylation of KaiC [138, 166]. The period of the cyanobacterial circadian oscillation appears to be set purely by the rate of phosphorylation and dephosphorylation of KaiC [184], and is temperature compensated, even in the purified in vitro oscillator [135]. Crucially, the in vitro oscillation is also entrainable by temperature cycles [217]. Though the cyanobacterial clock is quite unlike that of eukaryotes, understanding its structure has provided important insights. In particular, mathematical models of the cyanobacterial oscillator [30, 195] have suggested that a network of reversible phosphorylation events, like that present in both prokaryotic and eukaryotic clocks, could be crucial for allowing temperature compensation of individual period-determining reactions.

## 1.3 Biochemistry of the circadian clock

Biochemical research into circadian clocks has two main goals, aside from the mere enumeration of relevant reactions: first, to understand the mechanism which sets the highly unusual (for a biological regulatory network) twenty-four hour timescale of the circadian oscillation, and second, to explain the mechanism of temperature compensation. Clearly, these goals are closely related, since explaining the details of temperature compensation requires knowing the set of biochemical processes that need to be compensated (see Chapter 5 for more perspective on this). However, knowledge of the biochemical mechanisms of the clock remains fragmentary. The story of how the 24-hour period is set is not even tentatively complete, and at best there is partial knowledge of how some sub-reactions are regulated. We will lay out some of this knowledge here in order to give the reader a feel for the state of the field, and to provide context for our later investigations into temperature compensation. Further details can be found in a recent review [27].

The key processes of the circadian clock in *Drosophila* can be broken down as follows: transcription of *per* and *tim* and translation of the PER and TIM proteins, dimerization and nuclear translocation of PER and TIM, and finally repression of CLK and CYC and nuclear export/degradation of PER and TIM. Experiments in *Drosophila* cell culture have shown that PER and TIM dimerization occurs rapidly, but nuclear translocation takes roughly 6-8 hours [130]. It is also clear from a variety of time course measurements (see, for example [178]) that the delay between transcription of the *per* and *tim* genes and appearance of PER and TIM protein is unusually long, on the order of 4-5 hours. This is in contrast to, for example, the heat shock response, where transcrip-

tion and translation of new protein can occur in a matter of minutes [145, 164]. These processes can explain, at most, about half of the 24-hour circadian period, meaning that the process of nuclear degradation and export of PER and TIM must also require time on the order of hours, and in particular that, unlike in the cyanobacterial clock, no one rate-limiting reaction determines the period in eukaryotic circadian clocks.

Nuclear translocation of PER and TIM has been extensively studied by exogenous expression in cultured Drosophila S2 cells, which do not natively express the circadian clock [130]. It is largely due to this fact (and the lack of good in vitro systems for examining other aspects of the circadian oscillation) that nuclear translocation is biochemically the best understood of the period-determining processes mentioned above. As such, we will focus on describing the biochemistry of nuclear translocation in an effort to give a flavor for the workings of circadian post-translational regulation, and leave other aspects of clock regulation as an exercise in further reading (see [113] and [127] for more complete reviews).

The biochemistry of nuclear translocation, though it has been extensively studied, is not completely understood. However, by considering a variety of experimental results, we can begin to get a general picture. The process of nuclear translocation of PER and TIM involves a delicate balance between transport and degradation. Both PER and TIM are subject to daily rhythms of phosphorylation [45, 124]. Phosphorylation by the DBT kinase has been shown to destabilize PER protein [157] by targeting it for ubiquitinylation and degradation by the ubiquitin-targeted proteasome [99]. However, the role of DBT is not so straightforward. Two different mutations, $dbt^S$ and $dbt^L$, affect the clock by shortening

and lengthening the period, respectively [155]. Indeed, it has also been shown that phosphorylation by DBT can affect nuclear transport of PER [9, 29], and that DBT phosphorylation is required for subsequent phosphorylation by other kinases [93]. Additionally, there is evidence that DBT also translocates into the nucleus, possibly as part of a complex with PER and TIM, where it represses *per* and *tim* transcription by phosphorylating CLK [94]. As we can see, the role of DBT in setting the period of the clock is multifarious, and thus far, defies straightforward explanations. The role of CK2 appears to be more clear. Loss of CK2 activity leads to lengthening of the period [115], and phosphorylation of PER by CK2 promotes transport into the nucleus [1, 177]. Post-translational regulation of TIM has been relatively less explored to date, but it has been shown that the kinase SGG phosphorylates TIM, and that this promotes nuclear transport of the PER:TIM complex [124].

It is worth examining the regulation of PER phosphorylation in more detail. Even though a complete picture does not yet exist, much has been learned about the basic logical scheme of PER regulation. One method for discovering physiologically relevant phosphorylation sites on a protein involves developing a list of candidate sites, either by in vitro phosphorylation followed by mass spectrometry [57], or by computational prediction [189], and then testing each site by inserting a mutated construct into a *Drosophila* strain lacking the native wild-type protein. Phosphorylation occurs on serine or threonine residues, so predicted phosphorylation sites are generally mutated to either alanine (a simple amino acid lacking a large functional group) to mimic lack of phosphorylation, or aspartate (an amino acid with a phosphate as functional group) to mimic permanent phosphorylation. One pioneering study in this vein [56] found that blocking phosphorylation by mutating threonine 610 and serine 613 to alanine

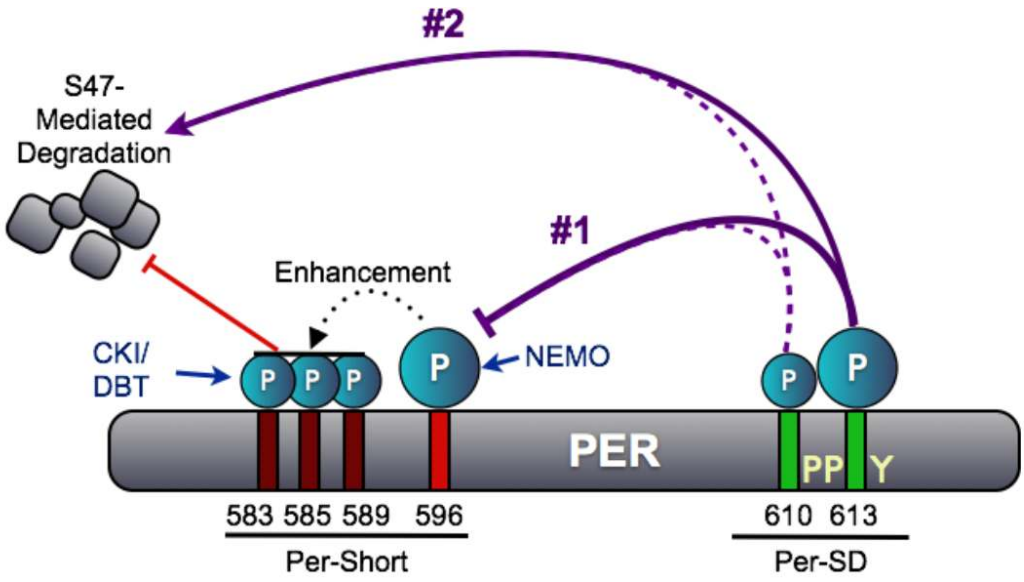


Figure 1.4: Variable and cooperative effects of PER phosphorylation. Phosphorylation of the Per-SD sites T610 and S613 by DBT leads to PER degradation either by promoting phosphorylation of S47 (#2), also by DBT, or by inhibiting phosphorylation at S596 by NEMO (#1). S596 phosphorylation promotes DBT phosphorylation at the Per-Short sites, T583, S585, and S589, which act to prevent S47-mediated degradation. From [56].

(T610A and S613A, respectively) lengthened the period and increased PER concentrations throughout the day. T610A alone has a near wild-type period, while S613A has a long period, but not as long as the double mutant, suggesting that the effects of the two mutations are cooperative. The T610A and S613A mutations also fail to lengthen the period in the presence of alanine mutations at known phosphorylation sites at T583, S585, S589, and S596. DBT is known to phosphorylate T583, S585, and S589, inhibiting DBT phosphorylation at S47 [22], which is known to lead directly to ubiquitin-mediated degradation [99]. Interestingly, the original $per^S$ mutation is a point mutation at S589, preventing phosphorylation at that site [12]. Phosphorylation at S596 by the NEMO kinase promotes phosphorylation at the so-called per-short sites at T583, S585,

and S589 [23]. Notably, all of these phenotypes are affected by the activity of a principle dephosphorylation enzyme, protein phosphatase 2 (PP2) [56, 94], which is known to be modulated in a circadian manner [168]. In sum, PER is regulated by a network of reversible phosphorylation events, which can influence each other and which have multifarious effects on both protein stability and localization.

Clearly, the regulatory logic of phosphorylation of *Drosophila* PER is quite complicated, and we are far from full understanding. However, it is intriguing that both the prokaryotic and eukaryotic circadian clocks, though different in many respects, both rely on period-determining processes that are regulated by a network of interdependent reversible phosphorylations. We have previously noted, and will discuss further in the next chapter, the fact that these types of reactions are easily designed to produce overall rates that are temperature compensated. Indeed, one of the goals of understanding the biochemistry of the circadian clock is to understand the microscopic mechanisms of temperature compensation. As we will see in subsequent chapters, our incomplete knowledge of circadian biochemistry requires a different, non-microscopic, approach to understanding temperature compensation. It is nonetheless worthwhile to review the existing experimental results on temperature compensation.

Most experimental work on the biochemistry of temperature compensation has focused on processes associated with nuclear translocation. An experiment that altered gene dosages in *Neurospora* has shown that the activity of CK2 has a strong influence on the period of the circadian rhythm [128]. Additionally, increasing CK2 levels several-fold by gene duplication leads to a decreasing period at higher temperature, while decreasing CK2 levels leads to an increasing

period at higher temperature. Crucially, these experiments altered only concentrations of a single enzyme, not biochemical rate constants. Another experiment in mammalian cell culture used a chemical screen to identify CK1 as a key period-determining enzyme [86]. Knockdown of CK1 leads to a loss of temperature compensation, and most interestingly, the phosphorylation rate of CK1 was independently temperature compensated in an in vitro assay. It should be pointed out however, that the substrate in this assay was an artificial peptide, not a physiologically relevant CK1 target, making the in vivo implications of the experiment unclear at best. In *Arabidopsis*, it has been shown that temperature-dependent changes in concentration of CK2 and CCA1 are required for temperature compensation [153]. In *Drosophila*, the equilibrium level of PER/TIM binding is temperature compensated [83], but no direct experiments on kinase effects have been performed, aside from a variety of mutations in both kinases and PER and TIM, which have temperature compensation phenotypes (see [81] for a good overview). It is also important to note that, in spite of the variety of interesting results suggesting the importance of kinase/phosphatase balancing in compensating nuclear transport, no experiment in any organism has demonstrated that nuclear translocation as a whole is temperature compensated.

A key puzzle for any general theory of temperature compensation is explaining the ready entrainment of circadian clocks to external oscillations in temperature. Enzymes whose rates are essentially insensitive to temperature are not unheard of in nature (see [72] for a review). There are even examples of biological oscillations that are insensitive to temperature, including microbial metabolic oscillations [8, 120] and, amusingly, the bouncing of the so-called Mexican jumping bean [73]. However, the circadian clock is not temperature insensitive. This has led to two proposals. Under one theory, various subprocesses of the clock

are temperature sensitive, and compensation of the period occurs by an overall cancelation, so that no particular signaling pathway for temperature is needed (see [71] for one advocate of this view). This approach overwhelming dominates the modeling literature on temperature compensation (see [107] for a review), which we discuss further in subsequent chapters. Another theory (advocated in [53]) suggests that the core circadian clock is temperature insensitive, and that a specific signaling pathway for temperature is present. In order to preserve temperature compensation, this pathway must either be adaptive (so that it is only activated while temperature is changing), or must couple to the clock in a way that does not affect the period.

A number of experiments have found specific neural pathways for communicating temperature to the circadian clock. One line of work has shown that mutations in the genes $norp^A$ [61] and *nocte* [171] affect temperature entrainment. These genes are involved in the development and functioning of *Drosophila* chordotonal organs, which are responsible for touch and temperature sensation. Additionally, temperature-sensitive TrpA ion channels have been shown to affect circadian temperature entrainment [111], and are also implicated in other aspects of temperature sensation, both in *Drosophila* and other organisms [24]. Neural mechanisms represent an appealing solution to the problems posed above, because adaptation to constant inputs is a ubiquitous phenomenon in neural signaling pathways [34]. Another possible solution comes from transcriptional signaling. The period of the circadian oscillation in mammalian tissue culture has been shown to be compensated against large changes in overall transcription rates by the use of the transcriptional inhibitor $\alpha$-amanitin [35]. A similar result was obtained in *Drosophila* by generating transgenic animals with multiple copies of the *per* gene [25]. One strong candidate for tran-

scriptional coupling of the circadian oscillation to temperature is the heat shock pathway, which has been shown to be required for normal temperature resetting in the circadian clocks of isolated mouse cells [17, 182]. A more in depth discussion of these matters can be found in Chapter 5.

## 1.4 Anatomy of the circadian clock

The biochemical circadian oscillator is cell autonomous and able to function in single cultured animal cells as well as in unicellular organisms. However, the physiological functioning of the circadian rhythm in animals relies on a complex network of clocks expressed in different tissues. Many of the regulatory functions of the circadian clock are fulfilled by cells expressing the oscillation in peripheral tissues (see for example, [11, 212, 173]). However, these peripheral clocks tick under the control of a central pacemaker in the brain. In mice, the circadian clock is located in the suprachiasmatic nucleus (SCN), an approximately 20,000 neuron cluster inside the hypothalamus (see [200] for a review). In *Drosophila*, the circadian clock is present in about 200 neurons, but a variety of experiments have shown that the master pacemaker is contained in a small cluster of about ten neurons on each side of the brain (reviewed in [140]).

Figure 1.5 shows a fluorescence microscope image of a *Drosophila* brain expressing a fluorescent marker under the control of the *tim* promoter. The circadian neurons in *Drosophila* can be divided into two main groups, each consisting of three smaller clusters. The lateral neurons (LN) on either side of the brain are made up of about 5 small ventral lateral neurons (s-$LN_v$), 4-6 large ventral lateral neurons (l-$LN_v$), and 5-8 dorsal lateral neurons ($LN_d$). The dorsal neurons (DN)

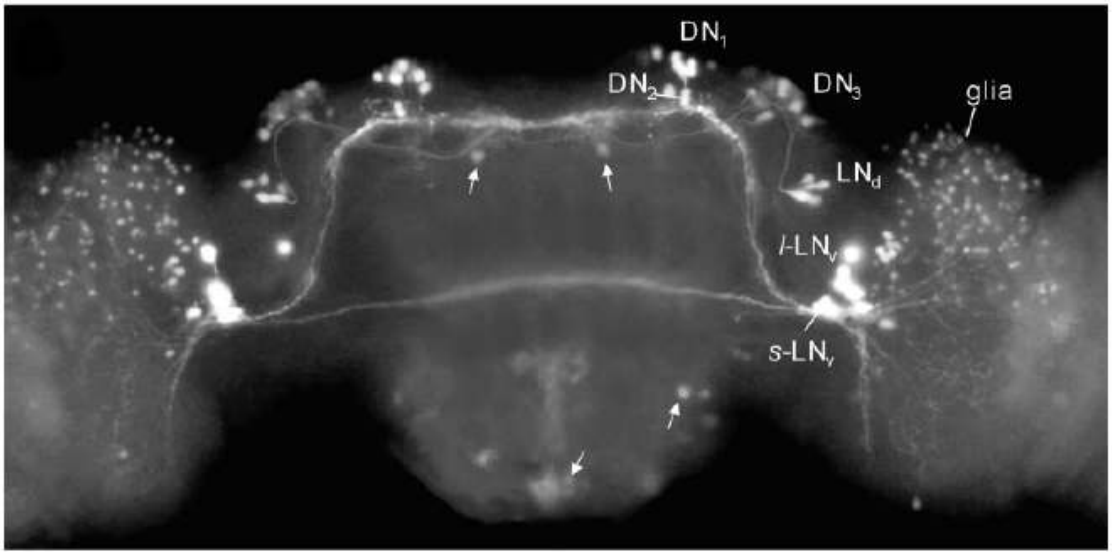


Figure 1.5: Fluorescence microscope image of a *Drosophila* brain expressing a fluorescent marker under the control of the *tim* promoter, with the major groups of circadian neurons marked. Arrows indicate cells with spurious ectopic expression. From [77].

consist of about 15 $DN_1$, 2 $DN_2$, and about 40 $DN_3$. Broadly speaking, the LN make up the master circadian pacemaker, and the DN are a downstream population involved in coordinating various outputs. The dorsal projection from the LN is responsible for mediating communication with the DN. The DN are themselves coupled to the *pars intercerebralis*, a region at the top of the brain responsible in part for hormonal signaling [75], and the mushroom bodies, dorsal brain regions implicated in the regulation of sleep [39]. The central projection connects the LN to the central body, which is known to be involved in controlling motor function (see [75] for an overview of *Drosophila* brain anatomy).

The DN are not required for normal circadian rhythmicity [54], though activity rhythms in flies lacking the DN do show increased noise [76]. In constant darkness the circadian rhythm in the $DN_1$ is damped [95]. Weakened rhythmic behavior is observed in flies expressing the circadian clock in only the s-$LN_v$

[162], or in only a single LN combined with the DN [74]. The l-$LN_v$ appear to play a role in coupling the s-$LN_v$ and $LN_d$. The LN express the neurotransmitter *pigment dispersing factor* (PDF), which couples them to each other and to the DN. *Drosophila* lacking PDF show largely normal behavior in light-dark cycles but quickly become arrhythmic in constant conditions [116]. A similar phenotype is observed after electrical silencing of the LN by ectopic expression of a persistently open $K^+$ channel, suggesting that electrical communication is involved in the PDF pathway [139]. Both LN and DN express cryptochrome and are involved in light entrainment [48], however, experiments with competing out-of-phase light and temperature cycles suggest that the LN are primarily responsible for light sensation, while the DN are more temperature-sensitive [132]. Ectopic expression of *per* and *cry* in null mutants has indicated that the presence of CRY may actually inhibit temperature sensation [60], and the $DN_2$ in particular do not express *cry* [149].

Detailed anatomical knowledge of the fruit fly circadian system has relied on the rich set of genetic tools available in *Drosophila*, and less is known about the anatomy of the clock in mouse. However, studies of the mechanics of intracellular coupling in the mouse have been greatly aided by the possibility of culturing and imaging individual live neurons as well as intact SCN slices. The SCN contains a structured population of cells, with different subgroups communicating via different characteristic neurotransmitters [91]. Additionally, the phase of the molecular circadian oscillation varies continuously from dorsal to ventral within the SCN [79]. Electrical coupling is also important in the mammalian clock, and application of the sodium channel inhibitor TTX rapidly abolishes collective rhythmicity in SCN explants, but does not eliminate individual cellular oscillations [199]. The average period of neurons in the SCN closely

matches the behavioral period of the animal from which the explant was taken [118]. However, dissociated neurons from the SCN show much greater variance in period than neurons in an intact slice [80]. Additionally, the amplitude of circadian oscillation in individual cells is considerably reduced when intercellular coupling is eliminated, either by dissociation [6] or application of TTX [215]. In fact, some single cell imaging experiments have suggested that the circadian oscillation in dissociated neurons is a noise-induced resonance phenomenon, rather than a true stable limit cycle [196].

CHAPTER 2

# THEORETICAL CONSIDERATIONS

The circadian clock is a prime example of a biological pathway possessing both major regulatory significance as well as rich and complex dynamical properties. As such, it has been a popular subject for mathematical modeling from the very beginning of circadian biological research (see, for example, [146], as well as [112] for a review). Indeed, a lack of genetic or molecular tools for studying circadian rhythms meant that much early circadian research was phenomenological in nature, and relied heavily on mathematical models for interpretation of data (a variety of examples can be found in the proceedings of the seminal 1960 Cold Spring Harbor symposium [151]). The basis of many of these early mathematical models was the analysis of systems of coupled oscillators, and in fact, the first model demonstrating spontaneous synchronization of nonlinear oscillators was introduced in the 1967 Cornell undergraduate thesis [205] of the circadian biologist and mathematician Art Winfree, whose work we discuss in more detail in Chapter 4.

## 2.1 Coupled oscillator models

Winfree's 1967 proof involved qualitative arguments based on general topological properties of limit cycles. Later work on coupled oscillator populations has tended to rely instead on concrete but simple models derived from generic normal form equations (see the textbook of Kuramoto [106]). Following this practice, we begin by considering a model of two oscillators, each with dynamics described by the normal form of the Hopf bifurcation, and with an attractive coupling proportional to the linear distance between the two oscillators in the

plane. In Cartesian coordinates, the equations describing the position $(x_1, y_1)$ of the first oscillator are as follows

$$\dot{x}_1 = -\rho A x_1 - \omega y_1 - \rho x_1(x_1^2 + y_1^2) + \frac{K}{2}(x_2 - x_1) \tag{2.1}$$

$$\dot{y}_1 = -\rho A y_1 + \omega x_1 - \rho y_1(x_2^2 + y_2^2) + \frac{K}{2}(y_2 - y_1) \tag{2.2}$$

where $\omega_1$ is the frequency of the first oscillator, $\rho$ is the rate of relaxation towards the limit cycle, $A$ is the amplitude of the limit cycle, and $K$ is the strength of coupling between the oscillators. The equation for the second oscillator is identical except with the subscripts exchanged. The solutions to these equations can be found most easily by changing to polar coordinates and considering the distance between the two oscillators, so that the equations for the radial and phase differences, $r_1 - r_2$ and $\Delta\phi = \phi_1 - \phi_2$, are given by

$$\dot{r}_1 - \dot{r}_2 = \rho\left[(r_1 - r_2)A^2 + r_2^3 - r_1^3\right] + \frac{K}{2}(r_2 - r_1)(\cos(\phi_2 - \phi_1) + 1) \tag{2.3}$$

$$\Delta\dot{\phi} = (\omega_1 - \omega_2) - \frac{K}{2}\left(\frac{r_2}{r_1} + \frac{r_1}{r_2}\right)\sin(\phi_1 - \phi_2) \tag{2.4}$$

It is important to note that the $\Delta\phi$ equation can only have a stable fixed point if $|\Delta\phi| < \pi/2$. This can be seen by first assuming that $\omega_1 > \omega_2$, and noting that $\sin\Delta\phi > 0$ at the fixed point and $d\sin\Delta\phi/d\Delta\phi$ must be positive for stability of the fixed point. The radial difference equation has a stable equilibrium at $r_1 = r_2$ as long as the $r_i$ are not too much smaller than $A$. A situation where the $r_i << A$ can arise in cases when the coupling is very strong and the frequency difference is large, but this is not relevant for our purposes (see below for more on this). If $r_1 = r_2$ and the frequency difference $\Delta\omega = \omega_1 - \omega_2$ is smaller than the coupling strength $K$, then Eq. 2.4 will have a stable fixed point given by

$$\Delta\phi = \sin^{-1}\frac{\Delta\omega}{K} \tag{2.5}$$

From this one can see that for sufficiently strong coupling, the two oscillators will maintain a constant phase relationship, known as *phase locking*, and that the oscillators will be separated by a phase difference that grows with the difference in their native frequencies. If the frequency difference and resulting phase lag are large, then the coupling can pull the oscillators away from their native limit cycles, and a phenomenon known as "amplitude death" can result, in which the only stable equilibrium occurs when $r_1 = r_2 = 0$ . This can be seen by considering the equation for $\dot{r}_1 + \dot{r}_2$

$$\dot{r}_1 + \dot{r}_2 = \rho\left[(r_1 + r_2)A^2 - r_1^3 - r_2^3\right] + \frac{K}{2}\left[(r_1 + r_2)\cos\Delta\phi - (r_1 + r_2)\right] \tag{2.6}$$

where if $\cos\Delta\phi$ is small and $K$ is very large, the only solution will be $r_1 = r_2 = 0$ because the first term is bounded form above. However, as long as $\Delta\omega$ and $\Delta\phi$ are not too large, coupled oscillators in the strong coupling regime can be safely treated as a single oscillator with positive amplitude. In general, since circadian clocks can be safely assumed to be in a regime where their constituent oscillators are phase-locked and oscillating with positive amplitude, we will restrict ourselves to this case in our analyses (note that this is not the same as assuming coupling is strong, since phase-locking can occur at weak coupling if $\Delta\omega$ is small). Further analysis of the strong coupling dynamics of coupled oscillator populations can be found in [131].

In Chapter 4, we will analyze the results of an experiment in which a precisely tuned pulse of light is used to disrupt the *Drosophila* circadian clock such

that the concentration of constituent proteins positions the state of the clock near the unstable fixed point at the center of its native limit cycle. A slow recovery of the clock back to the limit cycle could then be modeled in two ways: as the result of weak coupling between individual neuronal oscillators (i.e. small $K$), or as the result of slow relaxation of individual oscillators back to their individual limit cycles (i.e. small $\rho$). In the first case, we can consider the relaxation dynamics of Equation 2.3, which can be reduced to the following form

$$\Delta\dot{\phi} = -K\Delta\phi => \Delta\phi(t) = \Delta\phi_0 e^{-Kt} \tag{2.7}$$

where we have assumed $\omega_1 = \omega_2$ for the sake of simplicity. The prediction is therefore that amplitude will rapidly recover to an intermediate value (set by the initial phase difference $\Delta\phi_0$), followed by a long exponential decay to the native value. In the second case, since $K$ is large, we can assume that the oscillators synchronize rapidly, and, again assuming that $\omega_1 = \omega_2$, the system can simply be modeled as a single oscillator by the equation

$$\dot{r} = \rho r(A^2 - r^2) \Rightarrow r(t) = \left[\frac{1}{A^2} + \left(\frac{1}{r_0^2} + \frac{1}{A^2}\right)\exp(-2A^2\rho t)\right]^{-1/2} \tag{2.8}$$

In this case, the recovery of amplitude will feature a rapid initial phase due to resynchronization, followed by slow sigmoidal relaxation to the native value. Figure 2.1 shows a simulation of these two possibilities for a system of ten coupled oscillators. Of course, a mixture of the two scenarios is also possible, and in principle it can be difficult to disentangle the effects of weak coupling and slow relaxation. These issues are addressed in more detail in Chapter 4.

We will now turn to an analysis of populations of $N$ coupled oscillators in

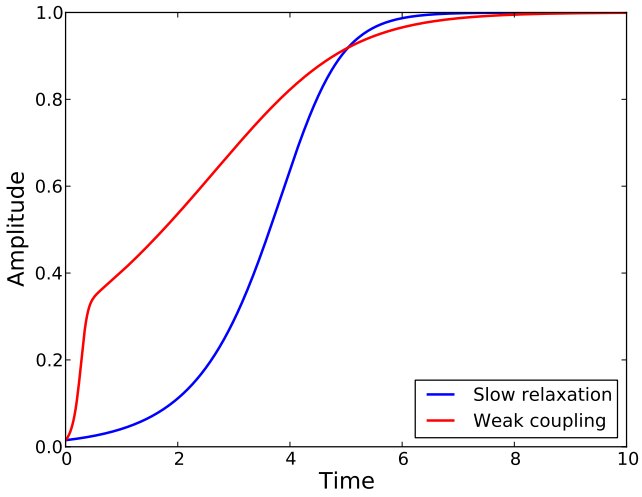


Figure 2.1: Recovery of overall amplitude in two simulations of ten coupled oscillators initialized near the phase singularity. One simulation (blue curve) features strong coupling between oscillators but weak relaxation of individuals to their native limit cycle. The other (red curve) features strong relaxation but weak coupling.

the thermodynamic limit $N \to \infty$. We will use the mean field approximation in which all oscillators are globally coupled. It is worth noting that this is likely not the case for most circadian oscillator populations, but we lack sufficient anatomical information to justify any other assumption. Additionally, it is likely that most clocks are governed by a "central pacemaker" cell population which is globally coupled within itself. Following the work of Kuramoto [106], we assume that the coupling between the oscillators is weak, so that we can analyze the dynamics purely in terms of a phase equation of the form

$$\dot{\phi}_i = \omega_i + \frac{K}{N} \sum_{j=1}^{N} \sin(\phi_j - \phi_i) \tag{2.9}$$

By considering an order parameter $\Phi = \frac{1}{N} \sum_j e^{i\phi_j} = Re^{i\theta}$, we can recast the equa-

tions in the form

$$\dot{\phi}_i = \omega_i + KR\sin(\theta - \phi_i) \tag{2.10}$$

We would like to see if it is possible to find a solution of these equations in which the average phase $\theta$ rotates with a constant frequency, $\dot{\theta} = \bar{\omega}$, and each individual oscillator has a fixed phase relationship to the average, so that $\Delta\phi_i = \theta - \phi_i$ is a constant in time. If we assume for the sake of argument that $\dot{\theta}$ is constant in time, then the above equation can be rewritten in terms of the phase differences $\Delta\phi_i$ and frequency differences $\Delta\omega_i = \bar{\omega} - \omega_i$

$$\frac{\mathrm{d}}{\mathrm{d}t}\Delta\dot{\phi}_i = \Delta\omega_i + KR\sin(\Delta\phi_i) \tag{2.11}$$

Much like the two oscillator case, this equation will have a solution as long as $\Delta\omega_i$ is not too large compared to $KR$. However, we do not yet know the value of $R$, and in general, it could be the case that some oscillators are part of a phase-locked population while others are not. The exact threshold for partial synchronization ($R > 0$ at long times) can be derived by writing down a self-consistent equation for $R$ that must hold if a phase-locked population is present. We first pass to the continuum limit, and describe the oscillator population in terms of a continuous frequency distribution $g(\omega)$, which we will assume is symmetric about some average $\bar{\omega}$. Keeping in mind our previous assumption that $\dot{\theta}$ is constant in time for the phase-locked population, we can use a rotating coordinate frame in which both $\theta$ and $\bar{\omega}$ are zero. In this case, Eq. 2.11 gives the relation $\omega/KR = \sin\phi$ for oscillators in the phase-locked state. This leads to the following formula for $R$ in terms of an integral over frequencies $\omega$

$$R^2 = \left( \int_{-\infty}^{\infty} \cos(\sin^{-1}(\omega/KR)) g(\omega) \mathrm{d}\omega \right)^2 + \left( \int_{-\infty}^{\infty} \frac{\omega}{KR} g(\omega) \mathrm{d}\omega \right)^2 \tag{2.12}$$

The second term is zero due to the symmetry of $g(\omega)$. We rewrite the first term by changing variables from $\omega$ to $\phi$ and replacing $\mathrm{d}\omega$ with $KR\cos\phi \mathrm{d}\phi$, obtaining

$$R = KR \int_{-\pi}^{\pi} \cos^2\phi g(KR\sin\phi) \mathrm{d}\phi \tag{2.13}$$

This equation has the trivial solution $R = 0$, corresponding to totally incoherent oscillations, but also has a branch of non-zero solutions which satisfy the equation

$$1 = K \int_{-\pi}^{\pi} \cos^2\phi g(KR\sin\theta) d\phi \tag{2.14}$$

The critical value of the minimal coupling for synchronization is found by setting $R = 0$ and integrating, giving $K = 2/(\pi g(0))$. This threshold criterion will hold for any symmetric distribution $g$, and specific values values have been found for a variety of examples, including uniform, Gaussian, and Lorentzian distributions. Details of these calculations, as well as wealth of information on the dynamical phase diagram of coupled oscillator models, can be found in [125].

## 2.2 Period and phase of circadian rhythms

Almost any circadian rhythm experiment depends upon methods for classifying activity data as rhythmic or not, and for quantifying the period and phase of

rhythmic time series. A variety of methods exist in the field for performing these analyses, the most commonly used is the chi-square periodogram [50]. To compute a chi-square periodogram for a time series with point $\{x_i\}$, one first chooses a candidate period $\tau$. A list $\{y_i\}$ of length $\tau$ is generated by summing points in $\{x_i\}$ that are separated by $\tau$, so that $y_0 = x_0 + x_\tau + x_{2\tau} + ...$, $y_1 = x_1 + x_{1+\tau} + x_{1+2\tau} + ...$ and so on. One then computes the variance of the list $\{y_i\}$ and the process is repeated for different periods $\tau$ covering some range of interest. The resulting variance values can then be analyzed by a chi-square test to determine the significance of rhythmicity in the data at each period. This clear criterion for the significance of rhythms is the main reason for the popularity of the chi-square method in circadian research, but it is deficient in certain other respects [41, 40]. In particular, it features relatively poor filtering of noise, leading to a loss of resolution in period calculations. It also offers no way of measuring phase, and in spite of the ubiquity of phase response measurements in circadian research,methods for phase determination are extremely primitive, often amounting to the finding of peaks in data by hand (see two recent methods papers [64, 183] for examples).

We have therefore sought a method for measuring the period of rhythmic data that offers high temporal resolution, a clear way of estimating errors, and which generalizes easily to a method of measuring phase relationships. All of these criteria are satisfied by time correlation functions. The autocorrelation function of a time series $Y$ is computed by multiplying the series by a lagged version of itself, normalized by the variance and length of the time series. If $Y(t)$ has length $T$ and is made up of a combination of a sinusoid with amplitude $A$ and frequency $\omega$ and a white noise term $x_t$, $Y(t) = A \sin \omega t + x_t$, then the time autocorrelation at lag $\tau$ is given by

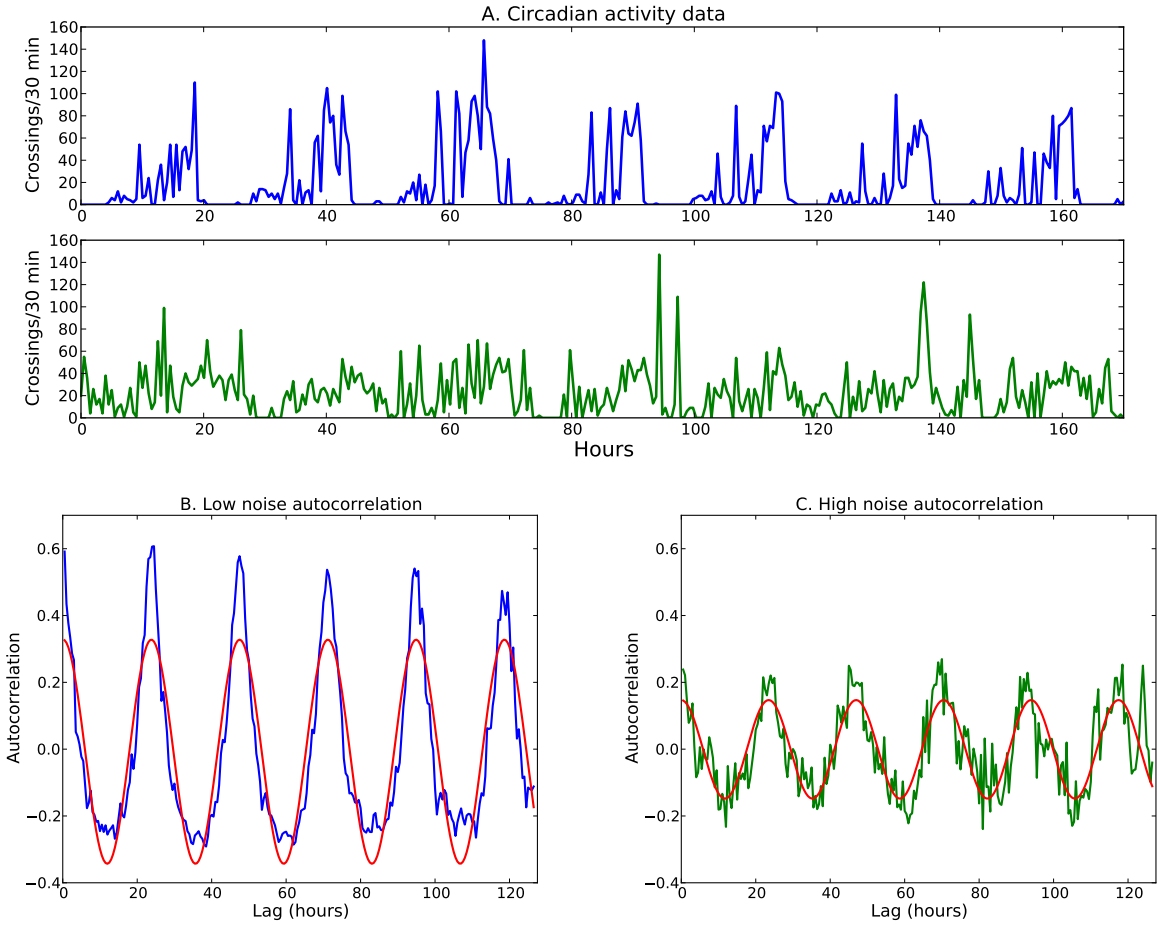


Figure 2.2: Example of period estimation for two typical circadian data sets. (A) Two raw circadian activity time series, one with relatively low noise (blue, top) and one with higher relative noise (green, bottom). (B) Autocorrelation (blue) with fit function (red) for the low noise data. (C) Autocorrelation (green) and fit function (red) for the high noise time series. The measured periods are 23.8 and 23.4 hours, respectively.

$$C_{YY}(\tau) = \frac{1}{\sigma_Y^2}\frac{1}{T-\tau}\int_0^{T-\tau}(A\sin\omega t + x_t)(A\sin\omega(t+\tau) + x_{t+\tau})dt \tag{2.15}$$

where the noise variance $\sigma_x^2$ is combined with the signal variance to give the overall variance $\sigma_Y^2 = A^2/2 + \sigma_x^2$. The expectation value of $C_{YY}(\tau)$ is given by

$$\langle C_{YY}(\tau)\rangle = \frac{A^2}{A^2 + 2\sigma_x^2}\cos\omega\tau \tag{2.16}$$

where we have omitted a term of order $1/T$. We can see from this that a perfectly periodic time series in the absence of noise will lead to a periodic autocorrelation with the same frequency as the time series and amplitude one. Adding white noise to a time series results in reduced amplitude of oscillation in the autocorrelation, while other types of noise can have different effects. Phase drift, for example, will lead to an exponential decrease in amplitude as lag increases. A cross-correlation between two time series of the same form can be computed in a similar fashion, and will have the same expectation value with an added phase equal to the phase difference between the two periodic functions. This makes time correlation functions a natural method for estimating both period and phase of circadian rhythm data. Figure 2.2 shows autocorrelation functions for a set of typical circadian activity data.

Period and phase can be measured from a computed correlation function by fitting a cosine function, which should have zero added phase and a variable frequency for period measurement, and a pre-determined frequency but variable added phase for phase measurement. Using fitting to measure period allows for high temporal resolution since a fit parameter can be specified to arbitrary accuracy. This is unlike a Fourier transform, where frequency resolution is lim-

ited by the number of observations in the time series, and can be increased only by padding, which can introduce artifacts. The value in fitting the correlation function rather than raw data is two-fold. First, initial phases are eliminated and harmonics are suppressed, reducing the number of parameters required for a good fit. Second, and more importantly, substantial averaging over noise occurs in the computation of the correlation function. For now we will assume that all noise in correlation functions is additive white noise, and will return to the subject of other types of noise at the end of this section. Given this, the expectation value of the noise terms in the correlation function is zero, and their variance is given by

$$\begin{aligned}\sigma_C^2 &= \left\langle \left( \frac{1}{T\sigma_Y^2} \int_0^T (Ax_{t+\tau} \sin \omega t + Ax_t \sin \omega(t+\tau) + x_t x_{t+\tau}) dt \right)^2 \right\rangle \\ &= \left\langle \frac{1}{T^2 \sigma_Y^4} \int_0^T (2A^2 x_t^2 \sin^2 \omega t + x_t^4) dt \right\rangle \\ &= \frac{1}{T} \frac{A^2 \sigma_x^2 + \sigma_x^4}{(A^2/2 + \sigma_x^2)^2}\end{aligned} \tag{2.17}$$

so that the characteristic size of fluctuations is reduced by a factor of $T^{-1/2}$ for a time series with $T$ observations, as long as $\sigma_x$ is not too large compared to the amplitude of the underlying periodicity. The accuracy of period estimation by this method can be estimated from a formula for the residual $f(\Delta\omega)$ of the fit, along with the size of fluctuations in the residual $\sigma_f^2$. The size of typical errors will be given by $\sqrt{\sigma_f / f''(0)}$. If the true correlation function is given by $a \cos \omega_0 t$ and the noise by $\eta_t$, then the residual is

$$f(\omega) = \int_0^T (a \cos \omega_0 t - a \cos \omega t + \eta_t)^2 dt \tag{2.18}$$

which has an expectation value given by (omitting terms that do not depend on $\omega$)

$$\langle f(\omega)\rangle = \frac{a^2 \sin 2\omega T}{4\omega} - \frac{a^2 sinT(\omega_0 - \omega)}{2(\omega_0 - \omega)} - \frac{a^2 sinT(\omega_0 + \omega)}{2(\omega_0 + \omega)} \tag{2.19}$$

The largest contribution will come from the second term, and, to highest order in $T$, is given by $f''(\omega = \omega_0) \approx a^2 T^3/2$. Since the noise variance $\sigma_C^2$ is small, the dominant contribution will be from the lowest order noise term given by

$$\left\langle \sigma_f^2 \right\rangle \approx \int_0^T 2a^2 \nu_t^2 \cos^2 \omega t dt = a^2 \sigma_C^2 T \tag{2.20}$$

Combining these results gives a typical error size $\Delta\omega \approx \sqrt{2\sigma_C/aT^{5/2}}$. Figure 2.3 shows a comparison of this expression, as well as Eqs. 2.12 and 2.13, using results from simulated data. The agreement is in general excellent, except in the estimate of errors for large values of the noise in Figure 2.3c. In this case the errors are slightly larger than predicted. This is due to the fact that the dominant noise term is of the form $x_t x_{t+\tau}$, which is non-Gaussian, and the fluctuations contributing to the error are not fully captured by the second moment shown in Figure 2.3b. In any case, as can be seen in Figure 2.2, typical noise magnitudes in circadian activity data are less than the amplitude of the underlying oscillations, so that the above method for period estimation can be expected to be accurate to within a few minutes.

We have shown that correlation function methods are highly effective at filtering white noise out of a periodic time series. However, it is worth considering other types of noise. Additive colored noise can be treated similarly to white noise, but will reduce the amount of effective averaging in the autocorrelation.

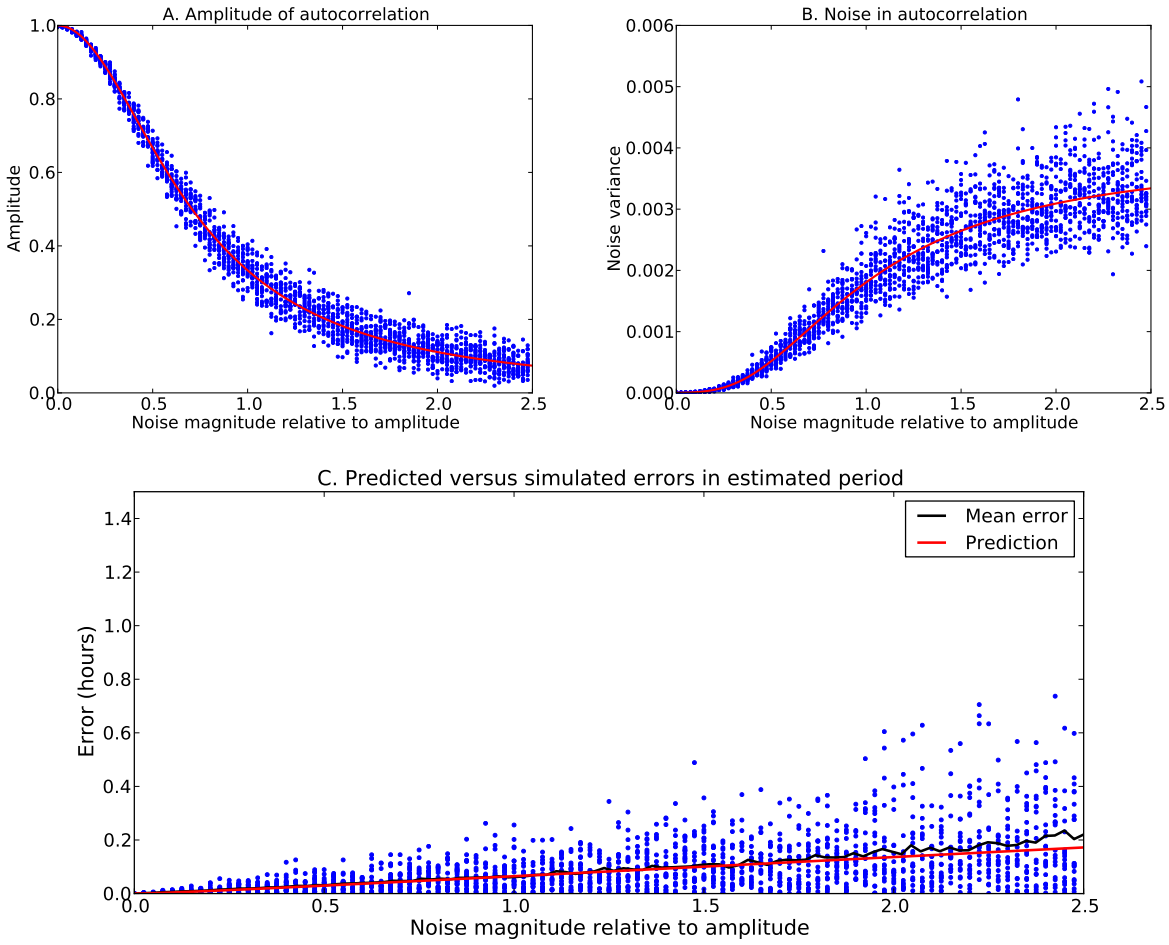


Figure 2.3: Performance of period estimating by fitting on simulated data consisting of a sine function with 24 hour period and length 240 hours combined with white noise of varying magnitude (magnitude here refers to standard deviation). (A) Comparison of measured autocorrelation amplitudes (blue dots) with the prediction from Eq. 2.16 (red line). (B) Noise in the correlation function (blue dots, measured by subtracting a fit and computing the variance of the remainder) compared to the prediction from Eq. 2.17. (C) Error in period estimation (blue dots), with a running average (black line) and the prediction from Eq. 2.20.

The noise in circadian time series is a combination of random fluctuations in behavior, and counting shot noise in the measured number of beam breaks from a moving fly. This latter type of noise does tend to have a circadian periodicity (since the shot noise is zero when the fly is not moving), but since it is uncorrelated at shorter times, it can still be filtered very effectively. It is also possible to have non-additive noise, such as fluctuations in amplitude or phase. We will see in Chapter 4 that the rate of phase drift in *Drosophila* circadian time series is very low. Amplitude fluctuations in circadian time series are also generally low, as can be seen in Figure 2.2. The data in Figure 2.2 also suggests that we are justified in not worrying too much about the presence of higher frequency harmonics in the time series, particularly given that their relative contribution to the signal is reduced in the autocorrelation, due to the squaring of amplitudes.

## 2.3 Modeling temperature compensation

As discussed in the previous chapter, temperature compensation is one of the most interesting and poorly understood properties of the circadian clock. Experimental understanding of the mechanisms of temperature compensation has been hindered by the lack of a complete understanding of the biochemical mechanisms which set the twenty-four hour circadian period. As a result, theoretical models have been a popular method for trying to understand temperature compensation. The earliest models (see [71] for an example) generally relied on a distributed form of temperature compensation, in which some parts of the circadian clock moved faster at higher temperature, and others slower, leading to an overall cancellation so that the period remained temperature independent. This approach has the advantage of solving the problem of temperature entrain-

ment, since the circadian clock remains sensitive to temperature.

However, here we describe an alternative approach, initially proposed in [53], in which the core circadian clock is completely temperature insensitive, and temperature entrainment is achieved by a specific pathway which acts without affecting the circadian period. Following [53], the idea can be illustrated via a simple model of a biological oscillator, the Goodwin oscillator [62]. The model consists of three species, an mRNA $X$, which is translated into a protein $Y$, which is then converted into a different protein $Z$, which in turn represses the transcription of $X$. The model is entirely linear except for the repression term, and is described by the following equations

$$\begin{aligned} \dot{X} &= \frac{k_1}{1+Z^n} - d_1 X \\ \dot{Y} &= k_2 X - d_2 Y \\ \dot{Z} &= k_3 Y - d_3 Z \end{aligned} \tag{2.21}$$

The Hill coefficient $n$ in the repression term must be greater than 8 in order for oscillations to result [66]. For values of parameters where oscillations occur, it is the case that $Z^n$ will be larger than 1, and by approximating the repression term as $k_1 Z^{-n}$ one can show that a rescaling of the form $x = \alpha X$, $y = \beta Y$, $z = \gamma Z$ with $\alpha = (k_2 k_3)^{\frac{n}{n+1}} k_1^{\frac{-1}{n+1}}$, $\beta = k_3^{\frac{n}{n+1}} (k_1 k_2)^{\frac{-1}{n+1}}$, and $\gamma = (k_1 k_2 k_3)^{\frac{-1}{n+1}}$ gives the modified system

$$\begin{aligned} \dot{x} &= z^{-n} - d_1 x \\ \dot{y} &= x - d_2 y \\ \dot{z} &= y - d_3 z \end{aligned} \tag{2.22}$$

in which the transcription/translation rates $k_i$ have vanished, without a rescaling of time. This implies that changes in the $k_i$ will not affect the period, but only the amplitude of oscillations. The Goodwin oscillator can therefore be temperature compensated by letting the degradation coefficients $d_i$ be independent of temperature, while remaining temperature entrainable via a signaling pathway that couples to the core oscillator through one or more of the parameters $k_i$ (for example, by increasing the transcription rate of the mRNA $X$).

One might object to this model by pointing out that chemical reaction rates are invariably temperature dependent. However, this objection can be answered in two ways. First, the relevant rates of circadian processes are determined not by first-order kinetics but by enzyme-catalyzed reactions, which can be rendered temperature independent by a balancing between changes in maximal rates and substrate binding coefficients. A variety of examples of such reactions have been observed in nature (see [72] for a review). Second, one can write down slightly more complicated models which exhibit similar properties without relying on temperature-independent reaction rates. An example is diagrammed in Figure 2.4. This model is a slight variant of the Goodwin model, in which each of the three original species is replaced by a pair of isoforms, with each isoform being reversibly converted into its partner. Each pair plays the same role as a single species did in the original model, with $X/X'$ leading to the production of $Y/Y'$, and so on. The only difference is that the basal degradation rates of the two proteins in a particular pair will be different, with one being degraded much more slowly than the other. This can be balanced by a temperature-dependent equilibrium constant, so that at higher temperatures, the balance within each pair will shift towards the more slowly-degraded isoform.

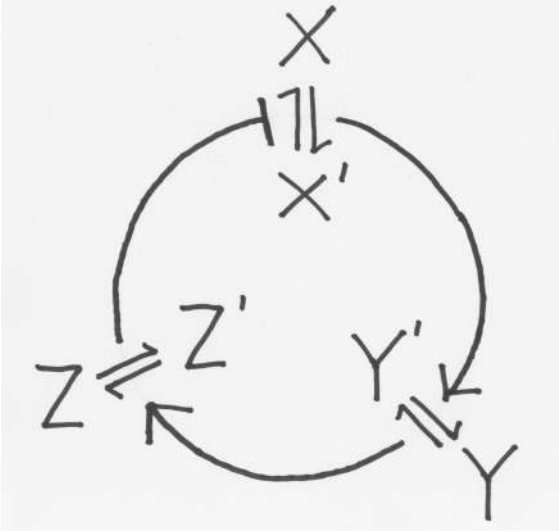


Figure 2.4: Variant of the Goodwin model oscillator in which the mRNA $X$ and proteins $Y$ and $Z$ have been replaced by reversibly interconvertible pairs of isoforms with differing degradation rates. This allows for temperature compensation by a balancing between the pair equilibrium constants and the degradation rates of each isoform.

As an example, the equations for $X$ and $X'$ take the form

$$\frac{\mathrm{d}}{\mathrm{d}t}X = \frac{k}{1+(Z+Z')^n} - dX - k_\mathrm{f}X + k_\mathrm{r}X' \tag{2.23}$$

$$\frac{\mathrm{d}}{\mathrm{d}t}X' = \frac{k}{1+(Z+Z')^n} - d'X' - k_\mathrm{r}X' + k_\mathrm{f}X \tag{2.24}$$

where $k_\mathrm{f}$ and $k_\mathrm{r}$ represent the forward and reverse rates for conversion of $X$ into $X'$. These equations can be combined to give

$$\frac{\mathrm{d}}{\mathrm{d}t}(X+X') = \frac{k}{1+(Z+Z')^n} - dX - d'X' \tag{2.25}$$

The terms associated with conversion between $X$ and $X'$ cancel out in this equation, and in any case we will assume that they are rapid compared to other

rates in the model, and that we can simply assume that $X/X' = k_r/k_f = K$ for some equilibrium constant $K$. The degradation term from the above equation can then be rewritten as follows

$$dX + d'X' = \left(d\frac{X}{X+X'} + d'\frac{X'}{X+X'}\right)(X+X') = \left(d\frac{K}{1+K} + d'\frac{1}{1+K}\right)(X+X') \quad (2.26)$$

So that the effective degradation rate for the combined species $X + X'$ is given by $d_{\text{eff}} = (dK + d')/(1 + K)$. The conditions required for temperature compensation can be found by assuming that the reaction rates are described by Arrhenius forms, $r \propto \exp(-E/kT)$, with the degradation rates determined by an energy $E_d$ and the difference between the energies of forward and reverse rates of conversion between isoforms given by $\Delta E_K$. In the simple limit that one isoform is not degraded at all, $d = 0$, and that $K \gg 1$ at room temperature, one finds that the condition for perfect compensation is simply $\Delta E_K = -E_d$. In other words, a factor of two increase in the degradation rate can be compensated by a factor of two shift in the equilibrium concentration of the isoform subject to degradation. In the limit of very fast equilibration of pairs of isoforms, the behavior of this model will be identical to that of the simpler model discussed above. The model is obviously somewhat artificial, and might be accused of being "unbiological" in some sense, but many of its key properties have been shown to be present in the circadian clock. As we discussed in Chapter 1, the circadian clock features a network of reversible phosphorylations of the PER and TIM proteins, which affect the stability of the proteins. Additionally, the *per* gene transcript undergoes temperature-dependent alternative splicing [121], so that alternate isoforms of circadian mRNA as well as protein are known to exist. In addition, the compensation of rate by commensurate changes in concentration has been found to be

involved in temperature compensation of other pathways, in particular *E. coli* chemotaxis [143].

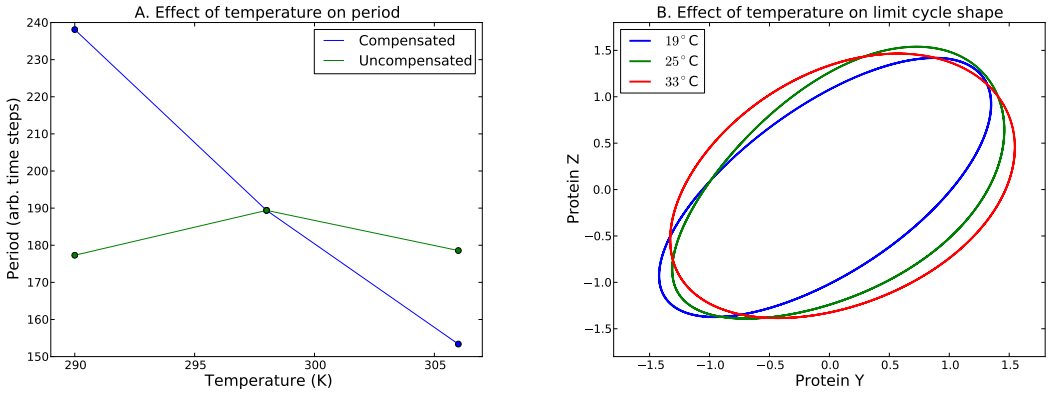


Figure 2.5: Simulation results from an alternative model of temperature compensation in the Goodwin oscillator, in which an increase in the degradation of $X$ and $Y$ at higher temperatures is compensated by a decrease in degradation of $Z$ (and *vice versa* at low temperatures). (A) Period as a function of temperature for the compensated model (green) compared to an uncompensated model (blue) in which all degradation rates increase with temperature. (B) Rescaled limit cycles in the $Y$-$Z$ plane,, showing the change in shape at different temperatures.

The Goodwin model can also be temperature compensated by balancing positive and negative changes in rates. Figure 2.5 shows an example in which the temperature changes of the degradation coefficients $d_i$ are determined by the Arrhenius form with effective "energies" of $E_1 = E_2 = 20$ kJ/mol and $E_3 = -40$ kJ/mol for the constants $d_1$, $d_2$, and $d_3$, respectively. In this case, as shown in Figure 2.5a, the period remains essentially constant from 19°C to 33°C, whereas if $E_1 = E_2 = E_3 = 20$ kJ/mol, the period decreases by about a third over the same range. However, the behavior of the system in this temperature-sensitive case is quantitatively different from the effectively temperature-insensitive case in Eq. 2.21. In the temperature-insensitive model, the scaling argument pre-

sented above predicts that changes in temperature should lead only to rescaling in overall amplitude of the oscillation, not to changes in the scale-free shape of the limit cycle. In the temperature sensitive case, the shape of the limit cycle will change with temperature due to incommensurate changes in the rates of different reactions in the system. Figure 2.5b shows the limit cycle at three different temperatures for the temperature-sensitive case, rescaled to have amplitude one and mean zero in order to emphasize the changes in scale-free shape. These cases are further discussed in Chapter 5, where a qualitative argument for the same conclusion is presented, in addition to experimental evidence from the *Drosophila* circadian clock.

## 2.4 Noise and bifurcations

A key issue in understanding the functioning of the circadian rhythm is explaining the ability of the clock to maintain accurate time in the presence of cellular noise. Intracellular proteins, particularly transcription factors, are often present at very low concentrations, such that their copy number inside a cell is less than 100, and the effect of simple counting noise can be significant [14]. It has long been theorized that the principal mechanism by which the circadian clock deals with noise is intercellular coupling, and that individual cells are themselves unreliable timekeepers [51].

The simplest means of analyzing the effect of noise on a single oscillator is to begin with the normal form for the Hopf bifurcation with added white noise

$$\dot{r} = r(A^2 - r^2) + \eta_r \tag{2.27}$$

$$\dot{\phi} = \omega + \eta_\phi \tag{2.28}$$

where we have made the simplifying assumption that the fluctuations $\eta$ in the $r$ and $\phi$ directions are uncoupled from one another. In this case, fluctuations in the $\phi$ direction are unchecked, and the phase of the oscillator will diffuse freely around the circle. In the absence of inter-oscillator coupling, this will lead to the gradual loss of synchrony in the population. The implications of this for circadian behavior in *Drosophila* will be discussed further in Chapter 4. This leaves the $r$ equation, which corresponds to the normal form of the pitchfork bifurcation with $A^2$ playing the role of the bifurcation parameter $\epsilon$. For $\epsilon < 0$, one stable fixed point is present, which branches into two stable fixed points separated by an unstable fixed point as $\epsilon$ becomes greater than zero. With the addition of a white noise term, $\eta_r$ ,with mean zero and variance $\sigma^2$, the density function for $r$, $\rho(r,t)$, is governed by the Fokker-Planck equation

$$\frac{\partial \rho}{\partial t} = -\frac{\partial}{\partial r}\left[(\epsilon r - r^3)\rho\right] + \frac{1}{2}\sigma^2 \frac{\partial^2}{\partial r^2}\rho \tag{2.29}$$

which has an invariant density given by

$$\rho(r) = \frac{1}{N}\exp\left[\frac{1}{\sigma^2}\left(\epsilon r^2 - \frac{r^4}{2}\right)\right] \tag{2.30}$$

where $N$ is a normalization constant. This calculation is carried out in [129], where the authors note that a key implication is that, unlike a bifurcation without noise, the transition in the behavior of the solution as $\epsilon$ crosses 0 is smooth. Figure 2.6 shows a plot of the invariant density $\rho$ for three values of $\epsilon$. For $|\epsilon|$ small, the shape of $\rho$ is very similar whether $\epsilon$ is positive or negative. Thus a

spontaneously oscillating (Hopf) system for which $A^2 < \sigma_r^2$ will be difficult to distinguish from one which is damped. In particular, the appearance of highly noisy circadian oscillations in a single cell (see Chapter 3 for an example) may not indicate the presence of a true spontaneous oscillator. The noise spectrum of a damped linear oscillator with frequency $\omega_0$ and damping rate $b$ will have a magnitude proportional to $((\omega^2 - \omega_0^2)^2 + \omega^2 b^2)^{-1/2}$, meaning that a spectral peak does not guarantee that a true oscillator is present.

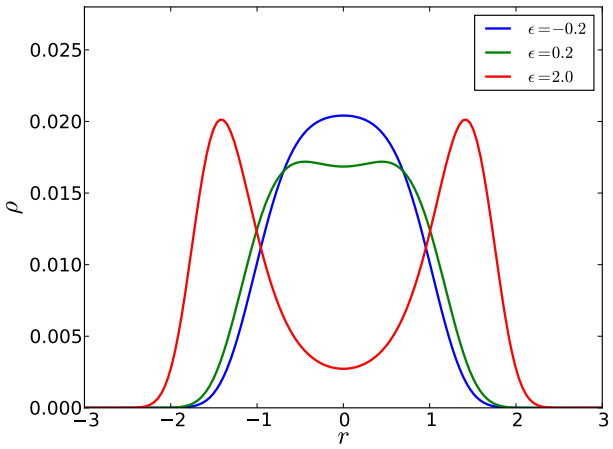


Figure 2.6: Invariant density of the Fokker-Planck equation for the pitchfork bifurcation (Eq. 2.29). Distributions close to the bifurcation point have similar shapes, regardless of whether the bifurcation parameter $\epsilon$ is positive (green) or negative (blue). For $\epsilon$ much greater than zero (red), the distribution takes on double-peaked shape characteristic of the bifurcation.

One experiment [202] compared luciferase rhythms measured in fibroblasts to simple models of damped and self-sustained noisy oscillators, and concluded that circadian rhythms in single cells cannot be distinguished from noise-induced oscillations. This suggests that intercellular coupling must play an important role in generating robust circadian rhythms in mammals. Indeed, a separate experiment [98] found that intercellular coupling is able to generate significant

stochastic oscillations in SCN explants from mice lacking the transcription actor Bmal1. Another experiment [117] has shown that individual knockouts of the *per1*, *per2*, and *cry1* genes do not eliminate behavioral rhythms in mice, and do not eliminate molecular rhythms in intact SCN explants, but *do* eliminate rhythms in fibroblasts or dissociated SCN neurons. This provides further evidence for strong interneuronal coupling in the mammalian circadian clock, and in particular suggests that, unlike in the Kuramoto model, the coupling between individual cellular oscillators must be *nonlinear* in order to explain the possibility of a spontaneously oscillating population arising from individually damped units. We can support this claim with a very simple example.

A model of a coupled oscillator population that exhibits spontaneous oscillations with individually damped units will have dynamics of the form

$$\begin{aligned} \dot{r} &= -ar + br^2 - r^3 \\ \dot{\phi} &= \omega \end{aligned} \tag{2.31}$$

where the coefficient $b$ is proportional to coupling strength. Individual units (with $b = 0$) will have the same dynamics as damped Hopf oscillators, but the population will have a stable limit cycle as long as $b > \sqrt{2a}$ (this can be found by setting the large $r$ local maximum of the $\dot{r}$ equation equal to zero). In order for the collective population oscillation to follow these dynamics, the inter-unit coupling must clearly be nonlinear, and a suitable coupling function could take the form (in $(x, y)$ coordinates)

$$K(\bar{x} - x_i + x_i(\bar{x}^2 + \bar{y}^2)^{1/2}) \tag{2.32}$$

where the bar denotes a population mean. The linear part of this expression will lead to synchronization while the nonlinear part will sum to provide the necessary $r^2$ term in the population average dynamics. It is interesting to note that this model has a stable fixed point at the center of its phase plane, and so an experiment like that discussed in Section 2.1 would observe amplitude recovery governed by noise-activated barrier crossing rather than by smooth increases like those shown in Figure 2.1. The implications of these results, as well as data on the nature and strength of intercellular coupling in mouse and *Drosophila*, will be discussed further in Chapter 4.

CHAPTER 3

# EXPERIMENTAL CONSIDERATIONS

The 1971 discovery of the *period* gene in *Drosophila* [101] and its subsequent cloning in 1984 [10, 160, 220] made circadian activity rhythms the first example of an animal behavior that could be studied by the techniques of molecular biology. Over the following decade, elucidation of the other genetic components of the core circadian clock led to a revolution in molecular neuroscience. In this chapter, we will discuss some of the experimental techniques used in the study of circadian rhythms.

## 3.1 *Drosophila* behavior experiments

*Drosophila* circadian behavior is measured using the Drosophila Activity Monitor or DAM (Trikinetics, Waltham, MA). Thirty-two slots in the monitor hold glass cuvettes in which individual flies are placed. The cuvettes also contain food, and are capped with a wax plug on one end and a cotton ball on the other. Each slot in the monitor features an IR LED and photodiode at the center, so that the movement of a fly along the length of a cuvette results in cutting of the IR beam, which is registered as a count by the monitor. Summed counts are transmitted to a computer via telephone cable every 60 seconds. A fully loaded DAM is shown in Figure 3.1a.

For light resetting experiments, a loaded DAM monitor is placed inside a custom box constructed from foam board, the top of which holds 15 bright blue LEDs (470nm, LEDSupply L1-0-B5TH15-1) shielded by a sheet of semi-transparent diffusing plastic (shown in Figure 3.1b-c). Each LED is wired in

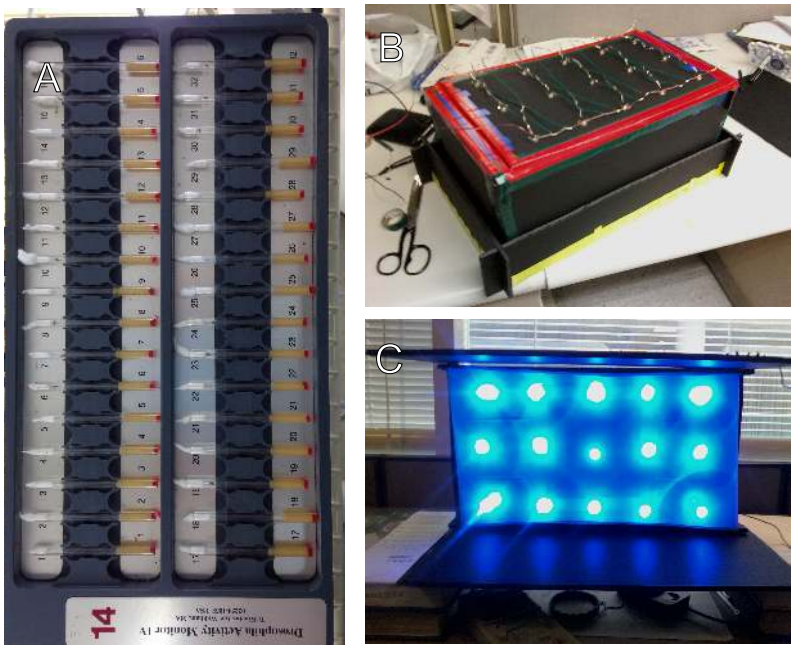


Figure 3.1: Equipment for *Drosophila* behavior experiments. (A) Drosophila Activity Monitor (DAM). Cuvettes containing individual flies with food are placed in slots in the DAM where movement is registered by the cutting of a light beam. (B) Top view of foam board box for light-resetting experiments. (C) Inside view of a partially-deconstructed box, showing light from 15 blue LEDs passed through a sheet of diffusing plastic.

series with a 100Ω resistor, and the 15 are connected in parallel to a computer-controlled power supply. Once inside the box, the DAM has a diode light sensor attached exactly at its center (phidgets.com, #1142). LEDs are powered from a computer-controlled DC supply (web-tronics.com, Model 3645A). The attached laptop computer runs a Visual Basic script which reads light levels and adjusts the voltage of the supply according to a pre-measured calibration curve, to achieve a level of 30 lux. For all light and temperature resetting experiments, adult *Drosphila* males are collected within 1-2 days of eclosion, loaded into a DAM, and subjected to a synchronizing protocol. For light-resetting experi-

ments involving $per^S$ flies (see Chapter 4), synchronization is achieved by placing animals in constant light (~ 500 lux white fluorescent light) for at least three days. For temperature-resetting experiments (Chapter 5), flies are subjected to a cycle consisting of twelve hours of light followed by twelve hours of darkness. In all cases animals are moved into constant darkness and left for a least 24 hours before a stimulus is applied. A 24 hour wait is necessary because the circadian dynamics generally take about a day to adapt from their form under a light cycle to their free-running form.

Temperature experiments requiring a step from one temperature to another (Figure 5.8) are performed by moving DAMs from an incubator set at the starting temperature to a different incubator set at the final temperature. However, for experiment involving rapid applications of high-temperature pulses (Figure 5.7), large temperature- and light-controlled incubators are unsuitable due to their long heating and cooling times. Therefore, a custom temperature-regulated box was constructed from 1/4" plexiglass, insulated on the outside by 1.5" construction foam. The interior of the box is 16"x8", and cables for DAMs enter through a small hole subsequently closed with silicone sealant. Heating and cooling are achieved by a Peltier effect thermoelectric element or TEC (Custom Thermoelectric, 19911-5M31-15CZ) with a maximum heat transfer rate of 225 watts. The TEC is embedded in an assembly (shown in Figure 3.2a) consisting of two heat sinks with mounted cooling fans, one on each side. The TEC is sandwiched between two lapped aluminum spacer plates, fixed with thermal epoxy (Arctic Silver). Spacer plates are coated in thermal grease (Arctic Silver 5) and thermal contact with the heat sinks is achieved via pressured applied by four bolts. Each bolt goes through both heat sinks, and both bolt and nut are separated from the metal surfaces by a 1.4" plastic jacket to avoid thermal

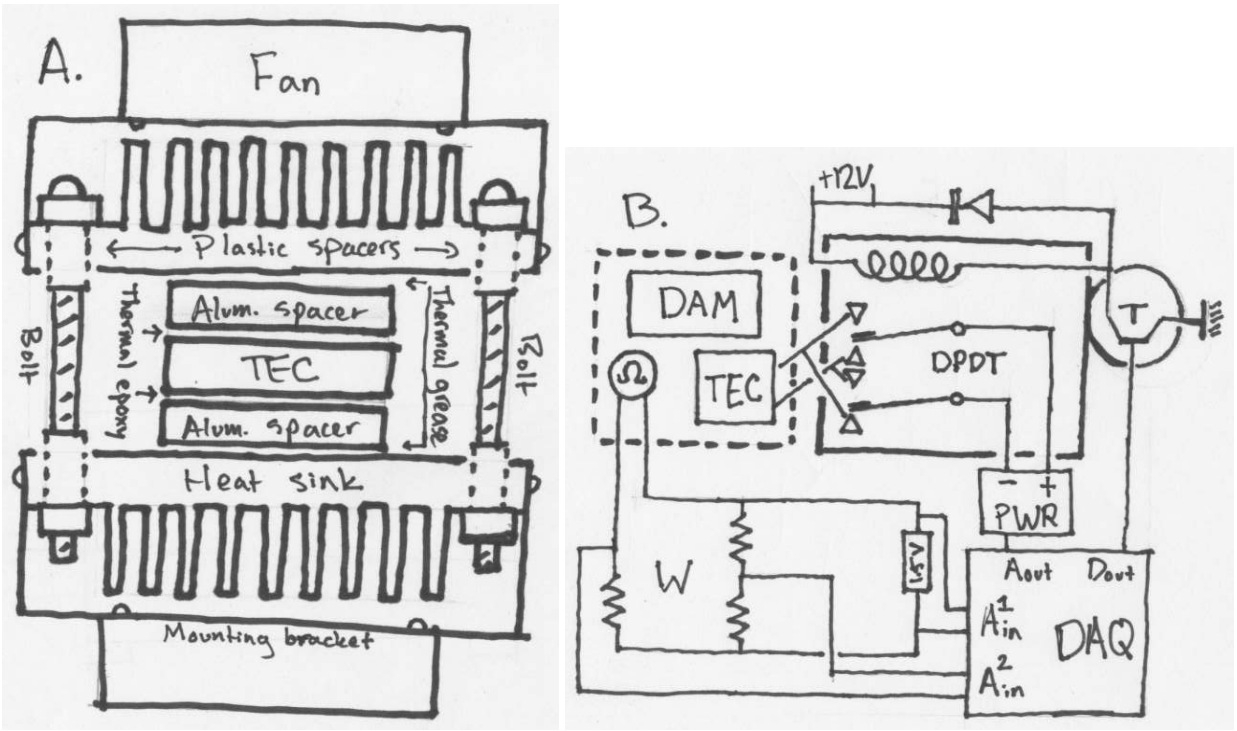


Figure 3.2: Designs for temperature-controlled box. (A) Cutaway diagram of the assembly for a thermoelectric cooler (TEC), placed into the lid of the box. The TEC is covered by aluminum spacer plates and sandwiched between two heat sinks held together by bolts, which are themselves thermally isolated by plastic spacers. A computer case fan is attached to each heat sink by a mounting bracket. (B) Control circuit for temperature feedback. A Data Acquisition (DAQ) card drives a variable-voltage power supply (PWR) via an analog output $A_{out}$. PWR output is passed through a DPDT relay switch controlled by the digital output ($D_{out}$) of the DAQ, via an amplifying transistor (T). Power is supplied to the relay coil by a 12V supply in parallel with a diode. Temperature is measured via a thermistor sensor ($\Omega$) in a Wheatstone bridge (W) powered by a 1.5V battery. Battery and bridge voltages are read by analog inputs of the DAW, $A^1_{out}$ and $A^2_{out}$, respectively.

contact.

Temperature control is implemented by a PID control circuit based on a data acquisition card or DAQ (National Instruments, USB-6009). A thermistor temperature sensor (Omega, #44030) inside the box is connected to an analog input of the DAQ via a Wheatstone bridge with a 1.5V battery as voltage source. The second analog input of the DAQ is connected across the battery to check the circuit voltage. The analog output of the DAQ controls the output voltage of a variable DC supply (Kepco, RKW24-14K) powering the TEC. The output of the power supply is passed through a DPDT relay switch (Digi-Key, PB1038-ND) for switching from heating to cooling. The relay coil is connected across a 12V DC supply in parallel with a diode (Digi-Key, 1N4001), and polarity switching is controlled by the DAQ digital output via a 4kΩ pull-up resistor connected to the base of a transistor (Digi-Key, ZTX692B-ND ) for amplification. The entire circuit is shown in Figure 3.2b. PID control is implemented in Matlab on the laptop connected to the DAQ. The circuit as constructed is able to heat the box from 25°C to 37° C in about 3 minutes, and to cool from 37°C to 25°C in about 10 minutes, while maintaining constant temperatures to within 0.1°C. The difference in heating and cooling rates is due to resistive heating in the TEC, which significantly reduces cooling efficiency.

## 3.2 Fluorescent imaging and tissue culture

Imaging circadian dynamics in the neurons of a living fly is difficult and cannot be maintained long-term (see [172] for one example). Imaging of circadian neurons is therefore generally done in fixed brains. Flies are decapitated and

heads are fixed in 5% paraformaldehyde on ice. Brains are then separated from the head cuticle with tweezers in phosphate-buffered saline (PBS), and stained with antibodies overnight in a solution of PBS supplemented with detergent (5% Triton-X 100) to permeabilize cell membranes. Details can be found in [78]. *Drosophila* brain are small (about 50 $\mu$m in their smallest dimension) and somewhat transparent, so they can be imaged by a confocal microscope without further dissection. Staining can be from primary antibodies against circadian proteins (PER and TIM are commonly used).

It is also possible to generate *Drosophila* lines expressing fluorescent reporters, usually green fluorescent protein (GFP), under the control of a circadian promoter. This is done by using the UAS-GAL4 system. GAL4 is a transcription factor from yeast, and UAS is its associated promoter target sequence. By crossing a fly carrying a transgene expressing GAL4 with a circadian promoter and a fly carrying a GFP transgene with the UAS promoter, one can generate a line in which GFP is effectively expressed by the circadian promoter of one's choice. A wide variety of GAL4 and UAS lines are available from common stock centers, making this method easy and inexpensive to carry out. Figure 3.3 shows an example image. Images of this sort can be used to quantify the expression of circadian proteins in *Drosophila* neurons (see, for example, [174]), but for many purposes, dynamical information is more useful.

*Drosophila* tissue culture lines such as S2 cells do not express the circadian clock, but several mammalian cell lines are available which do. The most commonly used among these are NIH3T3 fibroblasts. Circadian oscillations have frequently been observed in individual fibroblasts by the use of luciferase reporters (see for example, [141]), however, single-cell luciferase imaging requires

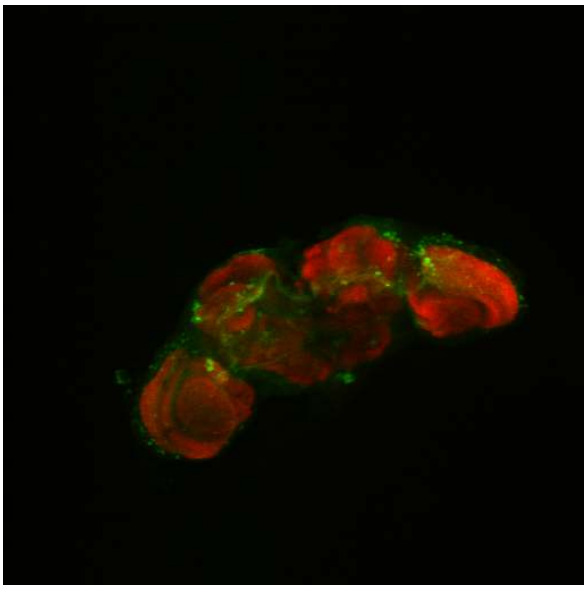

Figure 3.3: Maximal projection of a 10X confocal stack through a *Drosophila* brain. Green is a stain against GFP expressed by a *timeless* GAL4 driver. Lateral neurons are visible on the left and right between the optic lobes and the central brain, as are the projections from the lateral neurons to the dorsal brain. Red is a counterstain for nc82, a synaptic protein present in all neuropil tissue.

an ultra-cold CCD camera and a chamber specially designed to exclude 100% of ambient light (see [201] for a description). Fluorescent reporter proteins are far brighter and less demanding of specialized imaging equipment. The first experiment to use a fluorescent reporter to observe circadian oscillations in individual cells [136] relied on NIH3T3 cells transfected with a reporter construct consisting of the bright yellow fluorescent protein variant Venus, fused to a nuclear localization sequence (NLS) followed by a proteasome-activating proline-glutamate-serine-threonine-rich (PEST) sequence. The NLS targets the Venus protein for nuclear translocation, easing the process of automatic cell segmentation and fluorescence quantification. PEST sequences are a target for protein degradation machinery, and are necessary because the ordinary half-life of a

fluorescent protein is greater than 24 hours, complicating the observation of circadian oscillations in fluorescence [26]. The Venus construct was expressed by a flanking promoter sequence from the highly expressed downstream circadian transcription factor *rev-erbα*. The cells transfected with the Rev-Erb$\alpha$-Venus construct showed robust circadian rhythms in fluorescence, but also tended to die after about three days [136]. The short lifetime of cells subjected to constant fluorescent imaging is most likely due to free radical toxicity from excited fluorophores [175]. A similar experiment was done with the same reporter [52] to find evidence for coupling between circadian rhythms and the cell division cycle. These authors also did not image cells for longer than three days.

Following the work of [136], we generated a NIH3T3 cell line expressing two different fluorescent reporter constructs, one expressing Venus under the control of the *per2* promoter, and one expressing the red fluorescent protein mCherry under the *bmal1* promoter. The constructs were generated from a pGL3 (Promega) luciferase vector containing either *per2* or *bmal1* promoters (provided by A. Patke) by excising the luciferase cassette and replacing it with fluorescent protein sequence flanked by NLS and PEST. A schematic of the constructs used and image of the resulting cells are shown in Figure 3.4. The use of two promoters expressed at different phases of the circadian day was intended to be useful for amplitude recovery experiments (as discussed in Sections 2.1 and 4.1) as well for measurements of limit cycle shape at different temperatures (see sections 2.3 and 5.1).

For amplitude recovery experiments in particular, more than three days of data are required for a useful measurement. We therefore attempted to improve on the experiments of [136]. The clearest way to improve the health of cells

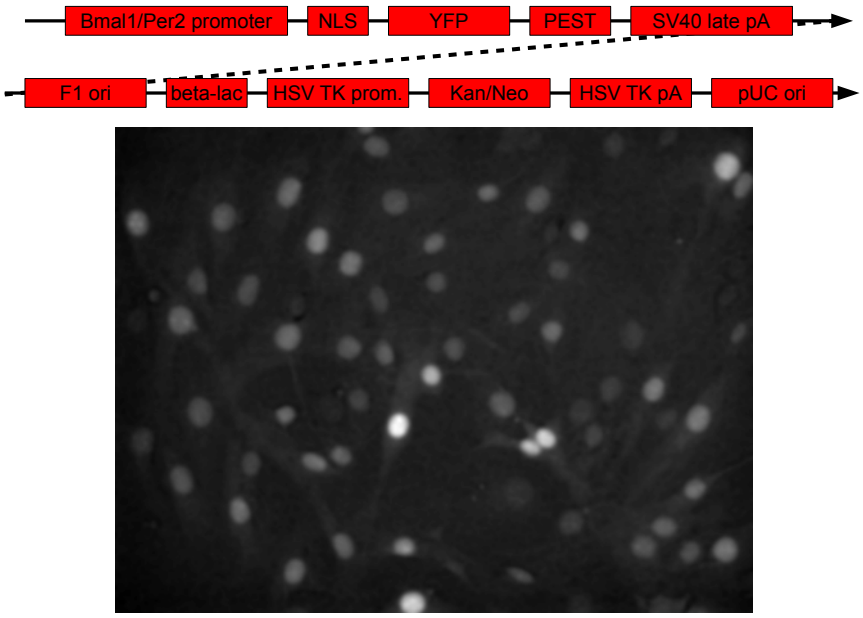


Figure 3.4: Fluorescent reporter construct and cells. (Top) Linearized schematic of the reporter construct, containing Bmal1/Per2 promoter followed by nuclear localization sequence (NLS), fluorescent protein (YFP or mCherry), PEST sequence, and polyA tail. The rest of the vector consists of origins of replication (bacterial F1 and eukaryotic pUC) and a resistance cassette containing both bacterial (beta-lac) and eukaryotic/herpes virus (HSV TK) promoters followed by kanamycin/neomycin antibiotic sequence and herpes virus polyA tail. (Bottom) NIH3T3 fibroblasts expressing Venus fluorescent protein from the above construct.

under fluorescent imaging is to reduce the total amount of exposure to fluorescent excitation. This was done in three ways. First, a top-down fluorescence microscope with computational autofocus (Olympus LCV110) was used, eliminating the need for taking confocal stacks as in [136]. Second, the required fluorescent exposure time was decreased by minimizing background fluorescence. All biological cells feature some amount of native autofluorescent material, but background fluorescence can be reduced by manipulating the cell culture medium. In particular, the standard mammalian future medium DMEM

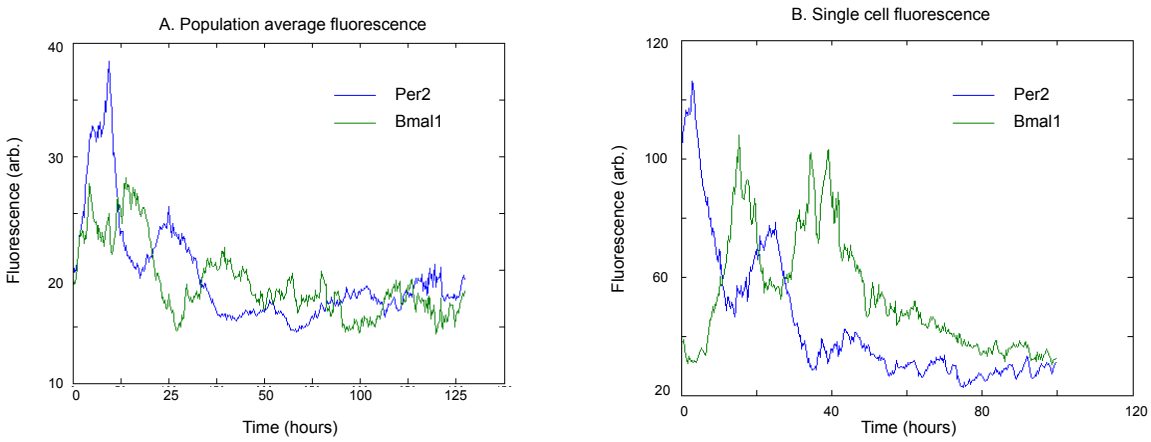


Figure 3.5: Quantitative fluorescence time-lapse data. (A) Population average of fluorescence from cells expressing Venus under the *per2* promoter and mCherry under the *bmal1* promoter. Cells were synchronized by application of the glucocorticoid hormone dexamethasone. (B) Data from an individual cell from the same reporter strain.

contains riboflavin and phenol red, both known to be autofluorescent. We therefore used a modified DMEM lacking riboflavin and phenol red (Gibco, provided by A. Warmflash). Finally, cells containing the reporter constructs were subjected to fluorescence-associated cell sorting in order to obtain lines with high, robust expression. The result of these efforts was that it was possible to image cells for up to five days without significant losses. Example data are shown in Figure 3.5. In Figure 3.5a, population-averaged oscillations in *per2*- and *bmal1*-generated fluorescence are shown, indicating that the reporters oscillated with roughly opposite phases, as expected.

In order to obtain single cell data, images were analyzed with custom Matlab code. The algorithm first uses image closing and opening to filter out cells and obtain a smoothed background. Background-subtracted images are segmented by a combination of threshholding and an algorithm that segmented regions

around local maxima (written by E. Siggia and A. Warmflash). Segmented cells are tracked over the imaging time series to generate individual cell fluorescence data like that shown in Figure 3.5b. Several problems prevented useful results from being obtained. First, unlike the data shown in Figure 3.5b, many cells did not display rhythmic oscillation of fluorescence, but instead essentially random fluctuations. Second, cells that did show oscillations could be difficult to track due to the trough of the circadian rhythm in fluorescence being barely different from background levels. Third, cells that showed robust oscillations over several days of tracking often showed a decay in amplitude, which can be seen in the above image. The combination of low throughput and a lack of consistent information about amplitude rendered the data essentially unusable for its intended purposes.

Several potential solutions to these problems exist. First, issues with decay in amplitude are almost certainly related to depletion of nutrients in the culture medium, which could be ameliorated by imaging cells inside a flow cell in which culture medium is constantly replenished. Second, as we will discuss in Chapter 4, many clock proteins, including *bmal1* and *per2*, are not strongly transcribed, contributing to noisiness in the data. Signal-to-noise ratios can be improved by finding candidate output genes with much higher expression levels, like *rev-erbα*. However, using output transcription factors rather than core circadian genes as reporters may lead to misleading conclusions about clock amplitude, and extensive control experiments would be required. In addition, single-cell luciferase experiments have produced observations of robust circadian rhythms using *bmal1* and *per2* promoters in NIH3T3 cells [201]. In [141], it is noted that the most coherent rhythms are observed in cells that have grown to confluence and ceased dividing. This is to be expected since the process of cell

division will inevitably scramble circadian phase at least slightly (evidence for this is discussed in [136]). However, NIH3T3 cells in our hands do not contact inhibit their growth at all, but continue dividing until nutrients are depleted and the cells die. This effect, which adds noise to circadian rhythms and also leads to relatively unhealthy cells due to nutrient depletion, is the most likely explanation for the low quality of the data obtained in our experiments. This suggests that best method for obtaining robust circadian rhythm data from single cell observations is not to switch reporters, but to experiment with a large number of cell lines until one is found that displays consistent, robust circadian rhythms and good contact inhibition of growth.

## 3.3 Western blots

The lack of live imaging methods for *Drosophila* means the best method for obtaining circadian molecular time series is direct measurement of protein concentrations by Western blot. The idea behind Western blotting is to isolate purified proteins from fly heads by using voltage to push denatured protein through a polymer matrix, separating different proteins by length. The contents of the polymer gel are then transferred to a thin membrane which can be stained with antibody and imaged [187]. Protein isolation from *Drosophila* heads begins by removing a sample of flies from a synchronized population at a specified time point and flash freezing them on dry ice. Frozen flies are shaken on a vortex machine, causing appendages to separate from the bodies, and heads are then isolated using a two-stage sieve cooled in liquid nitrogen. Heads are homogenized with a sterile pestle in 3X volume of RIPA buffer, and diluted with a further 1X volume of RIPA dilution buffer. RIPA is composed of 50mM TRIS buffer at pH

8.0, 150mM NaCl, 1mM EDTA, supplemented with, by volume, 20% glycerol, 1% Triton-X 100, 0.5% sodium deoxycholate (NDOC), and 0.02% sodium azide. EDTA is a chelater of magnesium and calcium ions, thereby acting as a potent suppressor of enzymatic activity. Detergents (Triton-X 100 and NDOC) are present to break up cellular and nuclear membranes. Glycerol and azide provide low temperature stability and sterility, respectively. RIPA dilution buffer is the same mixture without detergents. Before heads are homogenized, RIPA buffer is supplemented with 1% protease inhibitor cocktail (#3, Calbiochem) and 1mM dithiothreitol, a sulfur-containing compound that inhibits formation of inter-molecular disulfide bonds. The resulting slurry is centrifuged twice for ten minutes. At each centrifugation step, the soluble protein-containing layer is removed from between the insoluble pellet and a top layer containing lipids. The concentration of the resulting purified protein is then measured by Bradford assay [15], which uses a blue protein stain combined with a spectrophotometer and a series of protein concentration standards.

Approximately 25$\mu$g from each protein sample to be measured is mixed with water to equalize volumes and then added to an equal volume of loading buffer. The loading buffer consists of TRIS buffer, 2% sodium-dodecyl-sulfate, and 5% $\beta$-mercaptoethanol ($\beta$-ME). Samples are heated to 95°C to denature proteins and then loaded into the wells of a 7% poly-acrylamide gel (Bio-Rad). The gel is then subjected to 150V applied top-to-bottom in a standardized gel box (Bio-Rad) filled with running buffer consisting of TRIS and 1% SDS. $\beta$-ME breaks disulfide bonds, which, in combination with the SDS in the loading and running buffers, ensures that proteins are linearized and negatively charged. The result is that proteins will migrate through the poly-acrylamide polymer mesh at a rate inversely related to their length. A ladder standard consisting of a

few proteins of known size bound to dye molecules is also loaded on the gel to provide length markers. Once the proteins of interest are sufficiently well separated (about two hours in our case), the gel is removed and then layered under a polyvinylidene fluoride (PVDF) membrane in a plastic cassette. The cassette is inserted vertically into a box with sheets of metal on either side. The box is filled with running buffer and a voltage is applied to the metal sheets, leading a to a transverse electric field that pushes proteins out of the gel and into the PVDF membrane. PVDF is permeable to water and small molecules, but traps proteins, while being highly chemically inert and resistant to high temperatures. For the PVDF transfer process, a low voltage is used, generally around 30V for 6-8 hours, to avoid excess resistive heating, which can cause loss of protein.

Once protein has been transferred, the membrane is washed three times in TBST (TRIS buffer with 10% TWEEN detergent) to remove excess acrylamide. This is not a typical step in Western blotting, but is important for our purposes to minimize background signal, which can result from free antibody integrating into acrylamide fragments. Following the wash, the membrane is blocked for an hour in TBST supplemented with 5% powdered milk. Blocking the membrane fills vacant pores in the PVDF, preventing stray antibody binding. Then the membrane is incubated in a primary antibody mixture consisting of 5% powdered milk in TBST, with rat anti-TIM antibody (provided by L. Saez) added at 1:2000, and mouse anti-cadherin antibody (Santa Cruz Biotechnology) at 1:200. Primary antibody incubation occurs overnight at 4°C. Following this, the primary antibody is removed and the membrane is washed three times in TBST. Then anti-mouse and anti-rat secondary antibody (Jackson Immunolabs) is added in TBST with milk at 1:10000, the membrane is incubated for one hour at room temperature, and then washed three times again in TBST.

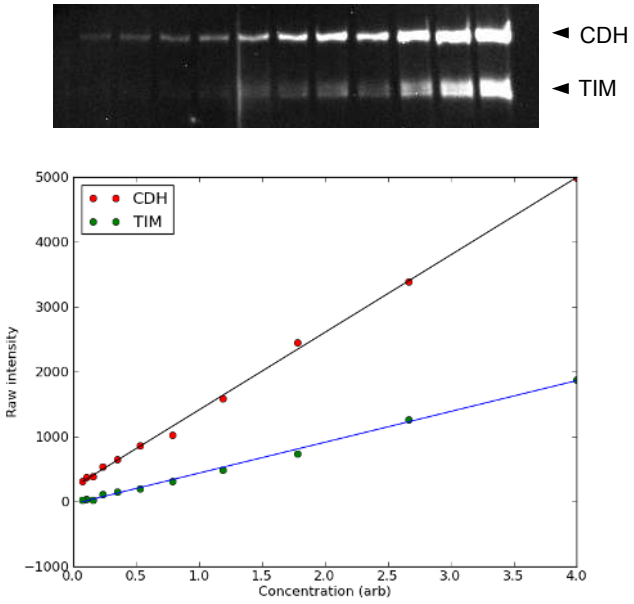


Figure 3.6: Dilution series of a single protein sample. (Top) Blot image with timeless (TIM) and cadherin (CDH) bands. Highest concentration on the right, with each subsequent band having 1.5X less protein than the previous. (Bottom) Quantification of TIM and CDH bands showing linearity of intensity measurements.

The secondary antibody is conjugated to horseradish peroxidase, which produces blue light by catalyzing the oxidation of luminol. The substrate (ECL, Thermo Scientific) is added for 60 seconds, then poured off and the membrane is imaged by a camera for a 6-8 minute exposure (Bio-Rad ChemiDoc). Bands in the image are quantified using custom image segmentation code written in Matlab. Background subtraction is not necessary. Intensities of bands from the protein of interest (TIM) are normalized by the intensities of the corresponding control band (cadherin, CDH) to control for small differences in loading volumes. In order to check the integrity of the blotting and quantification procedure, it is prudent to run a dilution series drawn from a single protein sample, such that the range of intensities measured covers the full physiological

range. An example image with associated quantification is shown in Figure 3.6. Linearity is preserved over a large concentration range (the physiological range corresponds to roughly the middle six of the twelve bands shown). This is particularly important for the experiments described in Chapter 5, in which Western blots are used to test the scaling hypotheses outlined in Section 2.3.

CHAPTER 4

# INTERNEURONAL COUPLING AND THE PHASE SINGULARITY

Cellular regulatory systems in all organisms must overcome the effects of noise, both intrinsic and extrinsic [47]. In eukaryotic cells, major contributions to molecular noise come from copy number fluctuations in transcription factors, which are generally present at very low concentrations, and from the varying size of bursts in mRNA transcription, among other sources [14]. It has long been theorized that one of the functions of the population of circadian clock cells in animals is to generate a reliable oscillator from units that are individually noisy [51]. The nature of intercellular coupling and communication in the animal brain is critical to generating such a robust collective oscillation. In addition, the structure of interneuronal coupling is important for determining the mechanisms of behavioral entrainment to environmental conditions as well as the regulation of circadian outputs (see [36] as well as Section 1.5 for a discussion of some of these issues).

The best studies of interneuronal coupling in an animal come from experiments in intact explants of the mouse suprachiasmatic nucleus (SCN). Coupling between the approximately 20,000 neurons of the SCN is mediated by both neurotransmitters and electrical communication [91, 199]. Coupling is not required for individual cellular oscillations, but does increase the amplitude and stiffness of oscillations in single cells [214], as well as reducing the variation in period present in a population of dissociated neurons [7]. In *Drosophila*, interneuronal coupling in the core circadian clock is mediated by the peptide *pigment-dispersing factor* (PDF), and mutants lacking PDF show rapidly damped circadian rhythms in the absence of external forcing by light or temperature

[116]. Studying the nature of the coupling between neurons is more difficult in the fly than in the mouse because the *Drosophila* brain cannot be cultured intact or observed at length *in situ*. However, some light has been shed on circadian interneuronal communication by genetic means. One recent study [216] used UAS-GAL4 drivers (see Chapter 3) to selectively express mutant alleles of the kinases *shaggy* and *doubletime* in subsets of circadian clock neurons in wild type *Drosophila*. Expressing the $DBT^S$ or $SGG^{CA}$ mutant proteins (both of which cause approximately 19-hour circadian rhythms in isolation) in PDF-positive neurons leads to a quasi-periodic circadian rhythm displaying both 19 and 24-hour periodicities. The properties of the *Drosophila* circadian clock as a population of coupled oscillators have also been examined by phenomenological experiments, the most notable of which are the work of the mathematician and biologist Art Winfree in the early 1970's, which we introduce in the next section.

## 4.1 Phase-resetting and the phase singularity

Before the era of circadian genetics was launched by the discovery of *per* by Konopka and Benzer [101], biological rhythm research relied on behavioral observations, generally based on the rhythmic eclosion of adult *Drosophila* from pupae, combined with environmental manipulations consisting of controlled light and temperature stimuli (see [152] for one historical account). The classic experiment of this type involves the measurement of a *phase-resetting* or *phase-response curve* (PRC). In a typical PRC experiment, a group of flies are synchronized by exposure to a common environmental light program, and then allowed to free-run in constant darkness. Then, at a particular time during the flies' subjective circadian cycle, they are exposed to a specific stimulus, for example a

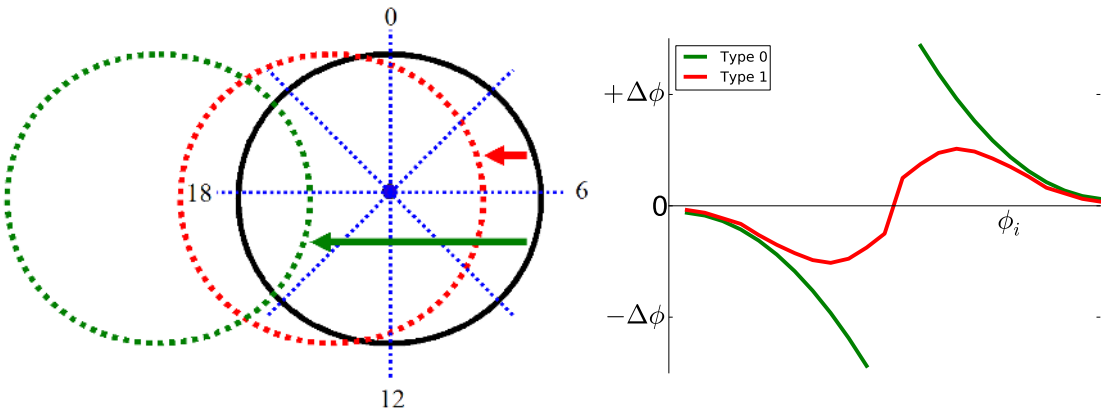


Figure 4.1: Schematic of a typical PRC experiment (left) and corresponding phase transition curves (right). The black circle indicates the native circadian limit cycle, and green and red curves indicate the results of strong and weak phase-resetting experiments, respectively. Lines of phase in the native phase plane are in blue, and the blue dot indicates the phase singularity.

step change in temperature or a light flash of a particular duration and intensity. The flies are then allowed to free run again, and the phase of their circadian oscillation is compared to a control group that did not receive the stimulus. New phases are then measured for a series of stimuli at different times spanning the subjective circadian day and plotted against the control phases, resulting in the PRC. A similar plot showing the difference between new and old phase is generally referred to as a *phase transition curve* (PTC). A schematic of a PRC experiment with its corresponding PTC is shown in Figure 4.1.

The twenty-four hour periodicity of the circadian rhythm requires that the PRC also be periodic, and the curve will therefore have an average slope of either zero or one. For weak stimuli, new phases will be close to old phases, and the average slope of the PRC will be one (the slope of the corresponding PTC will be zero). This is known as Type 1, or weak, phase resetting. For strong

stimuli, the circadian rhythm will tend to be reset to the same phase regardless of the time of day, and the PRC will be near constant, and have average slope zero (with the corresponding PTC having slope one). This is known as Type 0, or strong, phase resetting. The nature of the transition from Type 1 to Type 0 resetting can be understood by considering the diagram in Figure 4.1. The black circle is an abstract representation of the circadian limit cycle in an arbitrary planar coordinate system (consider, for example, a plot of TIM protein against *tim* mRNA concentration). Times of day and the associated phases of the circadian clock correspond to particular positions along the limit cycle. The points of phase along the limit cycle can be extended to lines of phase (dotted blue lines in the diagram) in the plane by considering the phase at which the circadian clock would relax back to the limit cycle if initialized at any arbitrary point. The effect of a stimulus is to move the state of the clock to the left in the phase plane (just as the effect of light is to degrade TIM protein). Applying a particular stimulus at every phase of the circadian limit cycle (as in a PRC experiment) then leads to a "shifted cycle" some distance to the left in the plane. The crossings of this shifted cycle with the original lines of phase predict the results of the PRC experiment. It can thus be seen from the diagram that a weak stimulus (red circle and arrow) will lead to a shifted circle crossing every line of phase, and thus to a Type 1 PRC, whereas a strong stimulus (green circle and arrow) will lead to a shifted cycle that crosses only a few lines of phase, leading to a Type 0 PRC. It can also be seen from the diagram that stimuli applied when the phase of the clock is in the top half of the circle result in a phase delay, while stimuli applied while the phase of the clock is in the bottom half of the circle result in a phase advance.

It was noted early on by Colin Pittendrigh, as well as by Winfree (his stu-

dent in Princeton at the time), that the transition from Type 0 to Type 1 resetting entailed a discontinuity in the behavior of animals exposed to stimuli of increasing strength [206] (and see [210] for an extensive discussion of Winfree's experiments). Indeed, one can see from the diagram in Figure 4.1 that a stimulus of a critical strength, exactly at the division between Type 1 and Type 0 resetting, applied at a critical time, at the phase where resetting switches from phase advance to delay, will result in the clock being shifted to a point of undefined phase (the blue dot in the center of the limit cycle). This point, known as the *phase singularity*, is located at the intersection of the lines of phase in the plane, and in a simple dynamical model, will correspond to the unstable fixed point at the center of the limit cycle. Winfree argued [206], and it has subsequently been proven on topological grounds [68], that any oscillator must feature a phase singularity corresponding to a point where lines of phase merge in the plane of the limit cycle. Therefore, it should be the case that a properly designed stimulus can lead to a random resetting of the phase of an oscillator, rather than the predictable resetting resulting from a typical stimulus.

Winfree performed a large number of phase resetting experiments using the fruit fly species *Drosophila pseudoobscura*, with blue light as the stimulus and the pupal eclosion rhythm as his reporter of the circadian rhythm [206]. By following the program outlined above, he was able show experimentally that a properly tuned blue light stimulus would lead to a vanishing of the collective population exclusion rhythm, due to random phase resetting of the individuals animals in the population. This proved that the phase singularity existed and could be accessed by a properly designed stimulus. Winfree was also able to show that the disruption of the circadian rhythm resulting from the critically tuned stimulus lasted much longer than the duration of the light pulse itself.

One can see from the diagram in Figure 4.1 that if the amplitude of the circadian rhythm were temporarily reduced (for example during recovery from the phase singularity), that a strong resetting stimulus would lead to a narrower range of new phases than if the amplitude of the oscillation were normal. In other words, the amplitude of a Type 0 PRC would be reduced, and could act as a reporter for the amplitude of the underlying circadian clock (which Winfree had no way of observing directly). Winfree performed such a two-pulse experiment, in which a large number of flies were exposed to the critical pulse, and then exposed to a series of assay light pulses of saturating intensity. The results showed that the amplitude of the circadian rhythm remained depressed for at least three days following the critical light stimulus [208]. Winfree argued that this was due to weak coupling between individual circadian neurons in the brain of the fly, so that even in individual animals, the overall amplitude of the circadian rhythm remained small after each neuron's phase was randomly reset by the initial light pulse. He had thereby shown that even a simple phase-resetting experiment could provide powerful insight into the nature of the circadian neuronal population inside the *Drosophila* brain.

However, Winfree's experiment did not distinguish between two possibilities: first, that the coupling between individual neurons in the fly brain was weak, or second, that interneuronal coupling was strong, but relaxation of individual oscillators from the unstable fixed point to the native limit cycle was slow (this was first pointed out in [2]). Resolving this ambiguity requires the ability to observe circadian rhythms in individual organisms, which Winfree did not have. However, a number of subsequent experiments have found phase singularities in other contexts. Random resetting of the phase by a critical light stimulus has been demonstrated in individual mosquitos using activity rhythms

as a reporter [148]. The presence of a phase singularity has also been demonstrated using light in *Neurospora* [82], as well as in human subjects, where body temperature and cortisol rhythms are disrupted [89]. The only experiment to obtain direct data on the amplitude of the circadian rhythm in an intact organism was preformed in the flowering plant *Kalanchoë*, where a critical light stimulus was shown to disrupt normal rhythms in petal movements for 3-6 days [49]. A phase singularity has also been found in individual mouse fibroblast cells supplemented with the light-sensitive protein melanopsin, where disruptions in luciferase reporter rhythms lasting 2-3 days were observed after a critical light pulse [193]. Unfortunately, none of these experiments were able to observe circadian amplitude in an intact animal with a population of coupled circadian neurons, and the question posed by Winfree's work remains open.

## 4.2 Phase singularity in individual *Drosophila*

Winfree's original work was performed on the pupated larvae of *Drosophila pseudobscura*, using population elocution measurements. Here we describe a new experiment demonstrating the existence of a phase singularity in individual *Drosophila melanogaster*. *Drosophila melanogaster* are known to be less light-sensitive than *pseudoobscura*, and the larvae of both species are known to be more light sensitive than the adults [209]. Winfree's procedures are therefore not directly applicable to an experiment on adult *Drosophila melanogaster*. However, the critical light stimulus required to pinpoint the phase singularity can be found by a similar approach. *Drosophila* $per^S$ mutants are known to be more light-sensitive than wild-type *Drosophila* [209], so phase-resetting experiments were performed using blue light stimulus on $per^S$ flies with Winfree's intensity

values as a starting point (the apparatus is described in Section 3.1). Since the period of $per^S$ flies is 19 hours, individual flies were synchronized by exposure to constant bright light followed by simultaneous shift into constant darkness, rather than by a day-night cycle (this is also the method used by Winfree). This works because prolonged exposure to light reduces PER and TIM protein concentrations to zero, fixing the phase of the oscillation when the lights are turned off. Activity rhythms of individuals were measured using DAM activity monitors (described in Section 3.1), and the phases of individual circadian rhythms were computed following the methods outlined in Section 2.2. Flies were allowed to free run in constant darkness for at least three days before application of a light stimulus, and stimulus times were chosen with reference to the peak in the 19-hour activity oscillation, averaged over the experimental population. Figure 4.2 shows the results of fourteen separate experiments, plotted as phase shifts (PTCs).

The PRC experiments in Figure 4.2 all involve a 30 lux blue light stimulus applied for varying durations beginning at varying times after the peak of daily activity. We can see (noting the sample plot in Figure 4.1) that for stimuli of longer than 120 minutes, the shape of the curves appears to be consistent with strong Type 0 phase resting, and for stimuli 90 minutes long, the curve is consistent with weak Type 1 resetting. Additionally, the crossover point from phase delay to phase advance occurs at about five hours after the time of peak activity in the population. Further experimentation showed that a stimulus of 105 minutes at 4.5 hours post-activity peak effectively desynchronizes the population. Activity data from a representative subset of flies in this experiment is shown in Figure 4.3. The light stimulus is applied at hour 60, and we can see that the flies are synchronized before the pulse, but distributed at more or less random

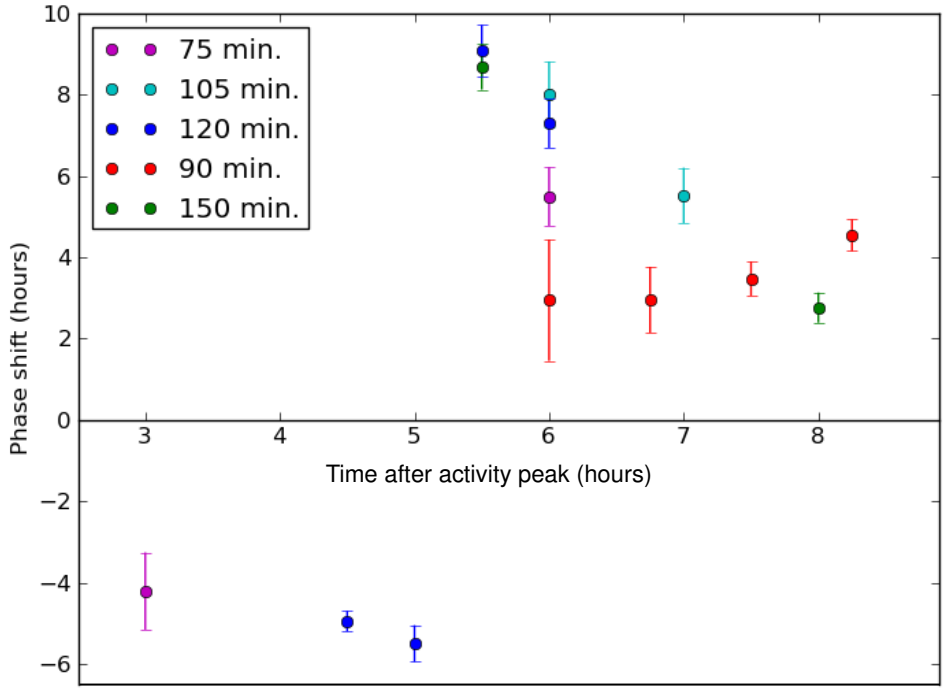


Figure 4.2: Phase-resetting of the *Drosophila* circadian activity rhythm in response to light. Light stimuli consisted of 30 lux of blue LED light applied at the indicated times after the population activity peak, and for the indicated durations. Phase shifts are measured relative to an unstimulated control population, and error bars indicate standard error of the mean.

phases after (see Figure 4.4A for quantification). Interestingly, most individual activity rhythms return to normal amplitude (at a new phase) essentially immediately after the light stimulus, seemingly contradicting the results of Winfree. However, it has been shown in prior experiments [198] that the amplitude of the activity rhythm is not a good indicator of the amplitude of the underlying molecular circadian oscillation. Additionally, a few of the individuals do show some disruption in their circadian rhythms after the stimulus (see, for example, the second and fourth rows).

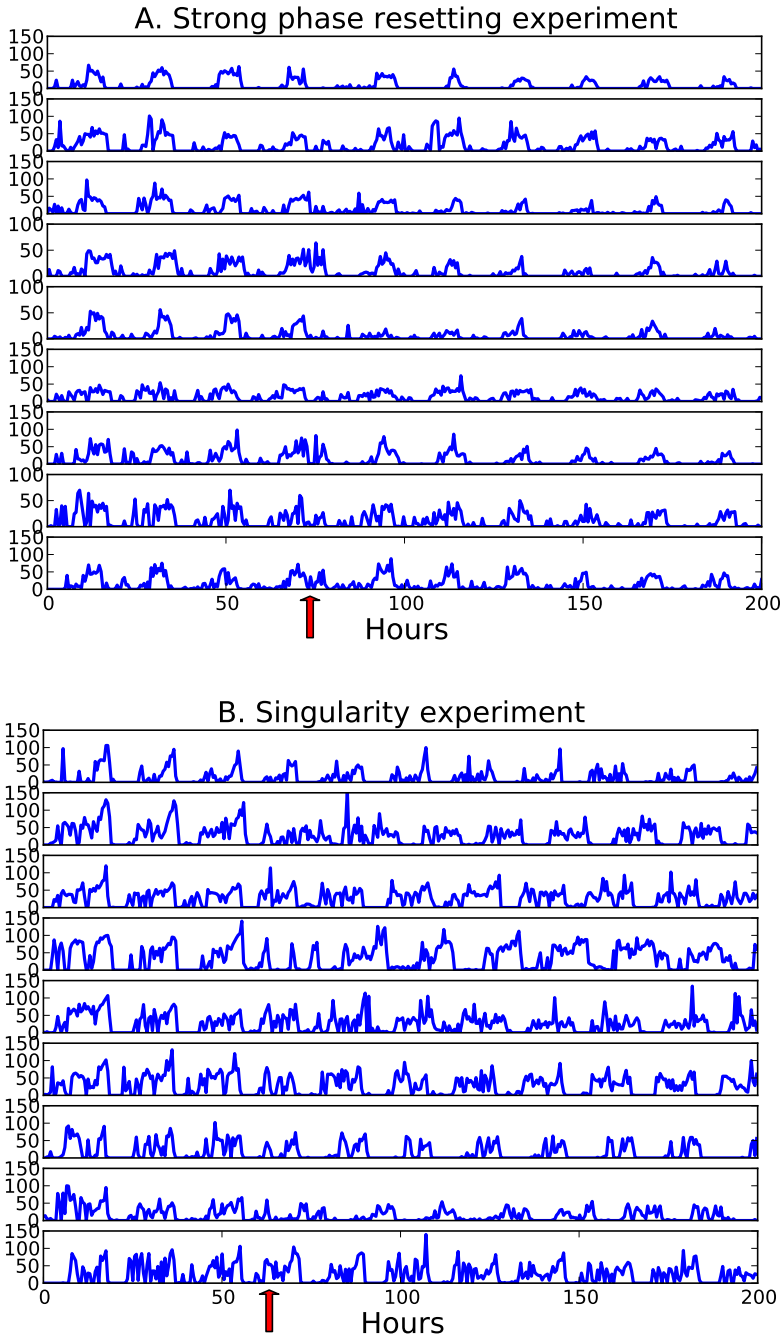


Figure 4.3: Raw data from two phase resetting experiments. (A) A typical strong phase resetting experiment in which a pulse of light applied at a certain time (red arrow) predictably shifts the phase of a whole population. (B) Singularity experiment in which a critical-timed stimulus (red arrow) randomly phase shifts a population. In both panels, pink shading indicates the active phase of the activity rhythms, with white space left around the time of the light stimulus as an aid to the eye.

One approach to quantifying this effect is to calculate a measure of overall *rhythmicity* of the circadian activity oscillation, rather than simple amplitude. One can imagine that a reduction in amplitude in the molecular oscillation might lead to an increase in noise in the activity output rhythm, if not to a change in amplitude. This can be quantified by calculating the time autocorrelation function of running subsets of the activity rhythm, according to the following equation

$$C_t(\tau) = \frac{1}{V}\frac{1}{T-\tau}\sum_{i=0}^{T-\tau} x(t+i)x(t+i+\tau) \tag{4.1}$$

where $x(t)$ is the time series, $T$ is the width of some subset centered at time $t$, and $V$ is the variance of the time series. $C_t(\tau)$ is thus the covariance between a subset of the time series centered at time $t$ and itself, shifted by $\tau$. In the measurements below, $\tau$ was varied from 0 to $3T/4$. $C_t(\tau)$ will be periodic with the same period as $x$, with an amplitude between zero and one, determined by the contribution of noise to the time series (see Section 2.2 for a more detailed discussion). We can call the amplitude of $C_t(\tau)$ the *normalized rhythmicity* at time $t$. Figure 4.4B shows a plot of normalized rhythmicity (computed using segments of width 60 hours) averaged over populations, for two different light stimuli. The control population received a 120 minute pulse 6 hours after the activity peak, producing an average phase shift of about 7 hours. The other population received the same critical stimulus as that shown in Figure 4.3.

Figure 4.4A shows a circle plot of the post-stimulus phases of individuals in both populations, relative to the full 19-hour cycle of the typical $per^S$ fly (computed by cross-correlation with a control population, see Section 2.2). The strongly-resetting stimulus applied to the control population leads to phases

clustered around hour 7 (relative to an unstimulated population) with a standard deviation of about 1.5 hours, while the critical stimulus leads to phases randomly distributed about the circle. Randomness can be judged by comparing the vector sum of the phases in the group to the expected value for a randomly distributed group of the same size, which is given by $\langle r^2 \rangle = (2N)^{-1}$. As can be seen from the figure, the magnitude of the vector sum for singularity population is consistent with a random distribution.

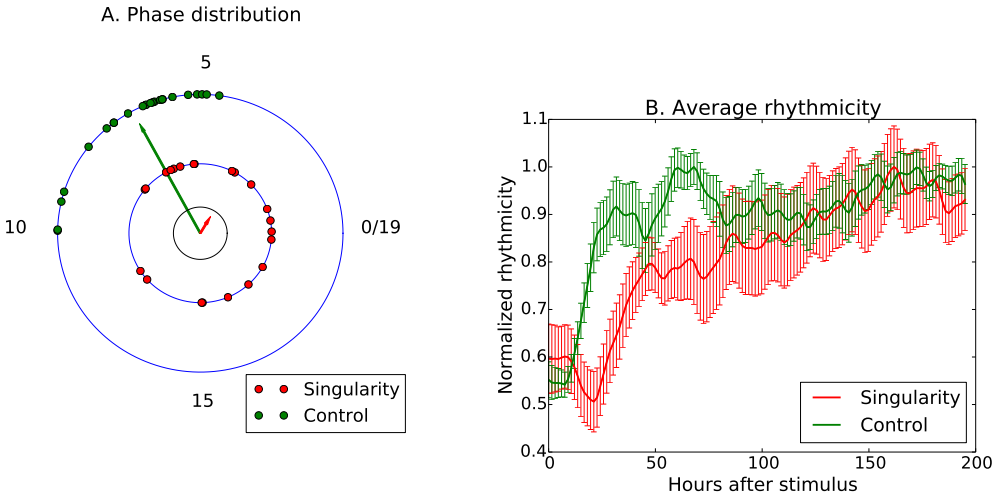


Figure 4.4: Effect of light stimuli on phase coherence and rhythmicity of *Drosophila* populations. (A) Phases of individual flies in populations subjected to the critical light stimulus and a strongly-resetting control stimulus. Arrows show the vector average of the phases in each group, and the black circle indicates the expected magnitude of the vector average for a randomly distributed sample of the same size as (red) population shown. (B) Recovery of normalized rhythmicity in the same populations, calculated for individuals and averaged. Error bars are standard error of the mean at each time point. The horizontal axis is hours after the beginning of the light stimulus.

The recovery of rhythmicity after the critical stimulus takes on the order of 100 hours, about 4-5 periods of the circadian oscillation, which is consistent with

the observations from Winfree's two-pulse experiment. Recovery of rhythmicity in the control population takes only about 30 hours, which is roughly the minimum possible considering the 60-hour width of the running window used for the computation. This is consistent with a variety of experiments showing that the circadian clock is reset essentially instantly by strong light stimuli [90]. Additionally, the shape of the recovery curve in the critical case is suggestive of the exponential relaxation of amplitude characteristic of weak coupling in the Kuramoto model or coupled oscillators (see Section 2.1). However, as can be seen from Figure 4.3 and the error bars in Figure 4.4, the variability between individuals in the population is significant, and it is far from clear that fitting a model like that discussed in Section 2.1 to the averaged curve in Figure 4.4 would be justifiable. Thus, while the experiment of Figure 4.3 proves that a phase singularity is present in the circadian oscillator of individual *Drosophila*, and is highly suggestive of long-term disruption of the circadian rhythm after the singularity is reached, it does not allow us to directly infer the strength of coupling between circadian neurons.

## 4.3 Inferring coupling from average rhythm data

The ideal system for studying coupling between circadian neurons is the cultured explant from the mouse suprachiasmatic nucleus. Oscillations in individual neurons in a cultured SCN can be observed by means of luciferase reporters [214] or firing rate measurements [7]. Normal coupling between the neurons is present in an intact SCN explant, but can be eliminated either by genetic means [7] (knocking out genes coding for either neurotransmitters or their receptors) or by blocking electrical communication using a chemical such as tetrodotoxin

(TTX) that inhibits sodium channel activity [214]. Experiments of this sort have suggested on two grounds that strong coupling exists between neurons in the SCN. First, the period of oscillation in neurons in an intact SCN varies by only about an hour, while in an SCN where coupling has been eliminated by knock-out of the neurotransmitter vasoactive intestinal peptide (VIP) the period varies by closer to ten hours between neurons [7]. Second, the amplitude and coherence of oscillations in individual neurons is significantly reduced when coupling is eliminated by application of TTX [214]. We saw earlier (see Section 2.4) that the low-amplitude oscillations in the absence of coupling may in fact be damped and noise-driven rather than truly self-sustained oscillations. In any case it clear that there are sting effects from coupling on both amplitude and frequency of individual cellular oscillators. Data from these experiments are shown in Figure 4.5.

An intact *Drosophila* brain has not been cultured, and methods for imaging the brain in living flies are limited [172]. However, there is potential for inferring facts about interneuronal coupling from phenomenological *Drosophila* data. The first such piece of data is the damping rate of circadian rhythms in *Drosophila* lacking the neuropeptide PDF. Upon transfer from a synchronizing light regime into constant darkness, the amplitude of activity rhythms in PDF-null flies decays to zero in about three days due to lack of interneuronal coupling [116]. This can be understood quantitatively by considering a simple model in which a population of oscillators has a phase distribution $p(\theta)$. In this case the amplitude $a$ of the collective oscillation is given from the amplitude $a_0$ of the individual oscillators by the convolution

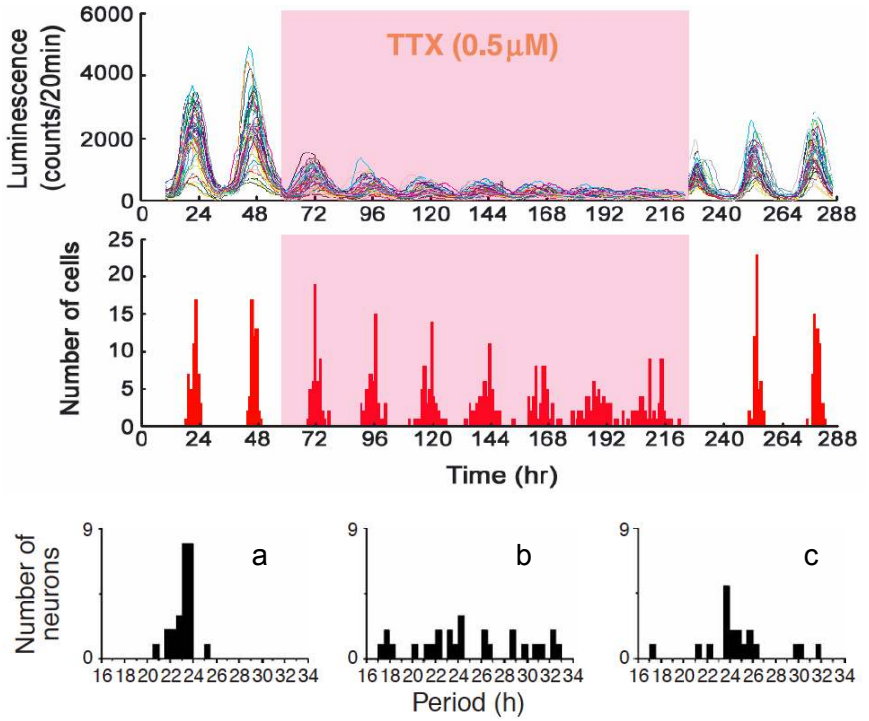


Figure 4.5: The effect of eliminating coupling on neuronal circadian oscillation in mouse SCN explants. (Top) Luciferase oscillations and peak phase distributions of neurons in an intact mouse SCN treated with the sodium channel-blocker TTX (shaded region). From [214]. (Bottom) Distribution of periods in an intact SCN explant from a wild-type mouse (a), or from a mouse lacking the gene for the neurotransmitter VIP (b), or the receptor for VIP, Vipr (c). From [7].

$$a = a_0 \int_0^{2\pi} p(\theta) \cos\theta d\theta. \tag{4.2}$$

In the case that the oscillators are strongly bound to their native limit cycle we can consider only the phase coordinate, and the effects of noise can be modeled as diffusion around the circle, so that the distribution $p(\theta)$ will be a Gaussian with variance $\sigma^2 \sim Dt$ for some diffusion constant $D$. This gives

$$a = \frac{1}{\sqrt{\pi\sigma^2}} \int_{-\infty}^{\infty} e^{-\theta^2/\sigma^2} \cos\theta d\theta = e^{-\sigma^2/2} = e^{-Dt/2} \tag{4.3}$$

where we set $a_0 = 1$. For analytical simplicity we use the standard Gaussian rather than a circularized distribution like the von Neumann distribution, which then requires the limits of integration to be set to $(-\infty, \infty)$ rather than $(-\pi, \pi)$.

Amplitude is thus expected to decay exponentially in time, with a time constant set by the phase diffusion rate of the individual oscillators. Note that the total number of oscillators does not appear in the formula. We can attempt to gain some information about coupling in the *Drosophila* brain by applying the same calculation to the activity rhythms of wild-type animals. Figure 4.6 shows a representative set of individual activity rhythms for wild-type flies as well as a calculation of their phase diffusion rate. The flies start in a 24-hour light-dark cycle and at hour 75 are transferred to constant darkness. The phase of the activity rhythm for each individual animal is measured relative to the population average for three segments of time, stretching from hour 100 to 183, 184 to 267, and 267 to 350. At each time point, the phases are converted to angles and summed as vectors of length one, giving a summed amplitude which can be fit to the form in Equation 4.4. The result is a decay time of 2950 hours, or about 123 days.

This rate of phase diffusion of the circadian oscillation is certainly acceptable for wild-type *Drosophila*, which generally live less than 60 days, but it is only about about 40 times less than that in PDF-null mutants. This 40-fold difference is roughly equal to the number of neurons in the DN cluster known to be responsible for circadian output (see Section 1.4), and is therefore about what would be expected from a mere summation of independent oscillators. It seems that,

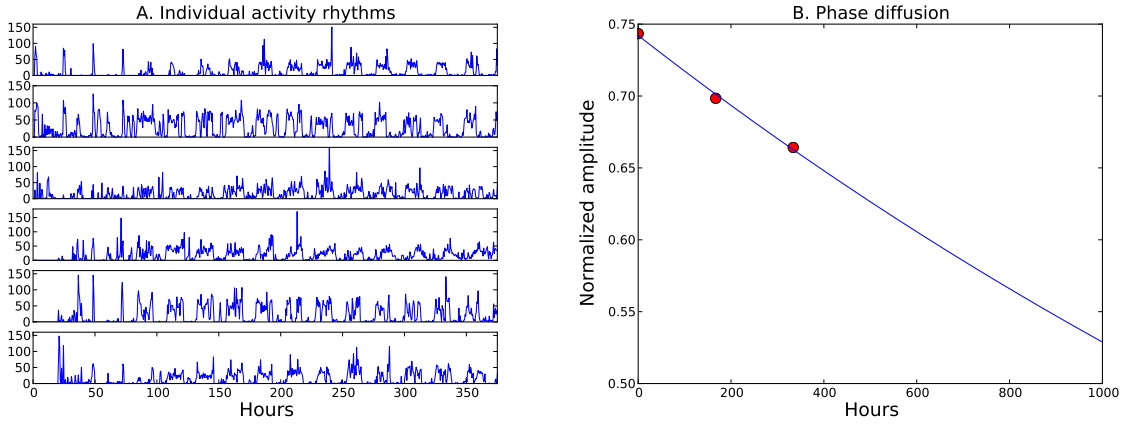


Figure 4.6: Phase synchrony in an initial synchronized *Drosophila* population. (A) Representative activity rhythms of individual flies starting in a 24-hour light dark cycle and moved into constant darkness at hour 75. (B) Measurement of the phase coherence of the population, computed by taking a vector sum of the phases of individuals in progressive time windows after the shift into darkness, and fit to the formula in Equation 4.4.

unlike in the mouse, the stiffness and coherence of individual neuronal oscillations in the fly is not strongly affected by intercellular coupling. It is important to note, however, that this is not a direct indication that interneuronal coupling is weak, *per se*. In the Kuramoto model with linear coupling between oscillators (see Section 2.1), the strength of coupling does not affect the rate of phase diffusion of the population average. This can be seen by diagonalizing the system of equations describing the oscillator population, which leads to the population averaged phase being given by a zero eigenvector that diffuses freely around the circle, regardless of coupling strength. An effect on phase drift must come from an increase in the amplitude or coherence of individual oscillators, which is does not happen in the Kuramoto model and does not appear to be present in *Drosophila*, unlike in the mouse. We can conclude, however, that if there is not a strong amplitude effect from coupling in *Drosophila*, that intercellular coupling

in the fly is in some sense weak, at least by comparison to mammalian clocks.

Direct evidence about the nature of interneuronal coupling in *Drosophila* will likely require an imaging experiment similar to those conducted in the mouse. There is some hope for achieving this without a major advance in tissue culture methods. Imaging of molecular circadian oscillations in fixed *Drosophila* brains is a well-established technique [78] (and see Section 3.5 for a discussion of confocal brain imaging). In particular, oscillations in PER and TIM proteins have been imaged over several days in brains fixed from a synchronized population, with reasonable quantitative accuracy [174]. By imaging two out-of-phase markers of the circadian oscillation in fixed brains taken from a synchronized population over the course of a day in constant darkness, it should be possible to build up a set of markers that would allow determination of the phase of oscillation in individual neurons in a fixed brain. It would then be possible, by applying the same imaging technique to brains fixed from flies exposed to the critical light stimulus, to measure the degree of phase synchrony between neurons in the brain of an animal recovering from the phase singularity. Enough measurements of this type should be sufficient to build up an estimate of the coupling strength between various circadian neurons in the *Drosophila* brain.

The above experiments have demonstrated clearly that a phase singularity is present in the *Drosophila* circadian oscillator, and that it can be reached by application of carefully chosen light stimuli. The behavior of individual flies exposed to the critical stimulus also suggests that there is long-term effect associated with recovery from the phase singularity. Phenomenological observations of rhythmic fly behavior indicate that coupling between circadian neurons in *Drosophila* is likely to be weak, further suggesting that the long-term effects

of the phase singularity (as seen in Figure 4.4b) are due to slow resynchronization of neurons after random phase resetting. This observation is interesting due to the contrast with evidence from the mouse, where interneuronal coupling appears to have strong effects on the coherence of oscillations in individual neurons. This is consistent with other experiments, which show that a period difference of about 5 hours between groups of neurons in the fly leads to quasi-periodic activity [216], while coupling in the mouse brain is able to synchronize neurons with native period differences as great as ten hours [7]. It seems likely that this difference in design between the circadian clocks of mice and flies is related to the large difference in the number of neurons between the two species, however, further speculation about the design of circadian oscillator populations will be reserved for the final chapter.

CHAPTER 5

# TEMPERATURE SENSATION AND TEMPERATURE COMPENSATION

*Temperature compensation* (having a temperature-independent period) and *temperature sensation* (being able to entrain to external oscillations in temperature) are defining properties of circadian clocks. Most biological reactions have temperature-sensitive rates, with typical $Q_{10}$ values falling in the range of 2-3 (meaning that reaction rates increase by a factor of 2-3 over a 10°C change in temperature) [72]. The period of the circadian clock actually lengthens slightly as temperature increases, going from about 23.5 hours at 17°C to 24 at 29°C, leading to a $Q_{10}$ of approximately 0.98 [102]. Enzymatic reactions whose rates are entirely insensitive to temperature are not unknown, particularly in organisms that experience large changes in temperature in their natural environment (those living in tidal pools, for example, see [72] for a review). However, the circadian clock is known to be highly temperature sensitive, *Drosophila* for example are able to entrain to temperature cycles with amplitudes as low as 1°C [207]. The puzzle of simultaneous temperature compensation and temperature sensation has been a key question in the field of circadian biology from the very beginning (see [203] for example).

Most theories of circadian temperature compensation have espoused what we will call the *network model* of compensation. In this model, the constitutive reactions of the circadian clock are temperature sensitive in the usual way. However, the quickening of some reactions (such as transcription and translation) tends to shorten the period of the circadian clock, while the quickening of other reactions (such as protein degradation in the cytoplasm) tends to lengthen the period of the clock. This leads to a lengthening of some processes (e.g. nu-

clear translocation) being cancelled out by a shortening of other processes (e.g. mRNA transcription), with the overall effect of a temperature change on the period being zero (see [71] for an early example of this argument). A significant mathematical literature has formalized the network model by the approach of developing a biochemical model of the circadian clock, with various rate constants $k_i$, and positing elasticities $\alpha_i$ of the form

$$\alpha_i = \partial \log \tau / \partial \log k_i$$

where $\tau$is the period of the circadian oscillation (see [165] for an early example, whose discussion we follow here, and [107] for a review). By substituting an Arrhenius form with temperature $T$, activation energies $E_i$, and attempt rates $A_i$ for the rate constants $k_i = A_i \exp(-E_i/RT)$, one can derive a constraint of the form

$$\frac{\partial \tau}{\partial T} = \frac{1}{RT^2}\left[\sum_i \alpha_i E_i\right]\tau = 0 \tag{5.1}$$

The elasticities $\alpha_i$ can be derived from the model, which then allows the activation energies $E_i$ to be fit to the constraint, resulting in a temperature compensated period. The appeal of this class of models lies in the fact that the temperature entrainment puzzle is solved along with the temperature compensation puzzle, because the clock is inherently temperature sensitive. However, there are a variety of objections to the network model. First, because most circadian clock models will have a large number of rate constants, the constraint (5.1) will not constrain most directions in parameter space, so the associated fits are highly non-unique and essentially any model of the clock can be compensated in this manner. In particular this means that various network models fail

to make specific predictions that could distinguish one from another. Additionally, it has been pointed out that the delicate balancing required would suggest that any mutation leading to a change in the circadian period should also have a temperature compensation phenotype, and this is not the case [81].

A variety of other models for temperature compensation have been proposed. In cyanobacteria, the circadian period is set largely by the phosphorylation and dephosphorylation rates of on enzyme, KaiC, meaning that only a single reaction needs to be temperature compensated []. Similar models have been proposed for the circadian clock in animals [81]. However, this mechanism is somewhat unappealing since it is known that multiple separate processes contribute to determining the period of the circadian clock in animals (see Section 1.3 for a detailed discussion). Another model posits that the effect of temperature is uniform across different sub-processes of the circadian clock, and that this leads to an increase in amplitude of the oscillation which is precisely cancelled out by a corresponding increase in reaction rates (see [109] for an example based on *Neurospora*). It is this class of models that we discuss in the next section.

## 5.1 Temperature-insensitive clocks?

A recent paper [53] explored the mechanism of temperature compensation using a genetic algorithm-based computer simulation of evolution. Using a fitness function that checked for a spontaneous oscillation with a temperature-compensated period as well as the ability to entrain to temperature cycles, the simulation found that most evolved oscillators did not conform to the above-described network model. Instead, the clocks resulting from the simulation

tended to consist of a core oscillator that lacked any temperature sensation, combined with an adaptive signaling pathway. Such a pathway would be activated in response to changes in temperature, but would adapt back to a quiescent state at any constant temperature, thus preserving temperature compensation. Adaptive signaling systems of this sort are common in biology, in neural sensory pathways [34] as well as in cellular pathways such as the *Escherichia coli* chemotaxis networks [3]. Another class of models emerging from the simulation also features a temperature-independent core oscillator, and couples temperature to the clock in a way that does not affect the period, eliminating the need for an adaptive signaling pathway. An example of this type of model can be built on the classic Goodwin model [62] of a biological oscillator, which we discuss in detail in Section 2.3.

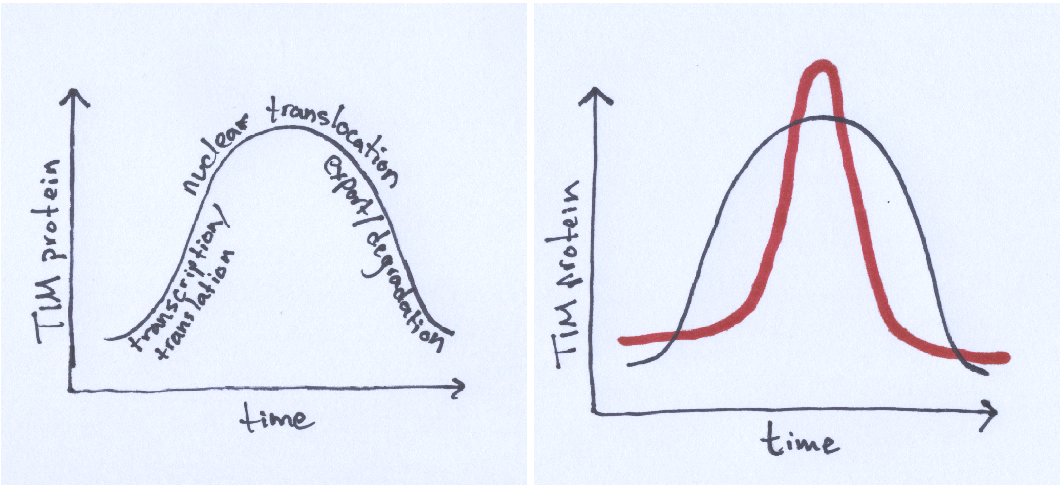


Figure 5.1: A cartoon of the circadian oscillation of TIM protein. On the left, various phases of the daily circadian cycle are marked on corresponding locations of the oscillation. On the right, a hypothetical scenario is shown in which a change in temperature causes a shortening of nuclear translocation time and a compensating increase in transcription time, leading to a change in shape of the oscillation.

One clear prediction of this model is that a specific system for signaling

temperature to the circadian clock should be present in *Drosophila* and other animals. In particular, it should be possible to reduce or eliminate circadian temperature entrainment by a single loss-of-function mutation in a temperature sensation pathway. This would not be possible in the network class of models, where the entire clock is temperature sensitive. A second prediction is that the dynamics of the clock should change with temperature only by a simple rescaling of amplitudes, and that there should not be changes in the scale-independent shape of the oscillation (see Section 2.2 for a detail argument). This prediction is also at odds with what would be expected from the network model. One can imagine, for example, that if temperature compensation was achieved by balancing a lengthening of the time required for transcription and translation of TIM and PER against a shortening of the nuclear translocation time, that this would lead to a change in shape of the oscillation due to the relative shortening of the period of time in which TIM and PER were present before repressing their own production. A cartoon of this situation is shown in Figure 5.1.

To test the prediction of simple scaling with temperature, one can measure the oscillation of various components of the circadian clock (protein and mRNA) at different temperatures. Figure 5.2 shows the oscillation of TIM protein at 18°C, 25°C, and 29°C. Flies were entrained in a light dark cycle, shifted to constant darkness, and then sampled by flash-freezing every hour on the second day in constant darkness. Protein was isolated from isolated heads, and TIM concentrations were measured by Western blot, with the structural protein cadherin (CDH) serving as control for loading volume.

Representative blot images are on the left of Figure 5.2, and quantifications

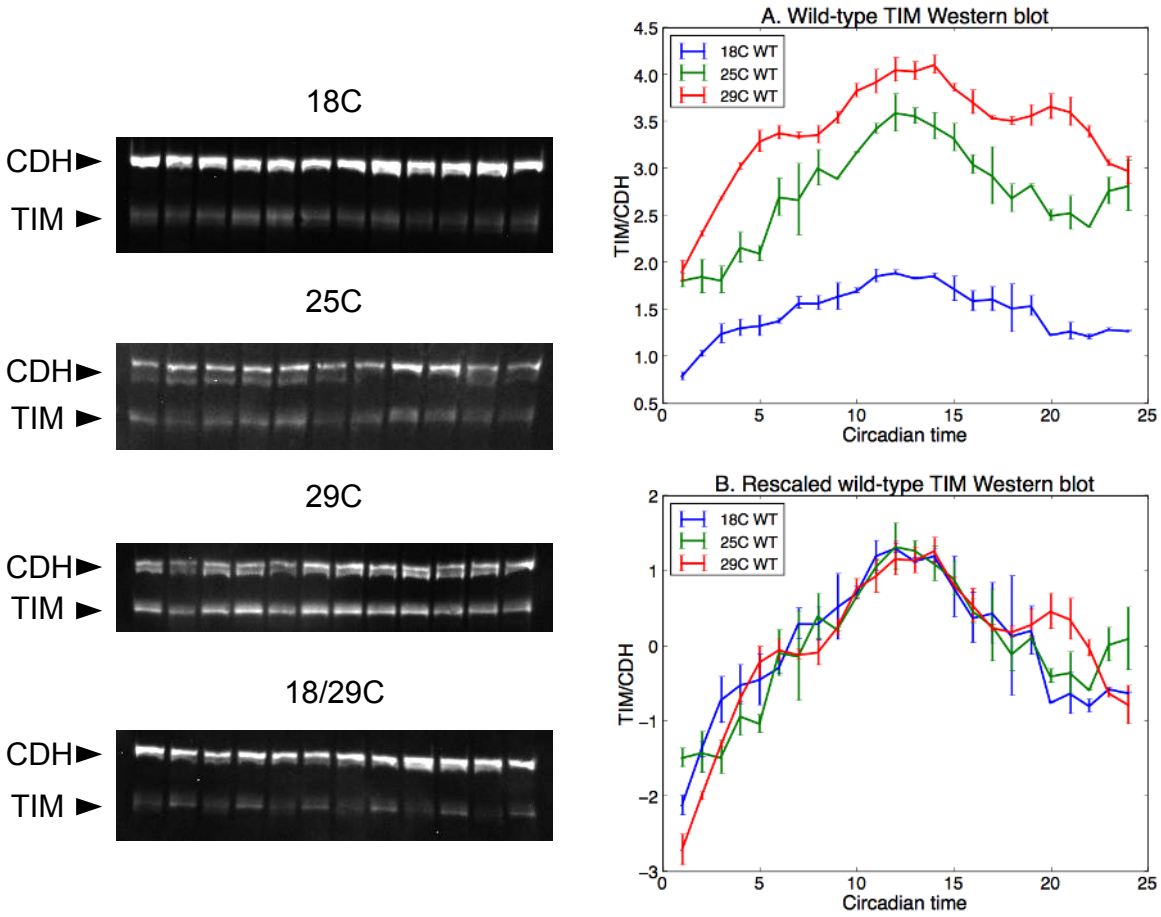


Figure 5.2: TIM protein Western blots at three different temperatures. Representative blot images are shown on the left. Bands correspond to time points two hours apart, covering on full day, except for the bottom band, which shows bands from the first 6 hours of the day at both 18°C (lighter bands) and 29°C (brighter bands). Panel A shows quantification of raw TIM concentrations relative to CDH. Panel B shows the same curves rescaled to have mean zero and amplitude one.

on the right. Figure 5.2A shows raw TIM concentrations over the subjective day, relative to CDH levels. Relative concentrations at different temperatures were adjusted by running gels with samples from two different temperatures side-by-side, as shown in the figure. We can see from the plot that average TIM levels increase at higher temperatures, and that the amplitude of the TIM oscillation is also somewhat larger at higher temperatures. Both of these observations are in agreement with the predictions of the Goodwin oscillator model discussed above. In order to test the prediction of simple rescaling with temperature, the mean is subtracted from each curve, and each curve is divided by its standard deviation, to produce oscillations with mean zero and amplitude one. The resulting scaling collapse is shown in Figure 5.2B, from which we can see that the shape of the TIM oscillation remains remarkably consistent across temperatures.

To further test the scaling hypothesis, it is desirable to measure oscillations from the transcriptional side of the circadian clock. Figure 5.3 shows data from flies expressing a transgenic firefly luciferase reporter. The coding sequence for firefly luciferase is inserted into the fly genome next to the promoter sequence from the *tim* gene, leading to circadian oscillations in luminescence. The construction of this *tim-luc* strain is discussed in detail in [179], where evidence is also presented that the expression of the *tim-luc* contract closely tracks native *tim* expression. To perform the measurement, luciferin substrate is mixed into standard *Drosophila* food in a 35mm plate. Roughly 50-100 male flies are placed on the food, and the plate is capped and put into a photomultiplier tube-equipped luminescence reader. The measurement is otherwise identical to the Western blot experiment, with animals being entrained by light dark cycles and then measured on the second day in constant darkness.

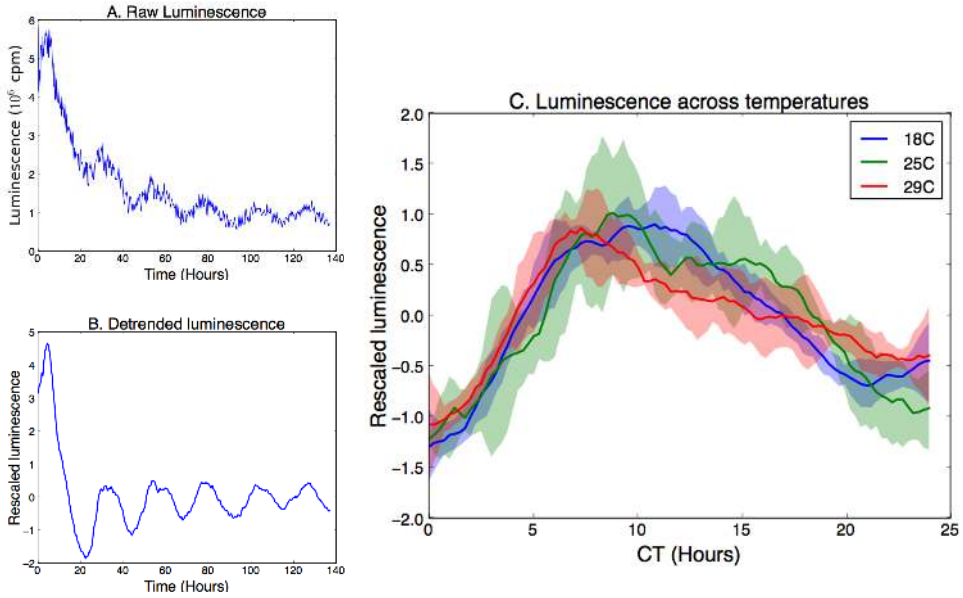


Figure 5.3: Luminescence from *tim-luc* flies at different temperatures. (A) A sample of raw luminescence data plotted in millions of photon counts per minute. (B) The same data after detrending and smoothing. (C) Rescaled luminescence curves from *tim-luc* flies at different temperatures, taken from the second day in constant darkness. Shaded areas indicate standard error of the mean across three repetitions of the experiment.

Consumption of the luciferin substrate by the flies leads to a decay in the average value of luminescence over time, as can be seen from the raw data shown in Figure 5.3A. The data also features white noise due to movement of the animals in the sample plate, and shot noise from photon counting. To account for these effects, the data are detrended by subtracting a 24-hour moving average, and smoothed by averaging over a 1-hour moving window. The effects of these manipulations are shown in Figure 5.3B. Figure 5.3C shows luminescence oscillations from the second day in constant darkness for flies measured at 18°C,

25°C, and 29°C, after the same rescaling procedure described above. As with the TIM protein oscillations, there is reasonable agreement between the shapes of the curves at different temperatures. The curve at 29°C features a slightly more shallow decay than the curves at 18°C and 25°C. This is likely due to the significantly greater rate of decay in average luminescence that occurs at higher temperatures, which in turn is likely caused by the lower stability of luciferase at high temperatures. Luciferase is known to become unstable at temperatures above about 30°C [192].

Indeed, all of the curves shown in Figures 5.2 and 5.3 feature slight differences in shape across temperature, which in general we could claim are due to the noise inherent in experimental measurements. In order to confirm this, it is useful to have a measurement of oscillations which the Goodwin model *would* predict to have different shape at different temperatures. The $per^L$ mutation causes a temperature-sensitive defect in binding between PER and TIM [59]. This leads to a long period at room temperature, caused by a delay in nuclear translocation caused by decreased PER/TIM dimerization, as well as a defect in temperature compensation [83]. The period of the circadian clock in $per^L$ flies is about 27 hours at 18°C, 29 hours at 25°C, and 31 hours at 29°C [156]. The argument described in Figure 5.1 suggests that the lengthening of a single subprocess of the clock (in this case, nuclear translocation) should lead to a change in shape of molecular oscillations at different temperatures.

Figure 5.4 shows the same Western blot time-course measurement discussed previously, performed using $per^L$ flies, and extending over 30 hours instead of 24. Figure 5.4A shows raw and Figure 5.4B rescaled data. The data shows that even the relatively minor temperature compensation defect present in the $per^L$

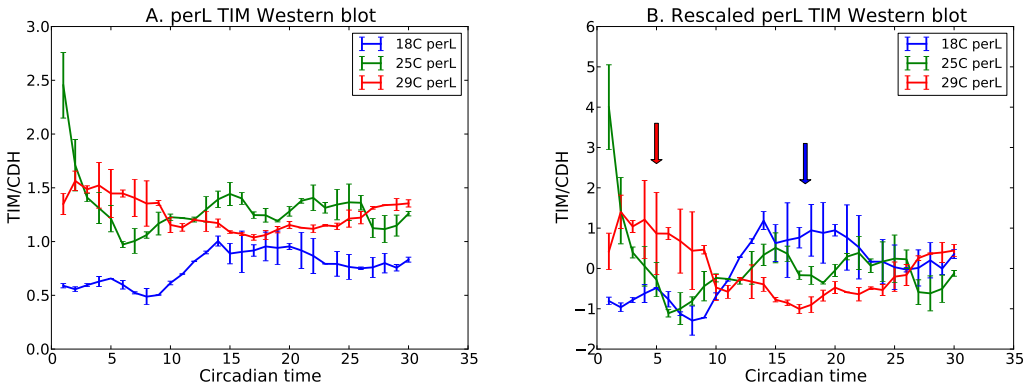


Figure 5.4: TIM protein oscillations in $per^L$ flies, measured by Western blot. (A) Raw TIM concentrations at three different temperatures, relative to cadherin. (B) TIM oscillations rescaled to have mean zero and variance one. Arrows indicate the position of peaks at 18°C and 29°C.

strain ($Q_{10}$ of 0.87 instead of 0.98) leads to a dramatic change in the shape of TIM oscillations across temperatures. The peak of the oscillation shifts from subjective mid-afternoon to late night/early morning, consistent with the delay in nuclear translocation (and therefore transcriptional repression) known to be present in the $per^L$ strain.

We have also performed luciferase reporter measurements in the $per^L$ background. The *tim-luc* construct was crossed into $per^L$ mutant flies to generate a reporter strain with the $per^L$ mutation that also carried *tim-luc* on both copies of the third chromosome. We then repeated the luciferase reporter experiment exactly as before. Results are shown in Figure 5.5. As we can see, the shifting of the peak phase with temperature is also present in the luminescence oscillations of the *tim-luc* transcriptional reporter. This further confirms the presence of measurable changes in limit cycle shape in the $per^L$ mutant.

The intuitive idea that a progressively increasing delay in nuclear transloca-

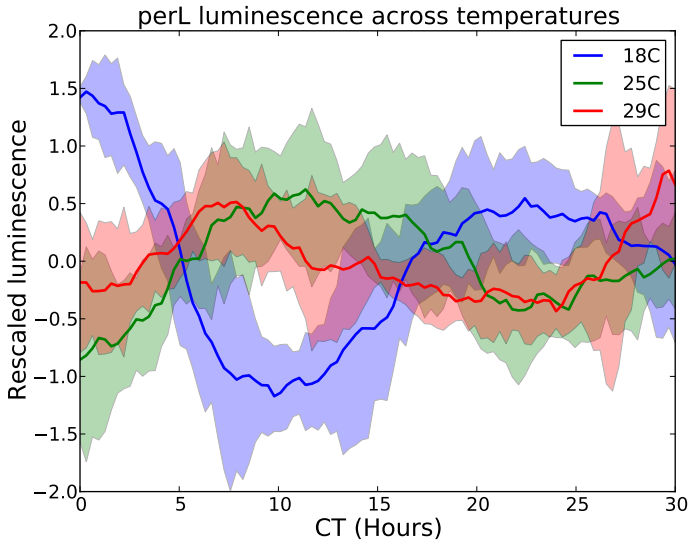


Figure 5.5: Rescaled luminescence curves from $per^L$ *tim-luc* flies at different temperatures, taken from the second day in constant darkness. Shaded areas indicate standard error of the mean across three different experiments.

tion should lead to a shift in the peak of circadian oscillations can be checked with a simple model. We use the model described in [191], in which an mRNA $M$ is translated into a protein $P_1$, which can form a homodimer $P_2$ that represses transcription of $M$. The equations are as follows

$$\frac{\mathrm{d}M}{\mathrm{d}t} = \frac{v_m}{1 + (P_2/P_{\mathrm{crit}})^2} - k_m M \tag{5.2}$$

$$\frac{\mathrm{d}P_1}{\mathrm{d}t} = v_p M - \frac{k_{p1} P_1}{J_p + P_1 + r P_2} - k_{p3} P_1 - 2k_a P_1^2 + 2k_d P_2 \tag{5.3}$$

$$\frac{\mathrm{d}P_2}{\mathrm{d}t} = k_a P_1^2 - k_d P_2 - \frac{k_{p2} P_2}{J_p + P_1 + r P_2} - k_{p3} P_2 \tag{5.4}$$

The model features protein dimerization (given by the rate $k_a$), phosophorylation-regulated degradation (represented by the rates $k_{p1}$ and $k_{p2}$, and transcriptional repression, while being relatively simple and straightforward. We can model

the effect of temperature in the $per^L$ mutant by decreasing the value of the binding rate $k_a$ while leaving the dissociation rate $k_d$ constant. The experiment in Figure 5.4 can be simulated by initializing the model in a state where protein is low and mRNA is high (like at the end of the day in a light-dark cycle), and then plotting the oscillation of $P_1$ after one full period has passed. The results are shown in Figure 5.6. There is a qualitative similarity between the effect of increasing temperature in the model and in the experimental data. In particular we can see in both cases a shift in the peak of the oscillation towards the late night/early morning.

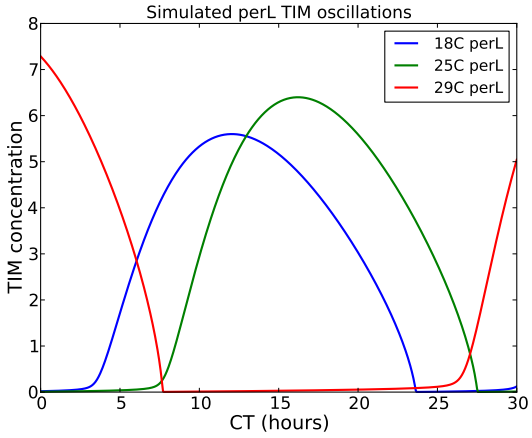


Figure 5.6: Simulation of the experiment shown in Figure 5.4 using the model developed in [191] to simulate different circadian mutations.

These results should of course be taken with a grain of salt since the model is oversimplified and our choice of parameters is somewhat arbitrary. However, they serve as a useful sanity check on our explanation of the experimental data. In general, we can conclude that quantitative Western blotting is a sufficiently sensitive measurement technique to detect the changes in shape of molecular oscillations associated with changing timescales in the circadian clock. This means that the above results constitute good evidence for the prediction that

the effect of temperature on the shape of circadian oscillations should be only simple rescaling of amplitude, and not changes in shape. We can therefore conclude that all the various sub-processes of the circadian clock in *Drosophila* are independently temperature compensated, and that the core clock is temperature insensitive. This leads us to the second prediction of the evolutionary model in [53], that there should be a specific separate pathway mediating temperature sensation of circadian oscillations.

## 5.2 Circadian temperature sensation

A variety of experiments have found sensory pathways involved in circadian entrainment to temperature cycles. *Drosophila* sensory bristles possess specialized structures, the *chordotonal organs*, that are involved in sensing tactile stimuli, as well as in thermotactic behavior [108]. Mutations in two genes, *nocte* and *norpA*, that are involved in chordotonal organ functions, have been shown to result in defects in circadian entrainment to external oscillations in temperature [171]. Additionally, a neural pathway involving the temperature-sensitive TrpA ion channel has also been shown to affect circadian activity under temperature cycles [111]. There is therefore good evidence for the type of signaling pathway required by our model. These results are particularly appealing because adaptive signaling is a ubiquitous feature of neural sensory systems. However, the argument for our model of temperature compensation has its roots in a simulation of evolution. Chordotonal organs and TrpA channels are known to play a role in general temperature sensation, and it is likely that they became connected to the circadian clock after the evolution of the circadian oscillation was in some sense complete. One could argue that a true satisfaction of the model's

predictions regarding temperature sensation requires a molecular pathway for circadian temperature sensation that is present in every cell, not just the brain.

Just such a pathway was proposed in experiments with flies carrying the $cry^b$ mutation. Cryptochrome (CRY) is a blue-light photoreceptor known to be responsible for circadian entrainment to light cycles. The $cry^b$ mutation leads to flies that have significantly reduced phase shifting in response to light pulses, and that, unlike wild-type *Drosophila*, are rhythmic in constant light [48]. A temperature PRC experiment found similar results for temperature sensation in $cry^b$ mutants [92]. A PRC using a 30 minute 37°C heat pulse found significantly reduced resetting amplitude in $cry^b$ mutants compared to wild-type animals. In particular, a 30 minute pulse applied at hour 15 of the subjective day was found to result in a 2.5 hour phase delay in wild-type flies, and only a 0.5 hour delay in $cry^b$ mutants. However, because the large incubators typically used for temperature control in *Drosophila* labs are not capable of heating and cooling to 37°C and back in a half hour, the temperature shock was applied by removing the cuvettes containing individual flies from the circadian activity monitor and dipping them into a 37°C water bath for 30 minutes. Figure 5.7 shows the results of an attempt to replicate the experiment using a custom incubator to avoid this methodological oddity.

Flies were entrained to light-dark cycles as in [92], and then placed in an insulated box with dimensions of about 18 by 8 inches. The small size of the box allows it be heated and cooled rapidly by a single thermoelectric Peltier element, with feedback control provided by thermistor temperature sensors (see Chapter 3 for a detailed description). At hour 15 of the first day in constant darkness, a 30 minute step to 37°C was applied, and the phase of the flies' activity rhythms

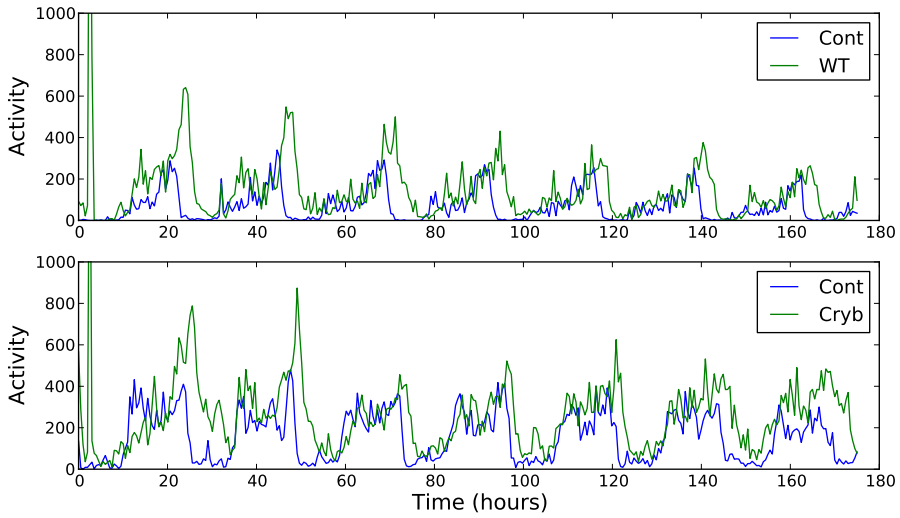


Figure 5.7: Average population oscillations of activity in a phase-resetting experiment. Control populations are shown in blue, populations exposed to a 30 minute temperature step from 25°C to 37°C are shown in green. The stimulus is applied at hour 2 in the plots, corresponding to hour 15 of the subjective day. Phase shifts are 2.45 ± 0.36 hours in wild-type animals (top), and 2.43 ± 0.59 hours in $cry^b$ mutants (bottom).

was compared to a control group. As can be seen in Figure 5.7, the phase shift in wild-type and $cry^b$ animals is similar, with both groups showing an approximately 2.5 hour phase *advance*. The results are in clear contradiction to those in [92], and no difference in temperature sensation appears to be present in the $cry^b$ mutant.

Fortunately, other results on cell autonomous circadian temperature sensation have subsequently been found. One experiment showed that mouse SCN explants expressing luciferase reporters showed significantly reduced phase resetting in a temperature PRC experiment when cultured in the presence of KNK437, a drug known to inhibit the heat shock response [17]. It has also been found that the heat shock transcription factor HSF1 is required for circadian synchroniza-

tion by temperature [182]. The same set of experiments also found an HSF1 binding site in the promoter region of the Per2 gene, and showed a physical association between HSF1 and the circadian transcription factor BMAL1. There is thus considerable evidence that the heat shock pathway plays a role in circadian temperature sensation in mammals. However, no such evidence yet exists in *Drosophila*.

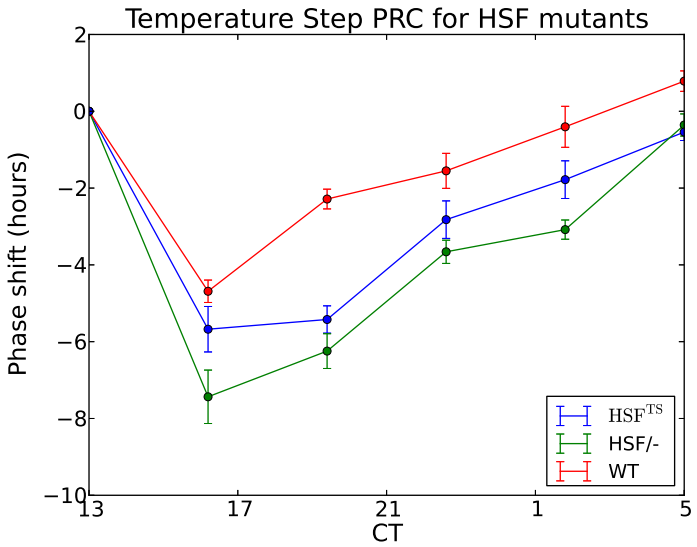


Figure 5.8: Results of a PRC experiment applying a temperature step from 18°C to 29°C to three strains of flies. WT denotes wild type, HSF/- a heterozygous knockout of the what shock transcription factor, and $HSF^{TS}$ a temperature-sensitive HSF mutant. Phase shifts are plotted against the hour of the subjective day at which the step occurred, and are calculated relative to the phase of the group at CT 13. Error bars are standard error of the mean.

Figure 5.8 shows the results of a temperature PRC experiment on two *Drosophila* strains bearing mutations in the heat shock pathway. The *Drosophila* heat shock transcription factor (HSF) is required for development even at normal temperatures, and so cannot be completely knocked out. One of the strains therefore features a heterozygous knockout of HSF, and the other strain bears a point mu-

tation rendering the HSF protein temperature-sensitive, such that it does not function above 29°C [88]. In order to fully exploit the temperature-sensitive mutant, the stimulus used in the PRC is a step up in temperature from 18°C to 29°C (higher temperatures are likely to kill flies with a nonfunctioning heat shock response). The expectation would be that flies bearing these mutations would show reduced or eliminated phase resetting in response to such a stimulus. However, as the figure shows, the opposite is the case. Both mutant strains show *increased* phase resetting in response to a temperature step. The most likely explanation for this is that the effect of the heat shock response on circadian phase is opposite to, and less than, the effect of other signaling pathways, perhaps the neural pathways mentioned above. This would suggest that although the heat shock pathway has some vestigial effect on circadian temperature sensation, it is no longer the primary pathway for temperature entrainment.

The phase shifts in Figure 5.8 are plotted relative to one of the stimulated groups, rather than by comparison to a control. This is because the shape of the circadian activity oscillation is markedly different at different temperatures (see Figure 5.9), making principled phase comparisons between oscillations at different temperatures impossible. It has long been known that temperature affects the circadian activity profile, with daytime sleep increased and nighttime sleep reduced at higher temperatures [85]. However, this effect is markedly reduced in the heat shock mutant strains. Figure 5.9 shows the sleep profile of wild-type and HSF/- flies in constant darkness at 18°C and 29°C. Wild-type animals show the usual increase in sleep during the subjective day (hours 0-12 in the plot) and decrease in sleep during the subjective night (hours 12-24). The heterozygous HSF knockout strain, however, has an essentially identical sleep profile at the two different temperatures. This provides further evidence for the

role of the heat shock pathway in communicating temperature information to the circadian clock.

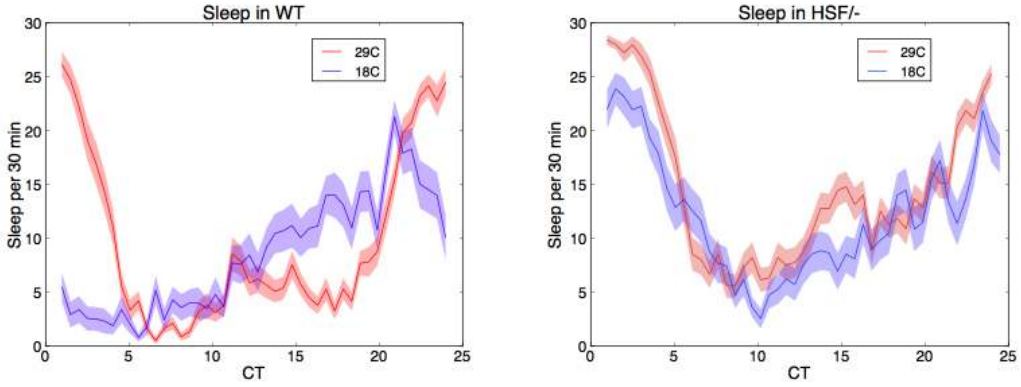


Figure 5.9: Effect of temperature on sleep profile in wild-type and heat shock mutant flies. Sleep per 30 minutes is shown over the course of the circadian day at 18°C and 29°C in wild-type flies (WT, left) and heterozygous heat shock transcription factor knockouts (HSF/-, right). Shaded regions indicate standard error of the mean across at least 15 individuals. Flies that have been motionless for at least 5minutes are considered to be asleep.

A variety of threads of evidence have shown that specific pathways for communicating temperature to the circadian clock exist, as required by our model. These pathways may take the form of an adaptive neural pathway (chordotonal organs and TrpA channels), or a transcriptional pathway that couples to the clock without changing the period (the heat shock response). We have shown that the structure of circadian temperature regulation consists of a core clock that is essentially temperature insensitive, coupled to an independent signaling pathway that communicates changes in temperature while preserving temperature compensation. The question of how the core circadian clock is compensated at the molecular level remains open. As we discussed in the Introduction, some partial results exist that suggest balancing between phosphorylation and dephosphorylation reactions plays an important role in temperature

compensation. Some simple models do show that networks of reversible reactions lend themselves well to robust temperature compensation (see Chapter 2). Firm experimental evidence on the global biochemical mechanisms of temperature compensation will likely require observation of the cellular molecular clock in action at different temperatures, perhaps by the use of fluorescent reporters or fusion proteins. Some preliminary work in this direction was discussed in Chapter 3, but much remains to be done.

# CHAPTER 6

# CONCLUSION

The circadian clock in *Drosophila melanogaster* is a crucial biological regulatory system that also displays rich dynamical behavior. This has led to a great deal of study of circadian rhythms from a mathematical point of view, some of which we reviewed in Chapter 2. The circadian clock has also been a fruitful system for the experimental study of behavior. The first genetic mutation known to influence animal behavior, in the *Drosophila period* locus, was found through a screen for alterations in circadian rhythmicity [102]. Some of the key experimental techniques in the study of circadian rhythms are discussed in Chapter 3.

In this thesis, we have attempted to understand features of circadian rhythm dynamics by synthesizing a mathematical point of view with quantitative experimental data. The experiments described in Chapter 4 used light stimuli to probe the dynamics of the clock in an effort to understand the structure of the cellular oscillator population in the *Drosophila* brain. Using a carefully tuned light pulse, phase synchronization of individual oscillators can be temporarily disrupted, as originally shown in the 1972 experiments of Art Winfree [208]. We have reproduced this effect for the first time in individual behaving animals, and shown that a careful analysis of behavioral rhythms in animals exposed to the so-called critical or singular light stimulus suggests that a long-term disruption in the dynamics of the clock occurs, consistent with Winfree's original observations. We then used some phenomenological observations of fly behavior in constant darkness to argue that this disruption could be explained by weak coupling between individual neurons in the *Drosophia* brain.

In Chapter 5, we study the effect of temperature on the dynamics of the clock in an effort to understand the mechanism of temperature compensation of the circadian period. Using Western blot measurements of protein concentrations and a luciferase reporter for transcriptional activity, we show that the effect of temperature change on the circadian clock can be described by a pure rescaling of amplitude. Using models described in Chapter 2 (in particular a model developed by Paul Francois [53]) we argue this simple scaling behavior indicates that various reactions making up the core circadian oscillator are independently temperature compensated. This suggests that, because the core circadian clock is essentially temperature-insensitive, a specific signaling pathway for communicating temperature to the clock should be present. We investigated the effect of a two candidate signaling pathways using temperature stimulus experiments, and present evidence that the heat shock pathway is likely involved in regulation of both circadian behavior and sleep in response to temperature changes.

## 6.1 Future directions

In Chapter 4, we used a measurement of the rate of phase drift in adult wild-type *Drosophila* activity rhythms to gain some information about the strength of coupling between circadian neurons. The premise of this measurement is that a combination of averaging between a large number of neurons and increased robustness of individual oscillations due to coupling should lead to a low rate of phase drift. We found that the rate of phase drift, while very low (the dephasing time is 120 days, longer than the lifespan of the fly) is only about 40 times higher than the dephasing time of an individual neuron. This is low enough that it can

be explained purely by averaging over the phase-locked population, without any additional effect from coupling.

However, this conclusion relies on an estimate of the number of neurons contributing to setting the circadian phase. The are about 120 circadian neurons in the *Drosophila* brain, but not all of them are part of the central pacemaker (see Section 1.4 for a more detailed discussion of circadian anatomy). In order to test how many (and which) neurons participate in setting the phase of circadian behavior, the phase diffusion measurement discussed in Chapter 4 can be repeated using mutant strains of fly in which the circadian clock is expressed in only a subset of the usual wild-type population. This can achieved by using the UAS-GAL4 system (see Chapter 3) to restore partial circadian expression in a clock-null mutant (usually either $per^0$ or $cyc^0$). GAL4 drivers can be used to restore the circadian clock specifically in $sLN_v$, $lLN_v$, $LN_d$, or DN neurons (see [67] for examples). Measuring phase diffusion rates in these partially expressing lines should provide insight into how various groups of neurons are coupled together, and which groups make up the central pacemaker.

The goal of the light pulse singularity experiment described in Chapter 4 is to gain insight into the strength of coupling between circadian neurons by observing the dynamics of amplitude recovery in animals exposed to the critical light stimulus. We found that this is not possible to achieve by observing activity rhythms alone, because the amplitude of activity rhythms is not tightly coupled to the amplitude of the underlying molecular oscillations. However, it is possible to observe amplitude recovery by directly imaging circadian neurons. This can be done in fixed brains with an antibody stain for circadian proteins (see Chapter 3 for details). Since time series data cannot be obtained, measur-

ing amplitude recovery and resynchronization rates will rely on assessing the position of the circadian clock in phase space for each neuron in an individual brain. From this average amplitude and synchrony values can be assessed in individual brains and further averaged over a large number of samples. This requires two independent markers of circadian phase to be imaged in each neuron. Previous quantitative observations of circadian rhythms in fixed brains have used antibodies against PER or TIM (see [174]) for an example), but PER and TIM oscillate with roughly the same phase, so cannot be considered independent markers. CRY protein oscillates with a slightly different phase than PER or TIM, so could serve as a possible marker, though an observation of CRY oscillations in individual neurons has not been reported in the literature. CLK and CYC proteins do no oscillate, and so cannot be used as phase markers. A final possibility would be to use a circadian GAL4 driver to express a destabilized GFP, which could serve as a reporter of transcriptional oscillations.

In Chapter 5, we showed that mutations in the heat shock pathway cause the *Drosophila* circadian clock to respond differently to temperature shifts. However, in flies, unlike in mammalian cell culture, reductions in the heat shock response lead to *increased* phase-shifting after temperature steps. This is likely due to the presence of other pathways for communicating temperature to the circadian clock. In particular, alteration in the functioning of mechanosensitive chordotonal organs [171] or temperature-sensitive Trp ion channels [111] have been shown to affect circadian temperature entrainment. One way to disentangle the effects of these pathways is generate mutants in which all of the pathways have been knocked out and measure temperature responses in the knockout strains. Another possibility is to examine the effect of temperature shifts on circadian rhythms in isolated tissues. This could eliminate the influence of neural sen-

sation mechanisms such as chordotonal organs and Trp channels, isolating the effects of the heat shock pathway. Circadian rhythms have been observed in a variety of isolated tissues including legs, wings, and abdomens, and have also been shown to be temperature-sensitive in these contexts [61].

The temperature scaling measurements shown in Chapter 5 also indicate that different sub-processes of the circadian clock are independently temperature compensated. However, they don't tell us anything about *how* these processes are compensated. As we saw in Section 1.3, our knowledge of the biochemical details of the workings of the clock is fragmentary and incomplete. We do not have a good understanding of how the period is set, or even how the lengths of individual sub-processes in the circadian rhythm are regulated. However, much more is known about the biochemical regulation of nuclear translocation of PER and TIM than about other parts of the clock. This is mostly due to experiments in the *Drosophila* S2 cell culture system (see [130] for a key early example). It is known that nuclear translocation is regulated by a complicated series of phosphorylation reactions (see Section 1.3 for details), and a number of phosphorylation site mutants with period phenotypes have been found on both PER and TIM [56]. Examining the temperature compensation phenotypes of these mutants, as well as the effect of kinase and phosphatase levels on nuclear translocation of the mutant proteins in S2 cells could shed significant light on the temperature compensation of nuclear translocation. Understanding how nuclear translocation is temperature compensated could in turn provide a blueprint for understanding the microscopic mechanisms of temperature compensation in other parts of the clock.

## 6.2 Evolution of circadian clocks

The experiments described in the preceding pages are all concerned in one way or another with understanding the *how* and the *why* of the construction of the circadian clock. Understanding the mechanism and structure of the clock is intimately related to understanding the evolution of the clock. As we discussed in Section 1.2, the evolutionary origins of the circadian clock are a subject of some debate. It is clear due to the significant differences in both sequence and structure that the cyanobacterial and eukaryotic clocks have independent origins. It also clear due the substantial sequence homologies present that all animal clocks have a common origin. However, the circadian clocks in fungus and plants have a very similar structure to that of the animals, but lack any significant sequence homology [219]. It is therefore unclear whether they evolved independently or not. The role of the circadian clock in the fitness of organisms is substantial and includes metabolic, immune system, and lifespan effects (see Section 1.1). However, the primary role played by the ancestral clock is also not known.

One popular theory [163] suggests that the circadian clock evolved to help organisms protect themselves form light-induced DNA damage. Sequence evidence from numerous different organisms indicates that the circadian clock co-evolved with blue light photo reception [58]. Animal cryptochrome proteins are part of an enzyme family known as the *photolyases*, most of which are light-inducible enzymes involved in DNA damage repair [185]. This theory still leaves the question of why the circadian *oscillations* evolved. A simple light-sensitive switch could be sufficient for regulation of DNA damage repair mechanisms, and indeed many photolyases serve in exactly this role [185]. The standard explanation of the need for a circadian clock rather than a circadian

switch is *anticipation*. That is, a clock allows the organism to anticipate the sunrise rather than just respond to it. However, even this does not require a clock. An hourglass mechanism could accomplish the same task, and in fact, some corals have been shown to keep circadian time via an hourglass-like mechanism [114]. However, an hourglass mechanism may not be sufficient to produce robust anticipation in the presence of seasonal variations in light level and day length. This claim has been supported by simulations of the evolutionary fitness of various timekeeping mechanisms [188].

One can ask similar questions about temperature compensation. Given that outside of the lab the circadian clock is always exposed to a strong entraining signal (light), why is temperature compensation actually necessary? One theory is that the temperature compensated clock is needed to produce the correct seasonal variations in wake and sleep times [122]. However, it seems easy to write down an uncompensated oscillator model that produces similar results. Another idea is that temperature compensation is important because different parts of the clock are responsible for downstream signaling to different targets, and that these targets must be kept in sync with each other. This would suggest that the clock must maintain a constant phase and shape at different temperatures (David Rand, personal communication). Another idea could be that temperature compensation originated in the evolution of the clock. One could imagine that the circadian clock resulted from a progression of light-sensing systems that included a switch and an hourglass. An hourglass mechanism would clearly need to be temperature compensated in order to accurately keep time in the face of daily temperature variations. It could respond to seasonal variation by sensing some combination of temperature and day length. This evolutionary story predicts that the circadian clock should be built on top of a switch-like

mechanism. One model of the clock [191] uses just such a mechanism, in which positive feedback comes from the stabilization of PER and TIM by dimerization. S2 cell experiments on the stability of PER and TIM as a function of concentration and light level could be used to test the predictions of this model.

Similar evolutionary considerations can shed light on the nature of coupling and communication in the circadian oscillator population. We argued that the necessity for a circadian oscillator rather than a switch lies in the need for robust timekeeping in the face of daily and seasonal variations in temperature, light levels, and day length. This has interesting implications for the structure of the clock because it means that the clock is not a sensory system designed to faithfully transmit information about environmental light and temperature. A comparison with another oscillating system, the hair bundle in the mammalian ear, is instructive. Sound information is transmitted to the optic nerve via a population of mechnosensitive hair bundles that respond selectively to particular frequencies. This is achieved via an active process involving mechanosensitive ion channels in the hair cell that make the bundle oscillate spontaneously with a characteristic frequency. The oscillation is poised very close to its associated Hopf bifurcation, which maximizes its sensitivity to external stimuli (see [84] for a review of hair bundle biophysics). This makes the hair bundle a faithful communicator of the amplitude, frequency, and phase of sound waves. The circadian clock, on the other hand, is not a faithful transmitter of amplitude or frequency. It is designed to oscillate only at one frequency, and with relatively fixed amplitude, and only to faithfully report the phase of external light and temperature oscillations. Even this reporting of phase should not be too sensitive to the variations that inevitably result from changes in weather and seasons.

The circadian clock must be entrainable in order to make behavioral and physiological rhythms responsive to environmental light and temperature. However, it must also be robust in the face of fluctuations in external forcing. Unlike the hair bundle, the circadian clock should be far from a Hopf bifurcation. As we saw in Chapter 2, this can be achieved either by having large amplitude oscillations in individual cells, or by having strong coupling between cells. A population of relatively weak individual oscillators with widely varying periods that are strongly coupled together (like that in the mouse) will have different properties than a population of individually strong oscillators weakly coupled together (as we suggest us the case for the fly in Chapter 4). It is likely that the explanation for the structure of oscillator populations in the fly and in mammals lies in the need for balancing between entrain ability and robustness.

## BIBLIOGRAPHY


[1] Bikem Akten, Eike Jauch, Ginka K Genova, Eun Young Kim, Isaac Edery, Thomas Raabe, and F Rob Jackson. A role for CK2 in the Drosophila circadian oscillator. *Nature Neuroscience*, 6(3):251–257, February 2003.

[2] J F Aldridge and T Pavlidis. Clocklike Behavior of Biological Clocks. *Nature*, 259(5541):343–344, 1976.

[3] U Alon, M G Surette, N Barkai, and S Leibler. Robustness in bacterial chemotaxis. *Nature*, 397(6715):168–171, 1999.

[4] Natsumi Aoki, Hiroyuki Watanabe, Kazuya Okada, Kazuyuki Aoki, Takuma Imanishi, Daisuke Yoshida, Ryosuke Ishikawa, and Shigenobu Shibata. Involvement of 5-HT3 and 5-HT4 Receptors in the Regulation of Circadian Clock Gene Expression in Mouse Small Intestine. *Journal of Pharmacological Sciences*, 124(2):267–275, 2014.

[5] Simon N Archer, Jayshan D Carpen, Mark Gibson, Gim Hui Lim, Jonathan D Johnston, Debra J Skene, and Malcolm von Schantz. Polymorphism in the PER3 promoter associates with diurnal preference and delayed sleep phase disorder. *Sleep*, 33(5):695–701, May 2010.

[6] Sara J Aton, Christopher S Colwell, Anthony J Harmar, James Waschek, and Erik D Herzog. Vasoactive intestinal polypeptide mediates circadian rhythmicity and synchrony in mammalian clock neurons. *Nature Neuroscience*, March 2005.

[7] Sara J Aton, Christopher S Colwell, Anthony J Harmar, James Waschek, and Erik D Herzog. Vasoactive intestinal polypeptide mediates circadian rhythmicity and synchrony in mammalian clock neurons. *Nature Neuroscience*, March 2005.

[8] I Balzer, U Neuhaus-Steinmetz, and R Hardeland. Temperature compensation in an ultradian rhythm of tyrosine aminotransferase activity in Euglena gracilis Klebs. *Experientia*, 45(5):476–477, May 1989.

[9] S Bao, J Rihel, E Bjes, J Y Fan, and J L Price. The Drosophila doubletimeS mutation delays the nuclear accumulation of period protein and affects the feedback regulation of period mRNA. *The Journal of Neuroscience*, 21(18):7117–7126, September 2001.

[10] T A Bargiello, F R Jackson, and M W Young. Restoration of Circadian Behavioral Rhythms by Gene-Transfer in Drosophila. *Nature*, 312(5996):752–754, 1984.

[11] J Bass and J S Takahashi. Circadian Integration of Metabolism and Energetics. *Science*, 330(6009):1349–1354, December 2010.

[12] M K Baylies, L B Vosshall, A Sehgal, and M W Young. New short period mutations of the Drosophila clock gene per. *Neuron*, 9(3):575–581, September 1992.

[13] D E Bianchi. An endogenous circadian rhythm in Neurospora cars. *Journal of general microbiology*, 35:437–445, June 1964.

[14] W J Blake, M Kaern, C R Cantor, and J J Collins. Noise in eukaryotic gene expression. *Nature*, 422(6932):633–637, 2003.

[15] M M Bradford. A rapid and sensitive method for the quantitation of microgram quantities of protein utilizing the principle of protein-dye binding. *Analytical biochemistry*, 72:248–254, May 1976.

[16] Steven A Brown, Gottlieb Zumbrunn, Fabienne Fleury-Olela, Nicolas Preitner, and Ueli Schibler. Rhythms of mammalian body temperature can sustain peripheral circadian clocks. *Current Biology*, 12(18):1574–1583, September 2002.

[17] E D Buhr, S H Yoo, and J S Takahashi. Temperature as a Universal Resetting Cue for Mammalian Circadian Oscillators. *Science*, 330(6002):379–385, October 2010.

[18] R M Buijs and A Kalsbeek. Hypothalamic integration of central and peripheral clocks. *Nature Reviews Neuroscience*, 2(7):521–526, July 2001.

[19] D Bushey, R Huber, G Tononi, and C Cirelli. Drosophila Hyperkinetic mutants have reduced sleep and impaired memory. *The Journal of Neuroscience*, 27(20):5384–5393, May 2007.

[20] María Casanova-Acebes, Christophe Pitaval, Linnea A Weiss, César Nombela-Arrieta, Raphaël Chèvre, Noelia A-González, Yuya Kunisaki, Dachuan Zhang, Nico van Rooijen, Leslie E Silberstein, Christian Weber, Takashi Nagasawa, Paul S Frenette, Antonio Castrillo, and Andrés Hi-

dalgo. Rhythmic Modulation of the Hematopoietic Niche through Neutrophil Clearance. *Cell*, 153(5):1025–1035, May 2013.

[21] Zheng Chen and Steven L McKnight. A conserved DNA damage response pathway responsible for coupling the cell division cycle to the circadian and metabolic cycles. *Cell Cycle*, 6(23):2906–2912, 2007.

[22] J C Chiu, J T Vanselow, A Kramer, and I Edery. The phospho-occupancy of an atypical SLIMB-binding site on PERIOD that is phosphorylated by DOUBLETIME controls the pace of the clock. *Genes & Development*, 22(13):1758–1772, July 2008.

[23] Joanna C Chiu, Hyuk Wan Ko, and Isaac Edery. NEMO/NLK Phosphorylates PERIOD to Initiate a Time-Delay Phosphorylation Circuit that Sets Circadian Clock Speed. *Cell*, 145(3):357–370, April 2011.

[24] D E Clapham, L W Runnels, and C Strubing. The TRP ion channel family. *Nature Reviews Neuroscience*, 2(6):387–396, June 2001.

[25] M K Cooper, M J Hamblencoyle, X Liu, J E Rutila, and J C Hall. Dosage Compensation of the Period Gene in Drosophila-Melanogaster. *Genetics*, 138(3):721–732, November 1994.

[26] P Corish and C Tyler-Smith. Attenuation of green fluorescent protein half-life in mammalian cells. *Protein Engineering*, 12(12):1035–1040, December 1999.

[27] Brian R Crane and Michael W Young. Interactive Features of Proteins Composing Eukaryotic Circadian Clocks. *Annual Review of Biochemistry*, 83(1):191–219, June 2014.

[28] S A Cyran, A M Buchsbaum, K L Reddy, M C Lin, NRJ Glossop, P E Hardin, M W Young, R V Storti, and J Blau. vrille, Pdp1, and dClock form a second feedback loop in the Drosophila circadian clock. *Cell*, 112(3):329–341, 2003.

[29] Shawn A Cyran, Georgia Yiannoulos, Anna M Buchsbaum, Lino Saez, Michael W Young, and Justin Blau. The double-time protein kinase regulates the subcellular localization of the Drosophila clock protein period. *The Journal of Neuroscience*, 25(22):5430–5437, June 2005.

[30] Bryan C Daniels, Yan-Jiun Chen, James P Sethna, Ryan N Gutenkunst, and

Christopher R Myers. Sloppiness, robustness, and evolvability in systems biology. *Current Opinion in Biotechnology*, 19(4):389–395, August 2008.

[31] T K Darlington, K Wager-Smith, M F Ceriani, D Staknis, N Gekakis, TDL Steeves, C J Weitz, J S Takahashi, and S A Kay. Closing the circadian loop: CLOCK-induced transcription of its own inhibitors per and tim. *Science*, 280(5369):1599–1603, 1998.

[32] A P de Candolle. *Physiologie Vegetale*. Paris: Bechet jeune, 1832.

[33] J J O de Mairan. Observation botanique. *Historie de lAcadmie Royale des Sciences*, page 3536, 1729.

[34] Giovanna De Palo, Giuseppe Facchetti, Monica Mazzolini, Anna Menini, Vincent Torre, and Claudio Altafini. Common dynamical features of sensory adaptation in photoreceptors and olfactory sensory neurons. *Scientific Reports*, 3, February 2013.

[35] Charna Dibner, Daniel Sage, Michael Unser, Christoph Bauer, Thomas d'Eysmond, Felix Naef, and Ueli Schibler. Circadian gene expression is resilient to large fluctuations in overall transcription rates. *The EMBO Journal*, 28(2):123–134, December 2008.

[36] Charna Dibner, Ueli Schibler, and Urs Albrecht. The Mammalian Circadian Timing System: Organization and Coordination of Central and Peripheral Clocks. *Annual Review of Physiology*, 72(1):517–549, March 2010.

[37] Theodosius Dobzhansky. Nothing in Biology Makes Sense Except in the Light of Evolution. *The American Biology Teacher*, 35(3):125–129, March 1973.

[38] T C Dockendorff, H S Su, SMJ McBride, Z H Yang, C H Choi, K K Siwicki, A Sehgal, and T A Jongens. Drosophila lacking dfmr1 activity show defects in circadian output and fail to maintain courtship interest. *Neuron*, 34(6):973–984, 2002.

[39] Jeffrey M Donlea, Diogo Pimentel, and Gero Miesenböck. Neuronal Machinery of Sleep Homeostasis in Drosophila. *Neuron*, 81(4):860–872, February 2014.

[40] H B Dowse and J M Ringo. The Search for Hidden Periodicities in Bio-

logical Time-Series Revisited. *Journal of Theoretical Biology*, 139(4):487–515, 1989.

[41] H B Dowse and J M Ringo. Comparisons Between Periodograms and Spectral-Analysis - Apples Are Apples After All. *Journal of Theoretical Biology*, 148(1):139–144, 1991.

[42] David Druzd, Alba de Juan, and Christoph Scheiermann. Circadian rhythms in leukocyte trafficking. *Seminars in Immunopathology*, 36(2):149–162, January 2014.

[43] J C Dunlap, J J Loros, H V Colot, A Mehra, W J Belden, M Shi, C I Hong, L F Larrondo, C L Baker, C H Chen, C Schwerdtfeger, P D Collopy, J J Gamsby, and R Lambreghts. A circadian clock in Neurospora: how genes and proteins cooperate to produce a sustained, entrainable, and compensated biological oscillator with a period of about a day. *Cold Spring Harbor Symposia on Quantitative Biology*, 72(1):57–68, 2007.

[44] Jay C Dunlap. *Chronobiology: Biological Timekeeping*. Sinauer Associates, 2003.

[45] I Edery, L J Zwiebel, M E Dembinska, and M Rosbash. Temporal phosphorylation of the Drosophila period protein. *Proceedings of the National Academy of Sciences*, 91(6):2260–2264, March 1994.

[46] Rachel S Edgar, Edward W Green, Yuwei Zhao, Gerben van Ooijen, Maria Olmedo, Ximing Qin, Yao Xu, Min Pan, Utham K Valekunja, Kevin A Feeney, Elizabeth S Maywood, Michael H Hastings, Nitin S Baliga, Martha Merrow, Andrew J Millar, Carl H Johnson, Charalambos P Kyriacou, John S O'Neill, and Akhilesh B Reddy. Peroxiredoxins are conserved markers of circadian rhythms. *Nature*, May 2012.

[47] Michael B Elowitz, Arnold J Levine, Eric D Siggia, and Peter S Swain. Stochastic gene expression in a single cell. *Science*, 297(5584):1183–1186, August 2002.

[48] P Emery, W V So, M Kaneko, J C Hall, and M Rosbash. CRY, a Drosophila clock and light-regulated cryptochrome, is a major contributor to circadian rhythm resetting and photosensitivity. *Cell*, 95(5):669–679, 1998.

[49] W Engelmann, A Johnsson, H G Karlsson, R Kobler, and M L Schimmel. Attenuation of Petal Movement Rhythm in Kalanchoe with Light-Pulses. *Physiologia Plantarum*, 43(1):68–76, 1978.

[50] J T ENRIGHT. The search for rhythmicity in biological time-series. *Journal of Theoretical Biology*, 8(3):426–468, May 1965.

[51] J T Enright. Temporal Precision in Circadian Systems - a Reliable Neuronal Clock From Unreliable Components. *Science*, 209(4464):1542–1545, 1980.

[52] Céline Feillet, Peter Krusche, Filippo Tamanini, Roel C Janssens, Mike J Downey, Patrick Martin, Michèle Teboul, Shoko Saito, Francis A Lévi, Till Bretschneider, Gijsbertus T J van der Horst, Franck Delaunay, and David A Rand. Phase locking and multiple oscillating attractors for the coupled mammalian clock and cell cycle. *Proceedings of the National Academy of Sciences of the United States of America*, 111(27):9828–9833, July 2014.

[53] Paul François, Nicolas Despierre, and Eric D Siggia. Adaptive temperature compensation in circadian oscillations. *PLoS Computational Biology*, 8(7):e1002585, 2012.

[54] B Frisch, P E Hardin, M J Hamblencoyle, M Rosbash, and J C Hall. A Promoterless Period Gene Mediates Behavioral Rhythmicity and Cyclical Per Expression in a Restricted Subset of the Drosophila Nervous-System. *Neuron*, 12(3):555–570, March 1994.

[55] Monica Gallego and David M Virshup. Post-translational modifications regulate the ticking of the circadian clock. *Nature Reviews Molecular Cell Biology*, 8(2):139–148, February 2007.

[56] David S Garbe, Yanshan Fang, Xiangzhong Zheng, Mallory Sowcik, Rana Anjum, Steven P Gygi, and Amita Sehgal. Cooperative Interaction between Phosphorylation Sites on PERIOD Maintains Circadian Period in Drosophila. *PLoS Genetics*, 9(9):e1003749, September 2013.

[57] Benjamin A Garcia, Jeffrey Shabanowitz, and Donald F Hunt. Analysis of protein phosphorylation by mass spectrometry. *Methods*, 35(3):256–264, March 2005.

[58] Walter Gehring and Michael Rosbash. The Coevolution of Blue-Light Photoreception and Circadian Rhythms. *Journal of Molecular Evolution*, 57(0):S286–S289, August 2003.

[59] Nicholas Gekakis, Lino Saez, Anne-Marie Delahaye-Brown, Michael P Myers, Amita Sehgal, Michael W Young, and Charles J Weitz. Isolation of

timeless by PER Protein Interaction: Defective Interaction Between timeless Protein and Long-Period Mutant PER1. *Science*, 270:811–815, 1995.

[60] Carla Gentile, Hana Sehadova, Alekos Simoni, Chenghao Chen, and Ralf Stanewsky. Cryptochrome Antagonizes Synchronization of Drosophila's Circadian Clock to Temperature Cycles. *Current Biology*, 23(3):185–195, February 2013.

[61] Franz T Glaser and Ralf Stanewsky. Temperature Synchronization of the Drosophila Circadian Clock. *Current Biology*, 15(15):1352–1363, August 2005.

[62] B C Goodwin. Oscillatory behavior in enzymatic control processes. *Advances in Enzyme Regulation*, 3:425–438, 1965.

[63] A L Gotter, T Manganaro, D R Weaver, L F Kolakowski, B Possidente, S Sriram, D T MacLaughlin, and S M Reppert. A time-less function for mouse Timeless. *Nature Neuroscience*, 3(8):755–756, August 2000.

[64] A Granada, R M Hennig, B Ronacher, A Kramer, and H Herzel. Phase Response Curves: Elucidating the Dynamics of Coupled Oscillators. *Methods in Enzymology*, 454:1–27, 2009.

[65] Rachel M Green, Sonia Tingay, Zhi-Yong Wang, and Elaine M Tobin. Circadian rhythms confer a higher level of fitness to Arabidopsis plants. *Plant Physiology*, 129(2):576–584, June 2002.

[66] J S Griffith. Mathematics of cellular control processes. I. Negative feedback to one gene. *Journal of Theoretical Biology*, 20(2):202–208, August 1968.

[67] Brigitte Grima, Elisabeth Chélot, Ruohan Xia, and François Rouyer. Morning and evening peaks of activity rely on different clock neurons of the Drosophila brain. *Nature*, 431(7010):869–873, October 2004.

[68] J Guckenheimer. Isochrons and phaseless sets. *Journal of Mathematical Biology*, 1:259–273, 1975.

[69] Franz Halberg, Germaine Cornélissen, George Katinas, Elena V Syutkina, Robert B Sothern, Rina Zaslavskaya, Francine Halberg, Yoshihiko Watanabe, Othild Schwartzkopff, Kuniaki Otsuka, Roberto Tarquini, Perfetto Frederico, and Jarmila Siggelova. Transdisciplinary unifying implications

of circadian findings in the 1950s. *Journal of circadian rhythms*, 1(1):2, October 2003.

[70] Stacey L Harmer. The Circadian System in Higher Plants. *Annual Review of Plant Biology*, 60(1):357–377, June 2009.

[71] J W Hastings and B M Sweeney. On the mechanism of temperature independence in a biological clock. *Proceedings of the National Academy of Sciences*, 43(9):804–811, September 1957.

[72] J R Hazel and C L Prosser. Molecular mechanisms of temperature compensation in poikilotherms. *Physiological Reviews*, 54(3):620–677, July 1974.

[73] Carlton Heckrotte. The influence of temperature on the behaviour of the Mexican jumping bean. *Journal of Thermal Biology*, 8:333–335, 1983.

[74] C Helfrich-Forster. Robust circadian rhythmicity of Drosophila melanogaster requires the presence of lateral neurons: a brain-behavioral study of disconnected mutants. *Journal of Comparative Physiology A*, 182(4):435–453, April 1998.

[75] C Helfrich-Forster. Neurobiology of the fruit fly's circadian clock. *Genes, Brain and Behavior*, 4(2):65–76, September 2004.

[76] C Helfrich-Forster, C Winter, A Hofbauer, J C Hall, and R Stanewsky. The circadian clock of fruit flies is blind after elimination of all known photoreceptors. *Neuron*, 30(1):249–261, April 2001.

[77] Charlotte Helfrich-Forster. The neuroarchitecture of the circadian clock in the brain ofDrosophila melanogaster. *Microscopy Research and Technique*, 62(2):94–102, September 2003.

[78] Charlotte Helfrich-Förster. Immunohistochemistry in Drosophila: sections and whole mounts. *Methods in molecular biology*, 362:533–547, 2007.

[79] E D Herzog, M E Geusz, SBS Khalsa, M Straume, and G D Block. Circadian rhythms in mouse suprachiasmatic nucleus explants on multimicroelectrode plates. *Brain Research*, 757(2):285–290, 1997.

[80] Erik D Herzog, Sara J Aton, Rika Numano, Yoshiyuki Sakaki, and Hajime Tei. Temporal Precision in the Mammalian Circadian System: A Reliable

Clock from Less Reliable Neurons. *Journal of Biological Rhythms*, 19(1):35–46, February 2004.

[81] Christian I Hong, Emery D Conrad, and John J Tyson. A proposal for robust temperature compensation of circadian rhythms. *Proceedings of the National Academy of Sciences*, 104(4):1195–1200, January 2007.

[82] Guocun Huang, Lixin Wang, and Yi Liu. Molecular mechanism of suppression of circadian rhythms by a critical stimulus. *The EMBO Journal*, 25(22):5349–5357, 2006.

[83] Z J Huang, K D Curtin, and M Rosbash. PER protein interactions and temperature compensation of a circadian clock in Drosophila. *Science*, 267(5201):1169–1172, February 1995.

[84] A J Hudspeth. Making an Effort to Listen: Mechanical Amplification in the Ear. *Neuron*, 59(4):530–545, August 2008.

[85] Hiroshi Ishimoto, Arianna Lark, and Toshihiro Kitamoto. Factors that Differentially Affect Daytime and Nighttime Sleep in Drosophila melanogaster. *Frontiers in neurology*, 3:24, 2012.

[86] Yasushi ISOJIMA, Masato NAKAJIMA, Hideki Ukai, Hiroshi Fujishima, Rikuhiro G Yamada, Koh-hei Masumoto, Reiko Kiuchi, Mayumi Ishida, Maki Ukai-Tadenuma, Yoichi Minami, Ryotaku Kito, Kazuki Nakao, Wataru Kishimoto, Seung-Hee Yoo, Kazuhiro Shimomura, Toshifumi Takao, Atsuko Takano, Toshio Kojima, Katsuya Nagai, Yoshiyuki Sakaki, Joseph S Takahashi, and Hiroki R Ueda. CKIepsilon/delta-dependent phosphorylation is a temperature-insensitive, period-determining process in the mammalian circadian clock. *Proceedings of the National Academy of Sciences of the United States of America*, 106(37):15744–15749, September 2009.

[87] Malgorzata Jasinska, Anna Grzegorczyk, Ewa Jasek, Jan A Litwin, Malgorzata Kossut, Grazyna Barbacka-Surowiak, and Elzbieta Pyza. Daily rhythm of synapse turnover in mouse somatosensory cortex. *Acta neurobiologiae experimentalis*, 74(1):104–110, 2014.

[88] Paul Jedlicka, Mark A Mortin, and Carl Wu. Multiple functions of Drosophila heat shock transcription factor in vivo. *The EMBO Journal*, 16:2452–2462, 1997.

[89] M E Jewett, R E Kronauer, and C A Czeisler. Light-Induced Suppression of Endogenous Circadian Amplitude in Humans. *Nature*, 350(6313):59–62, 1991.

[90] Chandrashekaran M K. Studies on phase-shifts in endogenous rhythms i. effects of light pulses on eclosion rhythms in drosophila pseudoobscura. *Zeitschrift fur Vergleichende Physiologie*, 56(2):154175, 1967.

[91] I N Karatsoreos, L Yan, J LeSauter, and R Silver. Phenotype matters: Identification of light-responsive cells in the mouse suprachiasmatic nucleus. *Journal of Neuroscience*, 24(1):68–75, 2004.

[92] Rachna Kaushik, Pipat Nawathean, Ania Busza, Alejandro Murad, Patrick Emery, and Michael Rosbash. PER-TIM Interactions with the Photoreceptor Cryptochrome Mediate Circadian Temperature Responses in Drosophila. *PLoS Biology*, 5(6):e146, 2007.

[93] E Y Kim, H W Ko, W Yu, P E Hardin, and I Edery. A DOUBLETIME Kinase Binding Domain on the Drosophila PERIOD Protein Is Essential for Its Hyperphosphorylation, Transcriptional Repression, and Circadian Clock Function. *Molecular and Cellular Biology*, 27(13):5014–5028, June 2007.

[94] Eun Young Kim and Isaac Edery. Balance between DBT/CKIepsilon kinase and protein phosphatase activities regulate phosphorylation and stability of Drosophila CLOCK protein. *Proceedings of the National Academy of Sciences*, 103(16):6178–6183, April 2006.

[95] A Klarsfeld, S Malpel, C Michard-Vanhee, M Picot, E Chelot, and F Rouyer. Novel features of cryptochrome-mediated photoreception in the brain circadian clock of Drosophila. *Journal of Neuroscience*, 24(6):1468–1477, 2004.

[96] A Knutsson. Health disorders of shift workers. *Occupational Medicine*, 53(2):103–108, March 2003.

[97] Caroline H Ko and Joseph S Takahashi. Molecular components of the mammalian circadian clock. *Human Molecular Genetics*, 15 Spec No 2:R271–7, October 2006.

[98] Caroline H Ko, Yujiro R Yamada, David K Welsh, Ethan D Buhr, Andrew C Liu, Eric E Zhang, Martin R Ralph, Steve A Kay, Daniel B Forger, and

Joseph S Takahashi. Emergence of Noise-Induced Oscillations in the Central Circadian Pacemaker. *PLoS Biology*, 8(10):e1000513, October 2010.

[99] Hyuk Wan Ko, Jin Jiang, and Isaac Edery. Role for Slimb in the degradation of Drosophila Period protein phosphorylated by Doubletime. *Nature*, 420(6916):673–678, December 2002.

[100] T Kondo and M Ishiura. The circadian clocks of plants and cyanobacteria. *Trends in plant science*, 4(5):171–176, May 1999.

[101] R J Konopka and S Benzer. Clock mutants of Drosophila melanogaster. *Proceedings of the National Academy of Sciences*, 68(9):2112–2116, September 1971.

[102] Ronald J Konopka, Colin Pittendrigh, and Dominic Orr. Reciprocal behaviour associated with altered homeostasis and photosensitivity of Drosophila clock mutants. *Journal of Neurogenetics*, 21(4):243–252, October 2007.

[103] Vesa-Petteri Kouri, Juri Olkkonen, Emilia Kaivosoja, Mari Ainola, Juuso Juhila, Iiris Hovatta, Yrjö T Konttinen, and Jami Mandelin. Circadian Timekeeping Is Disturbed in Rheumatoid Arthritis at Molecular Level. *PLoS ONE*, 8(1):e54049, January 2013.

[104] Shailesh Kumar, Ambika Mohan, and Vijay Kumar Sharma. Circadian Dysfunction Reduces Lifespan in Drosophila melanogaster. *Chronobiology International*, 22(4):641–653, January 2005.

[105] K Kume, S Kume, S K Park, J Hirsh, and F R Jackson. Dopamine is a regulator of arousal in the fruit fly. *Journal of Neuroscience*, 25(32):7377–7384, 2005.

[106] Y Kuramoto. *Chemical Oscillations, Waves, and Turbulence*. Springer, 1984.

[107] Gen Kurosawa and Yoh Iwasa. Temperature compensation in circadian clock models. *Journal of Theoretical Biology*, 233(4):453–468, April 2005.

[108] Young Kwon, Wei L Shen, Hye-Seok Shim, and Craig Montell. Fine thermotactic discrimination between the optimal and slightly cooler temperatures via a TRPV channel in chordotonal neurons. *The Journal of Neuroscience*, 30(31):10465–10471, August 2010.

[109] P L Lakin-Thomas, S Brody, and G G Coté. Amplitude Model for the Effects of Mutations and Temperature on Period and Phase Resetting of the Neurospora Circadian Oscillator. *Journal of Biological Rhythms*, 6(4):281–297, December 1991.

[110] C Lee, J P Etchegaray, FRA Cagampang, ASI Loudon, and S M Reppert. Posttranslational mechanisms regulate the mammalian circadian clock. *Cell*, 107(7):855–867, 2001.

[111] Y Lee and C Montell. Drosophila TRPA1 Functions in Temperature Control of Circadian Rhythm in Pacemaker Neurons. *Journal of Neuroscience*, 33(16):6716–6725, April 2013.

[112] M A Lema, J Echave, and D A Golombek. (Too many) mathematical models of circadian clocks (?). *Biological Rhythm Research*, 32(2):285–298, 2001.

[113] Chunghun Lim and Ravi Allada. Emerging roles for post-transcriptional regulation in circadian clocks. *Nature Publishing Group*, 16(11):1544–1550, October 2013.

[114] Che-Hung Lin, Keryea Soong, and Tung-Yung Fan. Hourglass Mechanism with Temperature Compensation in the Diel Periodicity of Planulation of the Coral, Seriatopora hystrix. *PLoS ONE*, 8(5):e64584, May 2013.

[115] Jui-Ming Lin, Analyne Schroeder, and Ravi Allada. In vivo circadian function of casein kinase 2 phosphorylation sites in Drosophila PERIOD. *The Journal of Neuroscience*, 25(48):11175–11183, November 2005.

[116] Yiing Lin, Gary D Stormo, and Paul H Taghert. The neuropeptide pigment-dispersing factor coordinates pacemaker interactions in the Drosophila circadian system. *The Journal of Neuroscience*, 24(36):7951–7957, September 2004.

[117] Andrew C Liu, David K Welsh, Caroline H Ko, Hien G Tran, Eric E Zhang, Aaron A Priest, Ethan D Buhr, Oded Singer, Kirsten Meeker, Inder M Verma, Francis J Doyle III, Joseph S Takahashi, and Steve A Kay. Intercellular Coupling Confers Robustness against Mutations in the SCN Circadian Clock Network. *Cell*, 129(3):605–616, May 2007.

[118] C Liu, D R Weaver, S H Strogatz, and S M Reppert. Cellular construction of a circadian clock: period determination in the suprachiasmatic nuclei. *Cell*, 91(6):855–860, December 1997.

[119] Y Liu, S S Golden, T Kondo, M Ishiura, and C H Johnson. Bacterial Luciferase as a Reporter of Circadian Gene-Expression in Cyanobacteria. *Journal of Bacteriology*, 177(8):2080–2086, April 1995.

[120] D Lloyd, S W Edwards, and J C Fry. Temperature-compensated oscillations in respiration and cellular protein content in synchronous cultures of Acanthamoeba castellanii. *Proceedings of the National Academy of Sciences*, 79(12):3785–3788, June 1982.

[121] Kwang Huei Low, Cecilia Lim, Hyuk Wan Ko, and Isaac Edery. Natural Variation in the Splice Site Strength of a Clock Gene and Species-Specific Thermal Adaptation. *Neuron*, 60(6):1054–1067, December 2008.

[122] J Majercak, D Sidote, P E Hardin, and I Edery. How a circadian clock adapts to seasonal decreases in temperature and day length. *Neuron*, 24(1):219–230, September 1999.

[123] Joseph S Markson and Erin K O'Shea. The molecular clockwork of a protein-based circadian oscillator. *FEBS Letters*, 583(24):3938–3947, December 2009.

[124] S Martinek, S Inonog, A S Manoukian, and M W Young. A role for the segment polarity gene shaggy/GSK-3 in the Drosophila circadian clock. *Cell*, 105(6):769–779, 2001.

[125] P C Matthews, R E Mirollow, and S H Strogatz. Dynamics of a Large System of Coupled Nonlinear Oscillators. *Physica D*, 52(2-3):293–331, September 1991.

[126] Colleen A McClung. Circadian genes, rhythms and the biology of mood disorders. *Pharmacology & Therapeutics*, 114(2):222–232, May 2007.

[127] Arun Mehra, Christopher L Baker, Jennifer J Loros, and Jay C Dunlap. Post-translational modifications in circadian rhythms. *Trends in Biochemical Sciences*, 34(10):483–490, October 2009.

[128] Arun Mehra, Mi Shi, Christopher L Baker, Hildur V Colot, Jennifer J Loros, and Jay C Dunlap. A Role for Casein Kinase 2 in the Mechanism Underlying Circadian Temperature Compensation. *Cell*, 137(4):749–760, May 2009.

[129] C Meunier and A D Verga. Noise and Bifurcations. *Journal of Statistical Physics*, 50:345–375, 1988.

[130] Pablo Meyer, Lino Saez, and Michael W Young. PER-TIM interactions in living Drosophila cells: an interval timer for the circadian clock. *Science*, 311(5758):226–229, January 2006.

[131] R E Mirollo and S H Strogatz. Amplitude Death in an Array of Limit-Cycle Oscillators. *Journal of Statistical Physics*, 60(1-2):245–262, July 1990.

[132] Y Miyasako, Y Umezaki, and K Tomioka. Separate Sets of Cerebral Clock Neurons Are Responsible for Light and Temperature Entrainment of Drosophila Circadian Locomotor Rhythms. *Journal of Biological Rhythms*, 22(2):115–126, April 2007.

[133] J R Montgomery, J P Whitt, B N Wright, M H Lai, and A L Meredith. Mis-expression of the BK K+ channel disrupts suprachiasmatic nucleus circuit rhythmicity and alters clock-controlled behavior. *AJP: Cell Physiology*, 304(4):C299–C311, February 2013.

[134] D Mulcahy, J Keegan, D Cunningham, A Quyyumi, P Crean, A Park, C Wright, and K Fox. Circadian variation of total ischaemic burden and its alteration with anti-anginal agents. *Lancet*, 2(8614):755–759, October 1988.

[135] Reiko Murakami, Ayumi Miyake, Ryo Iwase, Fumio Hayashi, Tatsuya Uzumaki, and Masahiro Ishiura. ATPase activity and its temperature compensation of the cyanobacterial clock protein KaiC. *Genes to Cells*, 13(4):387–395, April 2008.

[136] Emi Nagoshi, Camille Saini, Christoph Bauer, Thierry Laroche, Felix Naef, and Ueli Schibler. Circadian Gene Expression in Individual Fibroblasts. *Cell*, 119(5):693–705, November 2004.

[137] Masato Nakajima, Keiko Imai, Hiroshi Ito, Taeko Nishiwaki, Yoriko Murayama, Hideo Iwasaki, Tokitaka Oyama, and Takao Kondo. Reconstitution of circadian oscillation of cyanobacterial KaiC phosphorylation in vitro. *Science*, 308(5720):414–415, April 2005.

[138] Taeko Nishiwaki, Yoshinori Satomi, Yohko Kitayama, Kazuki Terauchi, Reiko Kiyohara, Toshifumi Takao, and Takao Kondo. A sequential program of dual phosphorylation of KaiC as a basis for circadian rhythm in cyanobacteria. *The EMBO Journal*, 26(17):4029–4037, September 2007.

[139] M N Nitabach, J Blau, and T C Holmes. Electrical silencing of Drosophila pacemaker neurons stops the free-running circadian clock. *Cell*, 109(4):485–495, 2002.

[140] Michael N Nitabach and Paul H Taghert. Organization of the Drosophila Circadian Control Circuit. *Current Biology*, 18(2):R84–R93, January 2008.

[141] T Noguchi, L L Wang, and D K Welsh. Fibroblast PER2 Circadian Rhythmicity Depends on Cell Density. *Journal of Biological Rhythms*, 28(3):183–192, June 2013.

[142] Hitoshi Okamura, Shun Yamaguchi, and Kazuhiro Yagita. Molecular machinery of the circadian clock in mammals. *Cell and Tissue Research*, 309(1):47–56, January 2014.

[143] Olga Oleksiuk, Vladimir Jakovljevic, Nikita Vladimirov, Ricardo Carvalho, Eli Paster, William S Ryu, Yigal Meir, Ned S Wingreen, Markus Kollmann, and Victor Sourjik. Thermal Robustness of Signaling in Bacterial Chemotaxis. *Cell*, 145(2):312–321, April 2011.

[144] N Öztürk, S H Song, S Özgür, C P Selby, L Morrison, C Partch, D Zhong, and A Sancar. Structure and Function of Animal Cryptochromes. *Cold Spring Harbor Symposia on Quantitative Biology*, 72(1):119–131, January 2007.

[145] T OBrien and J T Lis. Rapid Changes in Drosophila Transcription After an Instantaneous Heat-Shock. *Molecular and Cellular Biology*, 13(6):3456–3463, June 1993.

[146] T Pavlidis and W Kauzmann. Toward a quantitative biochemical model for circadian oscillators. *Archives of Biochemistry and Biophysics*, 132(1):338–348, June 1969.

[147] C B Peek, A H Affinati, K M Ramsey, H Y Kuo, W Yu, L A Sena, O Ilkayeva, B Marcheva, Y Kobayashi, C Omura, D C Levine, D J Bacsik, D Gius, C B Newgard, E Goetzman, N S Chandel, J M Denu, M Mrksich, and J Bass. Circadian clock NAD+ cycle drives mitochondrial oxidative metabolism in mice. *Science*, 342(6158):1243417–1243417, November 2013.

[148] E L Peterson. Phase-Resetting a Mosquito Circadian Oscillator .1. Phase-Resetting Surface. *Journal of Comparative Physiology*, 138(3):201–211, 1980.

[149] M Picot, A Klarsfeld, E Chelot, S Malpel, and F Rouyer. A Role for Blind DN2 Clock Neurons in Temperature Entrainment of the Drosophila Larval Brain. *Journal of Neuroscience*, 29(26):8312–8320, July 2009.

[150] C S Pittendrigh. On temperature independence in the clock system controlling emergence time in Drosophila. *Proceedings of the National Academy of Sciences*, 40(10):1018–1029, October 1954.

[151] C S Pittendrigh. *Biological Clocks*. Cold Soring Harbor Symposia, 1960.

[152] C S Pittendrigh. Temporal organization: reflections of a Darwinian clock-watcher. *Annual Review of Physiology*, 55(1):16–54, 1993.

[153] Sergi Portolés and Paloma Más. The Functional Interplay between Protein Kinase CK2 and CCA1 Transcriptional Activity Is Essential for Clock Temperature Compensation in Arabidopsis. *PLoS Genetics*, 6(11):e1001201, November 2010.

[154] Sheetal Potdar and Vasu Sheeba. Lessons From Sleeping Flies: Insights from Drosophila melanogasteron the Neuronal Circuitry and Importance of Sleep. *Journal of Neurogenetics*, 27(1-2):23–42, June 2013.

[155] F Preuss, J Y Fan, M Kalive, S Bao, E Schuenemann, E S Bjes, and J L Price. Drosophila doubletime Mutations Which either Shorten or Lengthen the Period of Circadian Rhythms Decrease the Protein Kinase Activity of Casein Kinase I. *Molecular and Cellular Biology*, 24(2):886–898, December 2003.

[156] J L Price. Insights into the molecular mechanisms of temperature compensation from the Drosophila period and timeless mutants. *Chronobiology International*, 14(5):455–468, September 1997.

[157] J L Price, J Blau, A Rothenfluh, M Abodeely, B Kloss, and M W Young. double-time is a novel Drosophila clock gene that regulates PERIOD protein accumulation. *Cell*, 94(1):83–95, July 1998.

[158] Jeffrey L Price. Genetic screens for clock mutants in Drosophila. *Applications of Chimeric Genes and Hybrid Proteins Pt B*, 393:35–60, 2005.

[159] E Pyza and I A Meinertzhagen. Neurotransmitters regulate rhythmic size changes amongst cells in the fly's optic lobe. *Journal of Comparative Physiology A*, 178(1):33–45, January 1996.

[160] P Reddy, W A Zehring, D A Wheeler, V Pirrotta, C Hadfield, J C Hall, and M Rosbash. Molecular Analysis of the Period Locus in Drosophila-Melanogaster and Identification of a Transcript Involved in Biological Rhythms. *Cell*, 38(3):701–710, 1984.

[161] Ludger Rensing and Peter Ruoff. Temperature effect on entrainment, phase shifting, and amplitude of circadian clocks and its molecular bases. *Chronobiology International*, 19(5):807–864, January 2002.

[162] D Rieger, C Wulbeck, F Rouyer, and C Helfrich-Forster. Period Gene Expression in Four Neurons Is Sufficient for Rhythmic Activity of Drosophila melanogaster under Dim Light Conditions. *Journal of Biological Rhythms*, 24(4):271–282, July 2009.

[163] Michael Rosbash. The Implications of Multiple Circadian Clock Origins. *PLoS Biology*, 7(3):e62, 2009.

[164] A E Rougvie and J T Lis. Postinitiation Transcriptional Control in Drosophila-Melanogaster. *Molecular and Cellular Biology*, 10(11):6041–6045, November 1990.

[165] Peter Ruoff and Ludger Rensing. The Temperature-Compensated Goodwin Model Simulates Many Circadian Clock Properties. *Journal of Theoretical Biology*, 179:275–285, 1996.

[166] M J Rust, J S Markson, W S Lane, D S Fisher, and E K O'Shea. Ordered Phosphorylation Governs Oscillation of a Three-Protein Circadian Clock. *Science*, 318(5851):809–812, November 2007.

[167] J E Rutila, V Suri, M Le, W V So, M Rosbash, and J C Hall. CYCLE is a second bHLH-PAS clock protein essential for circadian rhythmicity and transcription of Drosophila period and timeless. *Cell*, 93(5):805–814, 1998.

[168] Sriram Sathyanarayanan, Xiangzhong Zheng, Rui Xiao, and Amita Sehgal. Posttranslational regulation of Drosophila PERIOD protein by protein phosphatase 2A. *Cell*, 116(4):603–615, February 2004.

[169] Frank A J L Scheer, Michael F Hilton, Christos S Mantzoros, and Steven A Shea. Adverse metabolic and cardiovascular consequences of circadian misalignment. *Proceedings of the National Academy of Sciences of the United States of America*, 106(11):4453–4458, March 2009.

[170] K Schneider, S Perrino, K Oelhafen, S Li, A Zatsepin, P Lakin-Thomas, and S Brody. Rhythmic Conidiation in Constant Light in Vivid Mutants of Neurospora crassa. *Genetics*, 181(3):917–931, January 2009.

[171] Hana Sehadova, Franz T Glaser, Carla Gentile, Alekos Simoni, Astrid Giesecke, Joerg T Albert, and Ralf Stanewsky. Temperature Entrainment of Drosophilas Circadian Clock Involves the Gene nocte and Signaling from Peripheral Sensory Tissues to the Brain. *Neuron*, 64(2):251–266, October 2009.

[172] M T Sellix, J Currie, M Menaker, and H Wijnen. Fluorescence/Luminescence Circadian Imaging of Complex Tissues at Single-Cell Resolution. *Journal of Biological Rhythms*, 25(3):228–232, May 2010.

[173] Michael T Sellix and Michael Menaker. Circadian clocks in the ovary. *Trends in Endocrinology & Metabolism*, 21(10):628–636, October 2010.

[174] O T Shafer, M Rosbash, and J W Truman. Sequential nuclear accumulation of the clock proteins period and timeless in the pacemaker neurons of Drosophila melanogaster. *Journal of Neuroscience*, 22(14):5946–5954, 2002.

[175] I I Shemiakina, G V Ermakova, P J Cranfill, M A Baird, R A Evans, E A Souslova, D B Staroverov, A Y Gorokhovatsky, E V Putintseva, T V Gorodnicheva, T V Chepurnykh, L Strukova, S Lukyanov, A G Zaraisky, M W Davidson, D Shcherbo, and D M Chudakov. A monomeric red fluorescent protein with low cytotoxicity. *Nature Communications*, 3:1204–7, October 2012.

[176] Sandra M Siepka and Joseph S Takahashi. Forward genetic screens to identify circadian rhythm mutants in mice. *Applications of Chimeric Genes and Hybrid Proteins Pt B*, 393:219–229, 2005.

[177] Elaine M Smith, Jui-Ming Lin, Rose-Anne Meissner, and Ravi Allada. Dominant-negative CK2 alpha induces potent effects on circadian rhythmicity. *PLoS Genetics*, 4(1), January 2008.

[178] W V So and M Rosbash. Post-transcriptional regulation contributes to Drosophila clock gene mRNA cycling. *The EMBO Journal*, 16(23):7146–7155, December 1997.

[179] R Stanewsky, K S Lynch, C Brandes, and J C Hall. Mapping of Elements Involved in Regulating Normal Temporal period and timeless

RNA Expression Patterns in Drosophila melanogaster. *Journal of Biological Rhythms*, 17(4):293–306, August 2002.

[180] Nicholas Stavropoulos and Michael W Young. insomniac and Cullin-3 Regulate Sleep and Wakefulness in Drosophila. *Neuron*, 72(6):964–976, December 2011.

[181] Elizabeth F Stone, Ben O Fulton, Janelle S Ayres, Linh N Pham, Junaid Ziauddin, and Mimi M Shirasu-Hiza. The Circadian Clock Protein Timeless Regulates Phagocytosis of Bacteria in Drosophila. *PLoS Pathogens*, 8(1):e1002445, January 2012.

[182] Teruya Tamaru, Mitsuru Hattori, Kousuke Honda, Ivor Benjamin, Takeaki Ozawa, and Ken Takamatsu. Synchronization of Circadian Per2 Rhythms and HSF1-BMAL1:CLOCK Interaction in Mouse Fibroblasts after Short-Term Heat Shock Pulse. *PLoS ONE*, 6(9):e24521, September 2011.

[183] Özgür Tataroğlu and Patrick Emery. Studying circadian rhythms in Drosophila melanogaster. *Methods*, 68(1):140–150, June 2014.

[184] Kazuki Terauchi, Yohko Kitayama, Taeko Nishiwaki, Kurniko Miwa, Yoriko Murayama, Tokitaka Oyama, and Takao Kondo. ATPase activity of KaiC determines the basic timing for circadian clock of cyanobacteria. *Proceedings of the National Academy of Sciences*, 104(41):16377–16381, 2007.

[185] C L Thompson and A Sancar. Photolyase/cryptochrome blue-light photoreceptors use photon energy to repair DNA and reset the circadian clock. *Oncogene*, 21(58):9043–9056, 2002.

[186] Jun Tomita, Masato Nakajima, Takao Kondo, and Hideo Iwasaki. No transcription-translation feedback in circadian rhythm of KaiC phosphorylation. *Science*, 307(5707):251–254, January 2005.

[187] H Towbin, T Staehelin, and J Gordon. Electrophoretic Transfer of Proteins From Polyacrylamide Gels to Nitrocellulose Sheets - Procedure and Some Applications. *Proceedings of the National Academy of Sciences*, 76(9):4350–4354, 1979.

[188] Carl Troein, James C W Locke, Matthew S Turner, and Andrew J Millar. Weather and Seasons Together Demand Complex Biological Clocks. *Current Biology*, 19(22):1961–1964, December 2009.

[189] B Trost and A Kusalik. Computational prediction of eukaryotic phosphorylation sites. *Bioinformatics*, 27(21):2927–2935, October 2011.

[190] Benjamin P Tu and Steven L McKnight. Metabolic cycles as an underlying basis of biological oscillations. *Nature Reviews Molecular Cell Biology*, 7(9):696–701, September 2006.

[191] John J Tyson, Christian I Hong, C Dennis Thron, and Bela Novak. A Simple Model of Circadian Rhythms Based on Dimerization and Proteolysis of PER and TIM. *Biophysical Journal*, 77(5):2411–2417, November 1999.

[192] N N Ugarova, L Y Brovko, and N V Kost. Immobilization of Luciferase From the Firefly Luciola-Mingrelica - Catalytic Properties and Stability of the Immobilized Enzyme. *Enzyme and Microbial Technology*, 4(4):224–228, 1982.

[193] Hideki Ukai, Tetsuya J Kobayashi, Mamoru Nagano, Koh-hei Masumoto, Mitsugu Sujino, Takao Kondo, Kazuhiro Yagita, Yasufumi Shigeyoshi, and Hiroki R Ueda. Melanopsin-dependent photo-perturbation reveals desynchronization underlying the singularity of mammalian circadian clocks. *Nature Cell Biology*, 9(11):1327–1334, October 2007.

[194] Alexander M van der Linden, Matthew Beverly, Sebastian Kadener, Joseph Rodriguez, Sara Wasserman, Michael Rosbash, and Piali Sengupta. Genome-Wide Analysis of Light- and Temperature-Entrained Circadian Transcripts in Caenorhabditis elegans. *PLoS Biology*, 8(10):e1000503, October 2010.

[195] Jeroen S van Zon, David K Lubensky, Pim R H Altena, and Pieter Rein ten Wolde. An allosteric model of circadian KaiC phosphorylation. *Proceedings of the National Academy of Sciences*, 104(18):7420–7425, May 2007.

[196] Alexis B Webb, Nikhil Angelo, James E Huettner, and Erik D Herzog. Intrinsic, nondeterministic circadian rhythm generation in identified mammalian neurons. *Proceedings of the National Academy of Sciences of the United States of America*, 106(38):16493–16498, September 2009.

[197] Jonathan Weiner. *Time, Love, Memory: A Great Biologist and His Quest for the Origins of Behavior*. Knopf, 1999.

[198] Ron Weiss, Osnat Bartok, Shaul Mezan, Yuval Malka, and Sebastian Kadener. Synergistic Interactions between the Molecular and Neu-

ronal Circadian Networks Drive Robust Behavioral Circadian Rhythms in Drosophila melanogaster. *PLoS Genetics*, 10(4):e1004252, April 2014.

[199] D K Welsh, D E Logothetis, M Meister, and S M Reppert. Individual Neurons Dissociated From Rat Suprachiasmatic Nucleus Express Independently Phased Circadian Firing Rhythms. *Neuron*, 14(4):697–706, April 1995.

[200] David K Welsh, Joseph S Takahashi, and Steve A Kay. Suprachiasmatic Nucleus: Cell Autonomy and Network Properties. *Annual Review of Physiology*, 72(1):551–577, March 2010.

[201] David K Welsh, Seung-Hee Yoo, Andrew C Liu, Joseph S Takahashi, and Steve A Kay. Bioluminescence Imaging of Individual Fibroblasts Reveals Persistent, Independently Phased Circadian Rhythms of Clock Gene Expression. *Current Biology*, 14(24):2289–2295, December 2004.

[202] Pl O Westermark, David K Welsh, Hitoshi Okamura, and Hanspeter Herzel. Quantification of Circadian Rhythms in Single Cells. *PLoS Computational Biology*, 5(11):e1000580, November 2009.

[203] Zimmerman WF, Pittendrigh CS, and T Pavlidis. Temperature Compensation of Circadian Oscillation in Drosophila Pseudoobscura and Its Entrainment by Temperature Cycles. *Journal of Insect Physiology*, 14(5):669–&, 1968.

[204] Nicholas M Whitney, Yannis P Papastamatiou, Kim N Holland, and Christopher G Lowe. Use of an acceleration data logger to measure diel activity patterns in captive whitetip reef sharks, Triaenodon obesus. *Aquatic Living Resources*, 20(4):299–305, January 2008.

[205] A T Winfree. Biological Rhythms and Behavior of Populations of Coupled Oscillators. *Journal of Theoretical Biology*, 16(1):15–&, 1967.

[206] A T Winfree. Integrated view of resetting a circadian clock. *Journal of Theoretical Biology*, 28(3):327–374, September 1970.

[207] A T Winfree. Acute Temperature Sensitivity of Circadian-Rhythm in Drosophila. *Journal of Insect Physiology*, 18(2):181–&, 1972.

[208] A T Winfree. Unclocklike Behavior of Biological Clocks. *Nature*, 253(5490):315–319, 1975.

[209] A T Winfree and H Gordon. Photosensitivity of a Mutant Circadian Clock. *Journal of Comparative Physiology*, 122(1):87–109, 1977.

[210] Art Winfree. *The Geometry of Biological Time*. Springer, 2000.

[211] Mark A Woelfle, Yan Ouyang, Kittiporn Phanvijhitsiri, and Carl Hirschie Johnson. The adaptive value of circadian clocks: an experimental assessment in cyanobacteria. *Current Biology*, 14(16):1481–1486, August 2004.

[212] Kanyan Xu, Xiangzhong Zheng, and Amita Sehgal. Regulation of Feeding and Metabolism by Neuronal and Peripheral Clocks in Drosophila. *Cell Metabolism*, 8(4):289–300, October 2008.

[213] Ying Xu, Quasar S Padiath, Robert E Shapiro, Christopher R Jones, Susan C Wu, Noriko Saigoh, Kazumasa Saigoh, Louis J Ptáček, and Ying-Hui Fu. Functional consequences of a CKIdelta mutation causing familial advanced sleep phase syndrome. *Nature*, 434(7033):640–644, March 2005.

[214] S Yamaguchi, H Isejima, T Matsuo, R Okura, K Yagita, M Kobayashi, and H Okamura. Synchronization of cellular clocks in the suprachiasmatic nucleus. *Science*, 302(5649):1408–1412, 2003.

[215] Shun Yamaguchi, Hiromi Isejima, Takuya Matsuo, Ryusuke Okura, Kazuhiro Yagita, Masaki Kobayashi, and Hitoshi Okamura. Synchronization of cellular clocks in the suprachiasmatic nucleus. *Science*, 302(5649):1408–1412, November 2003.

[216] Z Yao and O T Shafer. The Drosophila Circadian Clock Is a Variably Coupled Network of Multiple Peptidergic Units. *Science*, 343(6178):1516–1520, March 2014.

[217] Takuya Yoshida, Yoriko Murayama, Hiroshi Ito, Hakuto Kageyama, and Takao Kondo. Nonparametric entrainment of the in vitro circadian phosphorylation rhythm of cyanobacterial KaiC by temperature cycle. *Proceedings of the National Academy of Sciences of the United States of America*, 106(5):1648–1653, February 2009.

[218] M W Young. The molecular control of circadian behavioral rhythms and their entrainment in Drosophila. *Annual Review of Biochemistry*, 67:135–152, 1998.

[219] M W Young and S A Kay. Time zones: A comparative genetics of circadian clocks. *Nature Reviews Genetics*, 2(9):702–715, September 2001.

[220] W A Zehring, D A Wheeler, P Reddy, R J Konopka, C P Kyriacou, M Rosbash, and J C Hall. P-element transformation with period locus DNA restores rhythmicity to mutant, arrhythmic Drosophila melanogaster. *Cell*, 39(2 Pt 1):369–376, December 1984.